



HAL
open science

Observer based fault diagnosis and fault tolerant control of nonlinear systems

Xue Han

► **To cite this version:**

Xue Han. Observer based fault diagnosis and fault tolerant control of nonlinear systems. Automatic. INSA de Toulouse, 2021. English. NNT : 2021ISAT0031 . tel-03738143

HAL Id: tel-03738143

<https://theses.hal.science/tel-03738143>

Submitted on 25 Jul 2022

HAL is a multi-disciplinary open access archive for the deposit and dissemination of scientific research documents, whether they are published or not. The documents may come from teaching and research institutions in France or abroad, or from public or private research centers.

L'archive ouverte pluridisciplinaire **HAL**, est destinée au dépôt et à la diffusion de documents scientifiques de niveau recherche, publiés ou non, émanant des établissements d'enseignement et de recherche français ou étrangers, des laboratoires publics ou privés.



THÈSE

**En vue de l'obtention du
DOCTORAT DE L'UNIVERSITÉ DE TOULOUSE
Délivré par l'Institut National des Sciences Appliquées de
Toulouse**

Présentée et soutenue par

Xue HAN

Le 9 avril 2021

**Diagnostic basé sur les observateurs et commande tolérante aux
fautes des systèmes non linéaires**

Ecole doctorale : **SYSTEMES**

Spécialité : **Automatique**

Unité de recherche :

LAAS - Laboratoire d'Analyse et d'Architecture des Systèmes

Thèse dirigée par

Boutaieb DAHOU

Jury

M. Mondher FARZA, Rapporteur

M. Dominique SAUTER, Rapporteur

Mme Olfa BOUBAKER, Examinatrice

M. Michel CABASSUD, Examineur

M. Boutaieb DAHOU, Directeur de thèse

Mme Louise TRAVE-MASSUYES, Présidente

Acknowledgments

I leave no trace of wings in the air, but I am glad I have had my flight.

– Rabindranath Tagore

My thesis was carried out at Laboratoire d'Analyse et d'Architecture des Systèmes du Centre National de la Recherche Scientifique (LAAS-CNRS) in the group Diagnostic, Supervision et CONduite (DISCO). First, special thanks to China Scholarship Council who gives financial support for my study in France. Besides, I would like to thank Liviu NICU, the director of LAAS, for having welcomed me to LAAS. I would also like to thank Yannick PENCOLE, head of the DISCO group, for welcoming me in the group.

I would like to express my sincere and deepest gratitude to my supervisor, Prof. Boutaib DAHHOU, for his enlightening guidance, constructive advice, and strong patience over the past few years. What I have benefited most from him is the rigorous and diligent attitude to scientific research. I would also like to extend my deepest gratitude to Prof. Zetao LI and Prof. Michel CABASSUD. I benefited a lot from their rich knowledge and experiences.

I would like to extend my sincere thanks to Prof. Mondher FARZA and Prof. Dominique SAUTER, for agreeing to be reporters of my thesis and for their precious and judicious remarks for this work. I also wish to thank Prof. Olfa BOUBAKER and Prof. Michel CABASSUD for having participated in my jury as examiners and giving valuable suggestions for my work. I would also like to express my thanks to research director Louise TRAVE-MASSUYES, for being the president of my jury.

Thanks should also go to my colleagues in the DISCO team. We had a wonderful time in the past years. I am sure I will miss our Tra-DISCO, miss our discussion about 'chocolatine' and 'pain au chocolat'.

Finally, a big thank to my parents for their love and constant support. Bisous.

Résumé

En raison de la demande croissante de sécurité et de fiabilité accrues des systèmes dynamiques, la détection et le diagnostic des défauts (FDD) ainsi que la commande tolérante aux fautes (FTC) deviennent des méthodes attrayantes pour éviter les pannes et les catastrophes des grands systèmes. Cette thèse porte sur le développement de stratégies de FDD et de FTC basées sur des observateurs pour des systèmes non linéaires complexes. Une étude de cas sur un réacteur/échangeur de chaleur (réacteur HEX) intensifié est proposée afin d'illustrer et de démontrer l'efficacité des algorithmes de commande tolérante aux fautes développés.

Dans le domaine du génie chimique, un réacteur HEX intensifié est un dispositif multifonctionnel qui combine un échangeur de chaleur et un réacteur chimique dans une unité hybride. Grâce à ses remarquables performances thermiques et hydrodynamiques, le réacteur HEX intensifié est un moyen prometteur de répondre aux exigences croissantes en matière de sécurité, de réduction des coûts et de déchets. Cependant, des défaillances telles que l'encrassement des canaux ou un mauvais contrôle thermique pouvant conduire à un emballement thermique constituent des menaces importantes pour la mise en œuvre de ce procédé intensifié. Pour résoudre ces problèmes, il est nécessaire de mettre en place des systèmes de diagnostic et de commande tolérante aux fautes afin de garantir des performances satisfaisantes, même en cas de d'apparition de certains défauts.

Un modèle mathématique du réacteur HEX est proposé dont la validité est prouvée en comparant les performances obtenues par simulation avec des données expérimentales. Afin de superviser le changement d'un paramètre susceptible de varier, un observateur adaptatif et un observateur par intervalles sont proposés. Ces observateurs qui portent non seulement sur l'estimation de l'état mais aussi sur le changement de paramètres, sont appliqués au réacteur HEX considéré. Les résultats montrent que la méthode FDD basée sur l'observateur adaptatif et la méthode FDD basée sur l'observateur par intervalles permettent de bien diagnostiquer les défauts dynamiques et les défauts liés à des capteurs.

Pour concevoir une stratégie de commande tolérante aux fautes pour le réacteur HEX, une loi de contrôle nominale basée sur l'approche Backstepping est proposée en premier lieu pour garantir que la température du fluide du procédé suive la valeur désirée. Ensuite, le contrôleur backstepping obtenu est combiné avec les schémas FDD basés sur les deux types d'observateurs, respectivement. Ainsi, deux stratégies de FTC

actives basées sur des observateurs sont proposées. L'idée principale de ces schémas FTC actifs est la reconfiguration de la commande. Une fois le défaut isolé et identifié, la loi de commande est reconstruite de façon à ce que le système continue à satisfaire les performances attendues en présence du défaut.

Les stratégies FTC développées sont appliquées au réacteur HEX considéré et leur efficacité est démontrée. Dans les deux cas, défaut dynamique ou défaut lié à un capteur, les résultats obtenus sont satisfaisants. On peut noter que la stratégie FTC utilisant l'observateur par intervalles présente une vitesse d'isolation de défaut plus rapide.

Mots clés: commande tolérante aux fautes; diagnostic de défauts; détection et isolation de faults; commande backstepping; observateur adaptatif; observateur d'intervalle; observateur non linéaire; systèmes non linéaires; échangeur de chaleur/réacteur

Abstract

Due to the increasing demand for higher safety and reliability of the dynamic system, fault detection and diagnosis (FDD), as well as fault tolerant control (FTC) are becoming effective methods to avoid breakdowns and disasters of major systems. Therefore, this thesis focuses on developing observer based fault diagnosis and fault tolerant control strategies for complex nonlinear systems. A case study on an intensified heat exchanger/reactor (HEX reactor) is proposed to illustrate and demonstrate the proposed fault tolerant control techniques.

In chemical engineering field, an intensified HEX reactor is a multifunctional device that combines heat exchanger and chemical reactor in one hybrid unit. Thanks to its remarkable thermal and hydrodynamic performance, the intensified HEX reactor is a promising way to meet the increasing requirements for safer operating conditions and lower cost as well as energy waste in the chemical engineering field. However, undesirable failures, such as thermal runaway, and fouling in channels, still pose a great threat to such intensified process. To solve this, FDD and FTC schemes are needed to make it have a satisfactory performance even under the faulty situation

To start, a mathematical model of the HEX reactor is proposed. The effectiveness of the proposed modeling is proved by comparing its performances obtained by simulation with the experimental data. In order to supervise the change of the possible faulty parameter, adaptive observer, and interval observer, which focus on not only the state estimation but also the parameter change, are applied to the considered HEX reactor. Simulation results show that both dynamic fault and sensor fault can be well diagnosed by the adaptive observer based FDD method and the interval observer based FDD method.

And then, to design a fault tolerant control strategy for the considered HEX reactor, a nominal control law based on the backstepping technique has been proposed firstly to guarantee the temperature of process fluid follows the desired value. After that, the designed backstepping controller is combined with the FDD schemes based on two kinds of observers, respectively. Thus, two active FTC strategies based on observers are obtained. The main idea of the active FTC schemes is the same, controller reconfiguration. Once the fault is isolated and identified by the observer, the control law is reconstructed to make the system still satisfy the expected performance under the faulty case. Both the dynamic fault and sensor fault are considered in this thesis.

After applying the proposed FTC strategies to the considered HEX reactor, their

effectiveness has been demonstrated. Even though the system is influenced by a dynamic fault or sensor fault, the temperature of process fluid still provides a satisfactory tracking performance. Besides, the interval observer based FTC strategy has a faster fault isolation speed after comparing the performances of the proposed FTC strategies.

Key words: fault tolerant control; fault diagnosis; fault detection and isolation; backstepping control; adaptive observer; interval observer; nonlinear observer; controller reconfiguration; nonlinear system; heat-exchanger/reactor.

List of Figures

1.1	Structure of the hardware redundancy scheme	4
1.2	Structure of the analytical redundancy scheme	5
2.1	Fault types and effects in system	9
2.2	Common types of actuator faults: (a) floating around trim, (b) lock-in-place, (c) hard-over failure, and (d) loss of effectiveness [130]	10
2.3	Common types of sensor faults: (a) bias, (b) drift, (c) performance degradation (or loss of accuracy), (d) sensor freezing, and (e) calibration [130]	11
2.4	Types of faults based on behavior [130]	12
2.5	Schematic diagram of model-based fault diagnosis	14
2.6	Schematic diagram of signal-based fault diagnosis	17
2.7	Schematic diagram of knowledge-based fault diagnosis	19
2.8	Architecture of the passive FTC	23
2.9	Architecture of the active FTC	24
3.1	Physical structure of the heat exchanger/reactor: (a) Process channel; (b) utility channel; (c) the heat exchanger/reactor after assembly	28
3.2	Block modeling description, showing (a) process plate, (b) utility plate, and (c) plate wall	29
3.3	Structure of units dividing	30
3.4	Internal description of one computing unit and convective heat exchange	30
3.5	Simulated temperature profiles for experiment 1 (reaction was introduced at 150 s)	35
4.1	Observer as the heart of control systems [14]	38
4.2	Temperature performances of the HEX reactor: dynamic h_p is faulty at 400s	51
4.3	Residuals of both adaptive observers: dynamic h_p is faulty at 400s	52
4.4	Estimated fault value \hat{f}_{p1} : dynamic h_p is faulty at 400s	52

4.5	Temperature performances of the HEX reactor: dynamic $T_{p,in}$ is faulty at 400s	53
4.6	Residuals of both adaptive observers: dynamic $T_{p,in}$ is faulty at 400s . .	53
4.7	Estimated fault value \hat{f}_{p2} : dynamic $T_{p,in}$ is faulty at 400s	54
4.8	Temperature performances of the HEX reactor: sensor T_p is faulty at 400s	54
4.9	Residuals of both adaptive observers: sensor T_p is faulty at 400s	55
4.10	Estimated fault value \hat{f}_{s1} : sensor T_p is faulty at 400s	55
4.11	Temperature performances of the HEX reactor: sensor T_u is faulty at 400s	56
4.12	Residuals of both adaptive observers: sensor T_u is faulty at 400s	56
4.13	Estimated fault value \hat{f}_{s1} : sensor T_u is faulty at 400s	57
4.14	Output errors e_{y,T_p} correspond to intervals of h_p when dynamic h_p is faulty at 400s	63
4.15	Output errors e_{y,T_u} correspond to intervals of h_p when dynamic h_p is faulty at 400s	64
4.16	Output errors e_{y,T_p} correspond to intervals of $T_{p,in}$ when dynamic h_p is faulty at 400s	64
4.17	Output errors e_{y,T_u} correspond to intervals of $T_{p,in}$ when dynamic h_p is faulty at 400s	65
4.18	Output errors e_{y,T_p} correspond to intervals of h_p when dynamic $T_{p,in}$ is faulty at 400s	66
4.19	Output errors e_{y,T_u} correspond to intervals of h_p when dynamic $T_{p,in}$ is faulty at 400s	66
4.20	Output errors e_{y,T_p} correspond to intervals of $T_{p,in}$ when dynamic $T_{p,in}$ is faulty at 400s	67
4.21	Output errors e_{y,T_u} correspond to intervals of $T_{p,in}$ when dynamic $T_{p,in}$ is faulty at 400s	67
4.22	Output errors e_{y,mea,T_p} correspond to variation intervals of Δ_{T_p} when sensor T_p is faulty at 400s	69
4.23	Output errors e_{y,mea,T_u} correspond to variation intervals of Δ_{T_p} when sensor T_p is faulty at 400s	69
4.24	Output errors e_{y,mea,T_p} correspond to variation intervals of Δ_{T_u} when sensor T_p is faulty at 400s	70
4.25	Output errors e_{y,mea,T_u} correspond to variation intervals of Δ_{T_u} when sensor T_p is faulty at 400s	70
4.26	Output errors e_{y,mea,T_p} correspond to variation intervals of Δ_{T_p} when sensor T_u is faulty at 400s	71

4.27	Output errors e_{y,mea,T_u} correspond to variation intervals of Δ_{T_p} when sensor T_u is faulty at 400s	72
4.28	Output errors e_{y,mea,T_p} correspond to variation intervals of Δ_{T_u} when sensor T_u is faulty at 400s	72
4.29	Output errors e_{y,mea,T_u} correspond to variation intervals of Δ_{T_u} when sensor T_u is faulty at 400s	73
5.1	Without chemical reaction case: measured process fluid temperature T_p and utility fluid flow rate F_u	87
6.1	Measured process fluid temperature T_p and utility fluid flow rate F_u in fault free case	93
6.2	h_p is faulty at 200s, without FTC case	94
6.3	h_p is faulty at 200s, with FTC case	94
6.4	Original residual r_i and auxiliary residual Dr_i when h_p is faulty at 200s	95
6.5	Zoom in 60s to 100s: original residual r_i and auxiliary residual Dr_i when h_p is faulty at 200s	95
6.6	Zoom in 170s to 280s: original residual r_i and auxiliary residual Dr_i when h_p is faulty at 200s	95
6.7	Estimated fault value \hat{f}_{p1} when h_p is faulty at 200s	96
6.8	$T_{p,in}$ is faulty at 200s, without FTC case	96
6.9	$T_{p,in}$ is faulty at 200s, with FTC case	97
6.10	Original residual r_i and auxiliary residual Dr_i when $T_{p,in}$ is faulty at 200s	97
6.11	Estimated fault value \hat{f}_{p2} when $T_{p,in}$ is faulty at 200s	98
6.12	Sensor of T_p is faulty at 200s, without FTC case	98
6.13	Sensor of T_p is faulty at 200s, with FTC case	99
6.14	Utility fluid temperature when sensor of T_p is faulty at 200s	100
6.15	Original residual r_i and auxiliary residual Dr_i when sensor of T_p is faulty at 200s	100
6.16	Estimated fault value \hat{f}_{s1} when sensor of T_p is faulty at 200s	100
6.17	Sensor of T_u is faulty at 200s, without FTC case	101
6.18	Sensor of T_u is faulty at 200s, with FTC case	101
6.19	Original residual r_i and auxiliary residual Dr_i when sensor of T_u is faulty at 200s	102
6.20	Estimated fault value \hat{f}_{s2} when sensor of T_u is faulty at 200s	102
6.21	Utility fluid temperature when sensor of T_u is faulty at 200s	103

6.22	Original residual r_1 and auxiliary residual Dr_1 correspond to bound 1 of h_p when dynamic h_p is faulty at 200s	104
6.23	Zoom in 60s to 100s: original residual r_1 and auxiliary residual Dr_1 correspond to bound 1 of h_p when dynamic h_p is faulty at 200s	105
6.24	Zoom in 170s to 280s: original residual r_1 and auxiliary residual Dr_1 correspond to bound 1 of h_p when dynamic h_p is faulty at 200s	105
6.25	Output errors e_{y,T_p} correspond to intervals of h_p when dynamic h_p is faulty at 200s	106
6.26	Output errors e_{y,T_u} correspond to intervals of h_p when dynamic h_p is faulty at 200s	106
6.27	Output errors e_{y,T_p} correspond to intervals of $T_{p,in}$ when dynamic h_p is faulty at 200s	106
6.28	Output errors e_{y,T_u} correspond to intervals of $T_{p,in}$ when dynamic h_p is faulty at 200s	107
6.29	Fault signature correspond to intervals of h_p when dynamic h_p is faulty at 200s	107
6.30	Fault signature correspond to intervals of $T_{p,in}$ when dynamic h_p is faulty at 200s	108
6.31	h_p is faulty at 200s, with FTC case	108
6.32	h_p is faulty at 200s, without FTC case	109
6.33	Original residual r_3 and auxiliary residual Dr_3 correspond to bound 3 of $T_{p,in}$ when dynamic $T_{p,in}$ is faulty at 200s	109
6.34	Output errors e_{y,T_p} correspond to intervals of h_p when dynamic $T_{p,in}$ is faulty at 200s	110
6.35	Output errors e_{y,T_u} correspond to intervals of h_p when dynamic $T_{p,in}$ is faulty at 200s	110
6.36	Output errors e_{y,T_p} correspond to intervals of $T_{p,in}$ when dynamic $T_{p,in}$ is faulty at 200s	111
6.37	Output errors e_{y,T_u} correspond to intervals of $T_{p,in}$ when dynamic $T_{p,in}$ is faulty at 200s	111
6.38	Fault signature correspond to intervals of h_p when dynamic $T_{p,in}$ is faulty at 200s	112
6.39	Fault signature correspond to intervals of $T_{p,in}$ when dynamic $T_{p,in}$ is faulty at 200s	112
6.40	$T_{p,in}$ is faulty at 200s, with FTC case	113
6.41	$T_{p,in}$ is faulty at 200s, without FTC case	113

6.42	Original residual r_1 and auxiliary residual Dr_1 correspond to bound 1 of Δ_{T_p} when sensor T_p is faulty at 200s	114
6.43	Output errors e_{y,mea,T_p} correspond to variation intervals of Δ_{T_p} when sensor T_p is faulty at 200s	114
6.44	Output errors e_{y,mea,T_u} correspond to variation intervals of Δ_{T_p} when sensor T_p is faulty at 200s	115
6.45	Output errors e_{y,mea,T_p} correspond to variation intervals of Δ_{T_u} when sensor T_p is faulty at 200s	115
6.46	Output errors e_{y,mea,T_u} correspond to variation intervals of Δ_{T_u} when sensor T_p is faulty at 200s	116
6.47	Fault signature correspond to variation intervals of Δ_{T_p} when sensor T_p is faulty at 200s	116
6.48	Fault signature correspond to variation intervals of Δ_{T_u} when sensor T_p is faulty at 200s	117
6.49	Sensor of T_p is faulty at 200s, with FTC case	117
6.50	Sensor of T_p is faulty at 200s, without FTC case	118
6.51	Utility fluid temperature when sensor of T_p is faulty at 200s	118
6.52	Original residual r_1 and auxiliary residual Dr_1 correspond to bound 1 of Δ_{T_u} when sensor T_u is faulty at 200s	119
6.53	Output errors e_{y,mea,T_p} correspond to variation intervals of Δ_{T_p} when sensor T_u is faulty at 200s	119
6.54	Output errors e_{y,mea,T_u} correspond to variation intervals of Δ_{T_p} when sensor T_u is faulty at 200s	119
6.55	Output errors e_{y,mea,T_p} correspond to variation intervals of Δ_{T_u} when sensor T_u is faulty at 200s	120
6.56	Output errors e_{y,mea,T_u} correspond to variation intervals of Δ_{T_u} when sensor T_u is faulty at 200s	120
6.57	Fault signature correspond to variation intervals of Δ_{T_p} when sensor T_u is faulty at 200s	121
6.58	Fault signature correspond to variation intervals of Δ_{T_u} when sensor T_u is faulty at 200s	121
6.59	Sensor of T_u is faulty at 200s, with FTC case	122
6.60	Sensor of T_u is faulty at 200s, without FTC case	122
6.61	Utility fluid temperature when sensor of T_u is faulty at 200s	123

List of Tables

3.1	Characteristics of the reaction of sodium thiosulfate oxidation by hydrogen peroxide [6]	34
4.1	Recent observers categorized under different classes	39
4.2	Physical data of the pilot	49
4.3	The value of interval bounds for h_p	63
4.4	The value of interval bounds for $T_{p,in}$	63
4.5	The value of variation Δ_{T_p} interval bounds for sensor T_p	68
4.6	The value of variation Δ_{T_u} interval bounds for sensor T_u	68
6.1	Comparison between adaptive observer based FTC strategy and interval observer based FTC strategy	124

List of abbreviations

FDD	Fault detection and diagnosis
FDI	Fault detection and isolation
FTC	Fault tolerant control
FTCS	Fault tolerant control systems
FD	Fault diagnosis
HEX	Heat-exchanger
SIFT	Scale invariant feature trans
LBP	Local binary patterns
DFT	Discrete Fourier transformation
FFT	Dast Fourier transformation
MCSA	Motor-current signature analysis
STFT	Short-time Fourier transform
WT	Wavelet transforms
HHT	Hilbert-Huang transform
WVD	Wigner-Ville distribution
QTA	Qualitative trend analysis
SDG	Signed directed graphs
PCA	Principle component analysis
PLS	Partial least squares
ICA	Independent component analysis
SVM	Suport vector machine
T-PLS	Total projection to latent structures
NN	Neutral network
ANFIS	Adaptive Neuro-Fuzzy Inference System
SMC	Sliding mode control
LQ	Linear quadratic
MPC	Model predictive control

HIP	Hot isostatic pressing
ODE	Ordinary differential equations
AE	Algebraic equation
ELO	Extended Luenberger observer
KF	Kalman filter
EKF	Extended Kalman filter
HGO	High gain observer
SMO	Sliding mode observer
AO	Adaptive observer
DOB	Disturbance observer
MDOB	Modified disturbance observer
UIO	Unknown input observer
NUIO	Nonlinear unknown input observer
AI	Artificial intelligence
ANN	Artificial neural networks
UO	Uniformly observable
LTI	Linear time invariant
LTV	Linear time variant
DDNO	Disturbance decoupling nonlinear observer

Contents

1	Introduction	1
1.1	Backgrounds	2
1.2	Motivations and objectives	3
1.3	Structure of the thesis	5
2	Fault diagnosis and fault tolerant control: the state of the art	7
2.1	Basic concepts	8
2.1.1	Definitions	8
2.1.2	Type of faults	9
2.2	Fault detection and diagnosis methods	13
2.2.1	Model-based approaches	13
2.2.2	Signal-based approaches	17
2.2.3	Knowledge-based approaches	19
2.2.4	Hybrid approaches	21
2.3	Fault tolerant control	22
2.3.1	Passive FTC	23
2.3.2	Active FTC	23
2.4	Summary	26
3	Modeling of the Heat-exchanger/Reactor	27
3.1	Introduction	28
3.2	Physical structure	28
3.3	Modeling	29
3.3.1	General Modeling of the Reactor	29
3.3.2	Modeling of process plate	31
3.3.3	Modeling of utility plate and plate wall	32
3.3.4	Reaction modeling	33
3.3.5	Simulation result	34

3.4	Summary	36
4	Observer based FDD schemes and their applications for the Heat-exchanger/Reactor	37
4.1	Introduction	38
4.2	Classification of nonlinear observers	38
4.3	Nonlinear model under consideration	40
4.3.1	Expressions of nonlinear system	41
4.3.2	Properties of nonlinear system	42
4.3.3	Dynamic and sensor faulty model	43
4.4	Adaptive observer	45
4.4.1	Structure of adaptive observer	46
4.4.2	Adaptive observer based FDD scheme	47
4.4.3	Application to HEX reactor: adaptive observer based FDD scheme	48
4.5	Interval observer	57
4.5.1	Structure of interval observer	57
4.5.2	Interval observer based FDD scheme	59
4.5.3	Application to HEX reactor: interval observer based FDD scheme	62
4.6	Summary	73
5	Backstepping controller design for the Heat-exchanger/Reactor	75
5.1	Backstepping design	76
5.1.1	Integrator backstepping	76
5.1.2	Backstepping for strict-feedback systems	77
5.1.3	Adaptive backstepping	79
5.1.4	Robust backstepping	81
5.2	Backstepping controller design for the considered HEX reactor	83
5.2.1	Controller design procedure	84
5.2.2	Simulation result	87
5.3	Summary	88
6	Backstpping fault tolerant control for the Heat-exchanger/Reactor based on different observers	89
6.1	Backstepping fault tolerant control based on observers	90
6.1.1	Dynamic FTC design	90
6.1.2	Sensor FTC design	91
6.2	Application to the HEX reactor	91

6.2.1	Backstepping fault tolerant control based on adaptive observers .	91
6.2.2	Backstepping fault tolerant control based on interval observers .	103
6.3	Comparison between these two methods	123
6.4	Summary	125
7	Conclusion and suggestion of future works	127
7.1	Conclusion	128
7.2	Future works	130
	Bibliography	133

Chapter 1

Introduction

Fault detection and diagnosis (FDD), as well as fault tolerant control (FTC), are critical techniques to ensure the safety and reliability of industrial systems. Based on the analysis of the background in this field, this chapter outlines the motivations and the objectives of this study. The structure of the thesis is also presented here.

1.1 Backgrounds

With the evolution of modern technologies, many engineering systems, such as aero engines, vehicle dynamics, chemical processes, manufacturing systems, power networks, etc, are becoming increasingly complex. As a consequence, one tiny component of the overall industrial system can cause an unanticipated economic cost due to unplanned shutdown and repairing/maintenance. Therefore, to guarantee the safety and reliability of these systems, it is of great interest to design advanced fault detection and diagnosis (FDD) techniques and fault tolerant control (FTC) programs to automatically supervise the behavior of industrial systems and prevent further degradation caused by unexpected faults.

A fault is defined as an unexpected deviation of at least one characteristic property or parameter of the system from its nominal condition [65]. This may be an intermittent event in the system, for example, sticking valves, leaks in the pipes, a pressure drop in hydraulic components, etc. It can also be a wrong control signal given by the controllers, or a change in ambient devices, such as sensor drift. In all cases, the fault can result in a degradation of system performance, such as reduced production and product quality, or worse, it can cause serious accidents in terms of human mortality and environmental impact. We can cite the following examples: [67] claims that the petrochemical industry in the United States loses between 10 to 20 billion dollars annually due to abnormal situation management. [117] declares that the operational unavailability of wind turbines reaches 3% of the lifetime of a wind turbine, and the maintenance for its onshore and offshore can account for 10% to 15% and 20% to 35% of the total life costs of wind conversion systems. Besides, faults can lead to fatalities in safety critical processes such as aircraft, nuclear reactors, etc. For example, due to complete loss of flying surface in the tail, Japan Airlines Flight 123 was crashed on 12 August 1984 killing 520 people [113]. Another famous example is the explosion that occurred in a huge nuclear power plant in the city of Chernobyl in 1986. The main cause for this tragedy was the faulty outdated technology and the lack of a fault handling mechanism. Therefore, to avoid, or at least minimize economic losses and fatalities, faults must be found as quickly as possible and decisions must be made to stop the spread of their effects [16]. Thus, even if a fault occurs in the system, the FDD scheme and FTC scheme can still ensure that the system maintains an acceptable performance.

In the chemical industries, the intensification of the process has become a growing interest in recent decades, see in [35, 52, 107]. It aims to replace the traditional energy

consuming unit operations with novel sustainable and economical ones by combining two or more traditional operations in one hybrid unit. Among the numerous options for intensifying a process, the conversion from a batch reactor to a continuous plug flow reactor is a good alternative when selectivity and heat exchange is a problem. As a consequence, an intensified heat-exchanger (HEX)/reactor is developed to remove the barrier related to the dissipation of the generated reaction heat [6, 34, 114]. It combines a heat-exchanger and a reactor in the same unit. Thus, by using HEX reactors, many benefits are expected such as waste reduction, energy and raw materials saving, increasing efficiency and selectivity, and cost reduction. Besides, thanks to its strong heat transfer capacity and good mixing performance, the safety of the chemical processes is improved because the temperature of chemical reactions can be guaranteed at a quite stable value.

However, for the considered HEX reactor, it is always possible to be affected by an unexpected fault during the production process, especially when it is assembled with ambient devices, for example, the sticking of the valves that control the flow rate of the reactants, the fouling caused by chemical reactions inside the reactors, etc. In addition, according to the investigation of its characteristics and performances, the HEX reactor presents high nonlinearities [6, 10, 112]. So, the development of FDD and FTC strategies for the intensified heat-exchanger/reactor is still necessary both in academia and industry.

1.2 Motivations and objectives

For the proposed HEX reactor, the most important objective is to guarantee a stable temperature for chemical reaction not only for a good productivity but also for the security of the production process, even in presence of a fault. Thus, the overall aim of this thesis is to propose and develop FDD schemes, as well as FTC systems for the considered intensified HEX reactor, which is an interesting class of chemical industries.

During the past decades, fruitful results have been reported on FD methods, FTC techniques and their applications in various industrial processes and systems. A number of survey papers and books were written. For instance, [41, 49, 63, 73, 88] give an review in FDD methods, and [15–17, 69, 70, 84, 97, 135] provide a review on the existing FTC technologies. When a fault occurs in the system, the desired performance can be achieved sometimes by designing a robust controller. However, a fixed controller is usually not flexible enough to deal with different kinds of fault. Therefore, to well

maintain the performance of the system in the presence of a fault, detailed information of the fault such as the location of the faulty component, the size of the fault etc, is highly required for the controller redesign, which are exactly the task of FDD.

FDD can be achieved by using the concept of redundancy, either hardware (or physical) redundancy or software (or analytical) redundancy. As shown in Figure 1.1, the idea of hardware redundancy is to use additional (redundant) components in parallel to the process components such as sensors, actuators, controllers and computers to perform the same function. If the behavior of a process component is different from that of the redundant component, it gives an indication of the occurrence of a fault. The hardware redundancy is reliable, but expensive and increasing weights and occupying more space [46, 73]. With the mature of modern control theory, the analytical redundancy technique has become the main stream of the fault diagnosis research since the 1980s. Functional relationships governed by physical laws and a fault diagnosis algorithm are employed to check the consistency of real-time process characteristic information carried by the input and output data against pre-knowledge about a healthy system, and fault information is then given by using diagnostic logic such as residual generation and evaluation, as presented in Figure 1.2. Compared with hardware redundancy methods, analytical redundancy diagnostic methods are more cost effective.

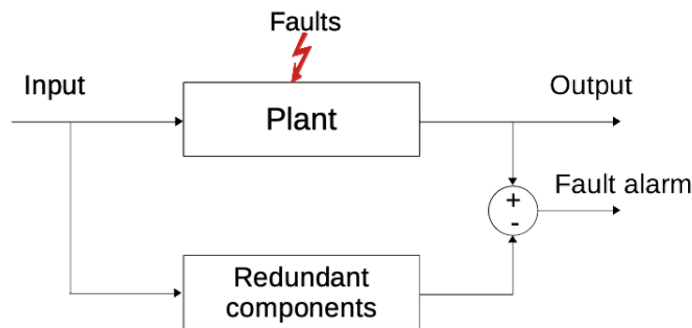


Figure 1.1: Structure of the hardware redundancy scheme

Among the analytical redundancy based fault detection schemes, analytical model-based techniques use the deepest knowledge of the monitored process and, therefore, are the most suitable approaches for FD when the mathematical model of the process is available. Among the model-based approaches, observer based methods have been widely applied because of their advantages such as, quick detection, less restrictions, requiring no excitation signal, possibility of online implementation etc [1].

Based on the before mentioned facts, this thesis focuses on developing observer based fault estimation and FTC strategies, which can be applied to the considered

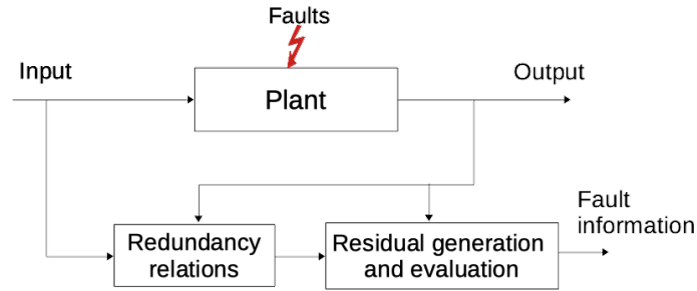


Figure 1.2: Structure of the analytical redundancy scheme

HEX reactor to increase system reliability and safety. The specific objectives of this thesis are the following:

- Review different FDD and FTC existing techniques and discuss their applicability in the HEX reactor;
- Develop a general mathematical model for the intensified heat-exchanger/reactor for control and diagnostic use;
- Review classical observers and compare their performances of state estimation;
- Design a nonlinear controller for the HEX reactor to make its performances follow the desired ones;
- Design different fault detection and diagnosis strategies combined with FTC scheme for the HEX reactor in presence of different kinds of fault;
- Test, over a simulation environment, the designed FDD and FTC techniques and compare their dynamics.

1.3 Structure of the thesis

This thesis is divided into eight chapters. Following the introduction in Chapter 1, Chapter 2 reviews recent FDD and FTC techniques. It begins with the definitions of basic concepts such as faults, failures etc. A classification of FDD and FTC methods, with a brief discussion on each approach, is also presented in this chapter.

Chapter 3 provides the modeling process of the intensified heat-exchanger/reactor. Physical structure and hydrodynamic and thermal performance of the HEX reactor are studied. A typical exothermic reaction, which was used in experiments, is also modeled in details. Finally, a non-linear numerical model of 255 calculating modules

is developed on the Matlab/Simulink platform. Simulations of this model are done under conditions with and without chemical reactions. In addition, simulation results are compared with reserved experimental data to show its validity and accuracy.

Chapter 4 introduces two kinds of FDD schemes based on adaptive observer and interval observer. First, an overview of observers are presented. Since the adaptive observer and interval observer focus on not only the state estimation but also the parameter estimation, they are used to develop fault diagnosis algorithms. And then, the presented FDD schemes are applied to the HEX reactor to verify their effectiveness.

Chapter 5 develops a nonlinear controller for the HEX reactor based on backstepping approach. The backstepping scheme is firstly introduced and studied. And then, the backstepping controller is designed for the HEX reactor, so as to make the output temperatures follow the desired values.

Chapter 6 presents two active FTC schemes for the considered HEX reactor by combining the nominal backstepping control law with the presented FDD schemes. The differences between these two methods are the fault detection and diagnose schemes, one is based on the adaptive observers, the other is based on the interval observers. For each FTC strategy, both dynamic fault and sensor fault are considered. Once the fault is detected, isolated and identified, the controller is redesigned to guarantee the performance of the HEX reactor follows the desired one. Simulation results proves the effectiveness of the presented FTC schemes. In addition, the performances of these two strategies are compared.

Chapter 7 summarizes and concludes the overall work described by this thesis and makes suggestions and recommendations as to how the research can be further developed in the future.

Chapter 2

Fault diagnosis and fault tolerant control: the state of the art

This chapter reviews the existing methods for fault detection and diagnosis (FDD) and fault tolerant control (FTC) in nonlinear systems. Fundamental concepts, such as fault, failure, fault detection, and fault isolation are introduced. And the different types of faults and their effects on the system performances are explained. In addition, several methods for FDD existed in the literature, and a widely accepted classification of these methods are presented in this chapter. Besides, a brief introduction of FTC and its classification are also presented in detail.

2.1 Basic concepts

In order to recognize the terminology in the field of fault diagnosis and to understand the goals of the specific contributions, the IFAC Technical Committee: SAFEPROCESS has launched an initiative to define a common terminology [65]. Throughout the text, a fault means an unpermitted deviation of at least one characteristic property or parameter of a system from the acceptable/usual/standard condition. It is the result of a defect in a component or subsystem which degrades the function and performance of the system. A very related term is failure which is a permanent interruption of the system's ability to perform a required function under specified operating conditions. Usually, failure means a complete breakdown of a component, whereas fault is the only deviation from normal characteristics, but a permanent fault may result in a failure.

From the viewpoint of the mathematical model, faults can be modeled as external inputs or parameter deviations which change the behavior of the process. Like faults, disturbances and uncertainties can also be modeled as external inputs, and they may have similar effects on the process. However, compared to faults, disturbances and uncertainties are present even during the normal operation of the process, so they should be taken into consideration in the controller design. By contrast, faults are considered as more severe changes and their effects cannot be overcome by a fixed controller. Thus, it is necessary to detect the fault so as to prevent any serious consequences.

2.1.1 Definitions

The purpose of FDD is to monitor the system and generate information about the abnormal behavior of its components. The procedure of FDD consists of three steps namely fault detection, fault isolation, and fault identification.

- **Fault detection:** to determine the presence of faults and when they occur in a system.
- **Fault isolation:** to determine the location of the fault.
- **Fault identification:** to estimate the size of the fault

In the literature, fault detection and isolation (FDI) or fault detection and identification (again, FDI) are often used. To avoid any confusion, this thesis has adopted FDI to stand for fault detection and isolation, while FDD stands for fault detection and diagnosis. Fault diagnosis (FD) consists of the determination of the kind, size, location,

and time of occurrence of a fault. The procedure of FD includes both fault isolation and identification.

Except for the basic steps of FDD, other definitions that are often used are introduced below.

(1) Monitoring

A continuous real-time task of determining the conditions of a physical system, by recording information, recognising and indicating anomalies in the behaviour.

(2) Quantitative model

Use of static and dynamic relations among system variables and parameters in order to describe a system’s behaviour in quantitative mathematical terms.

(3) Qualitative model

Use of static and dynamic relations among system variables and parameters in order to describe a system’s behaviour in qualitative terms such as causalities or if-then rules.

2.1.2 Type of faults

For a complex industrial system, the faults may occur at any level of the system, as shown in Figure 2.1. From a different point of view, faults can be classified into different categories.

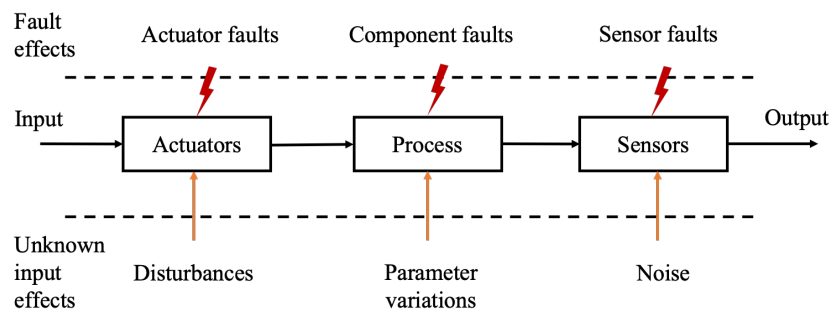


Figure 2.1: Fault types and effects in system

Based on the location of occurrence

Based on the physical location of their occurrence, faults can generally be categorized into three types: component fault, actuator fault, and sensor fault.

(1) Component fault

They are faults that appear in the process components. Component fault, which is also called the dynamic fault or process fault, alters the physical parameters of the

process which, in turn, leads to changes in the normal dynamics of the system. Component faults are usually caused by wear and tear, aging of components, etc. Some examples of component faults are leakages in tanks, breakages or cracks in gearbox systems, etc. For the considered HEX reactor, internal fouling can lead to a component fault. Component faults may result in instability of the process, therefore, it is extremely important to detect these faults.

(2) Actuator fault

Actuator faults act on the operative part of the control system and destroy the transformation from control signals into proper actuation signals. An actuator fault represents the discrepancy between the input command of an actuator and its actual output, and it may cause a total or partial loss of the actuator. A total loss of an actuator can occur, for example, as a result of a broken or cut-off of electrical wire connecting the actuator to the system. An example of partial loss of an actuator is hydraulic or pneumatic leakage or the drop in supply voltage. Actuator fault may result in higher energy consumption to a total loss of control [106], and therefore special attention is paid to the determination of this kind of fault. Examples of actuator faults include stuck-up of control valves, faults in pumps, motors, etc. The actuator faults can be classified into four types [33]: (a) lock-in-place, (b) hard-over failure, (c) float, and (d) loss-of-effectiveness, as shown in Figure 2.2, where dotted lines show the desired value of actuator and the solid lines show actual value.

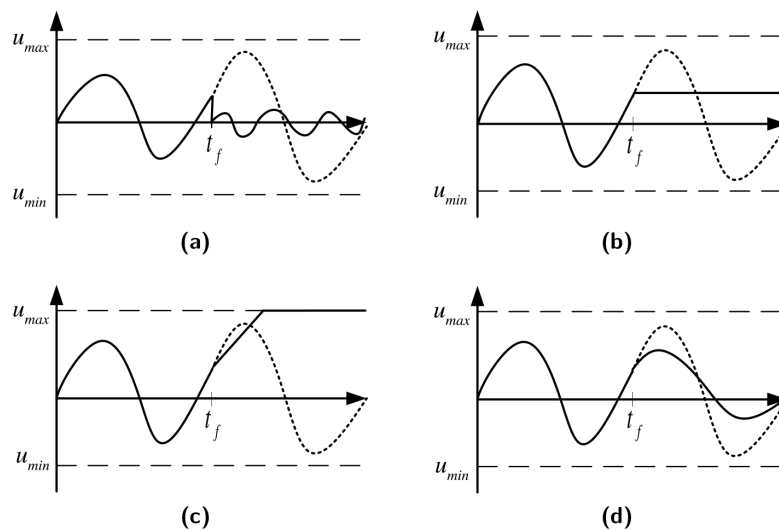


Figure 2.2: Common types of actuator faults: (a) floating around trim, (b) lock-in-place, (c) hard-over failure, and (d) loss of effectiveness [130]

(3) Sensor fault

Sensor faults represent the deviations between the measured and the actual value of a plant's output variable. In closed-loop systems, the measurements obtained by sensors are used to generate the control inputs. So, any fault in sensors can cause operating points far from the nominal ones, and then result in degradation in the performance of the system. Therefore, it is very important to detect these faults. Typical examples of sensor faults are listed in [33] [106]: bias, drift, performance degradation (or loss of accuracy), sensor freezing, and calibration error, as illustrated in Figure 2.3. Solid lines show the actual values whereas the dotted lines show the measured values.

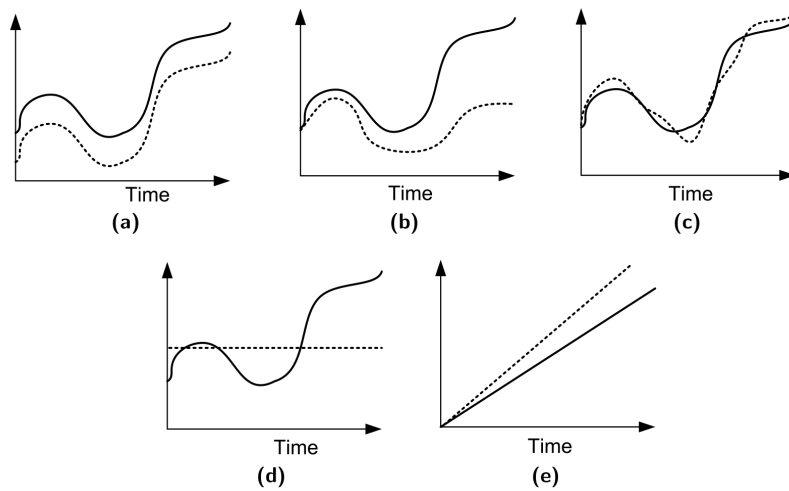


Figure 2.3: Common types of sensor faults: (a) bias, (b) drift, (c) performance degradation (or loss of accuracy), (d) sensor freezing, and (e) calibration [130]

Based on the behavior of fault

According to the time profiles of faults, they can be classified as abrupt, incipient, and intermittent fault [63], as shown in Figure 2.4, t_f is the time of fault occurrence.

(1) Abrupt fault

An abrupt fault is a nearly instantaneous occurring fault, like a step change, as described in (2.1). They have more severe effects and may result in damage to equipment. Fortunately, abrupt faults are easier to detect.

$$f(t - t_f) = \begin{cases} \delta, & t \geq t_f \\ 0, & t < t_f \end{cases} \quad (2.1)$$

(2) Incipient fault

An incipient fault is a slowly developing one, its magnitude develops over a period of time. It is often modeled as a time-varying change in the parameters of a system. Incipient faults can also degrade the performance of equipment, and this slowly changing behavior makes it difficult to detect.

$$f(t - t_f) = \begin{cases} \delta(1 - e^{-\alpha t}), & t \geq t_f \\ 0, & t < t_f \end{cases} \quad (2.2)$$

(3) Intermittent fault

An intermittent fault is a fault that shows up at some time intervals or operating conditions, not all the time, as shown in Figure 2.4 (c).

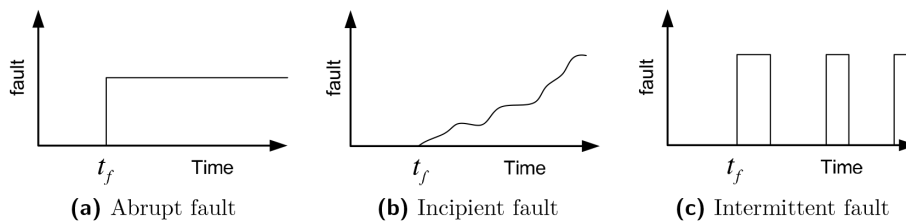


Figure 2.4: Types of faults based on behavior [130]

Based on the way faults are modelled

From the point of view of how the faults are added to the system, faults can be classified as additive faults and multiplicative faults [63].

(1) Additive fault

An additive fault is modeled by an additive term which can influence the input or output of the system. Additive faults are often dealt with by the FTC control. For a linear time invariant system (2.3), its state representation with an additive fault is given by (2.4):

$$\begin{cases} \dot{x}(t) = Ax(t) + Bu(t) \\ y(t) = Cx(t) \end{cases} \quad (2.3)$$

$$\begin{cases} \dot{x}(t) = Ax(t) + Bu(t) + Lf_i(t) \\ y(t) = Cx(t) + Mf_m(t) \end{cases} \quad (2.4)$$

where $x(t)$, $u(t)$, $y(t)$ represent the state, input and output of the system, respectively. The matrices A , B , and C are system matrix, input matrix and output matrix, respectively. $f_i(t)$ and $f_m(t)$ are additive faults, L and M are fault entry matrices.

(2) multiplicative fault

Multiplicative fault is modeled as changes in the parameter matrices ΔA , ΔB or ΔC , the process behavior becomes:

$$\begin{cases} \dot{x}(t) = (A + \Delta A)x(t) + (B + \Delta B)u(t) \\ y(t) = (C + \Delta C)x(t) \end{cases} \quad (2.5)$$

2.2 Fault detection and diagnosis methods

Since the 1970s, a number of FDD theories and methods have been developed, and many excellent survey papers were written, for example, [41, 49, 63, 73, 88]. In 2003, a comprehensive review on the development of FDD process has appeared in a series of papers including three parts [119–121], describing quantitative model-based methods, qualitative model-based methods, and process history based methods. These methods are also recalled below. Most recently, a two-part survey paper [46, 47] on fault diagnosis and fault tolerant techniques was presented in 2015, according to this, fault diagnosis approaches can be categorized into model-based methods, signal-based methods, knowledge-based methods, and hybrid/active methods.

2.2.1 Model-based approaches

Model-based fault diagnosis is suitable for non-stationary operations for engineering plants and can provide systematic design solutions. This method requires a well-known mathematical model of the system obtained by using either physical principles or systems identification techniques.

The model of the system is used to design a nominal system, i.e. a fault free system. Then, the behavior of the nominal system is compared with the behavior of the real system. In case of the absence of fault, the behavior of the real system is consistent with the behavior of the nominal system. However, a fault is detected when the behavior of the real system is different from the behavior of the nominal system. The reflected inconsistencies between nominal and faulty system operation are named as residual, and FDD can be achieved by inspecting the residual. The procedure of creating the residual signal, which is called residual generation, is the first part of the model-based fault diagnosis approach. The following part is called residual evaluation, i.e. the procedure of checking the residual. The schematic diagram of model-based fault diagnosis is illustrated in Figure 2.5.

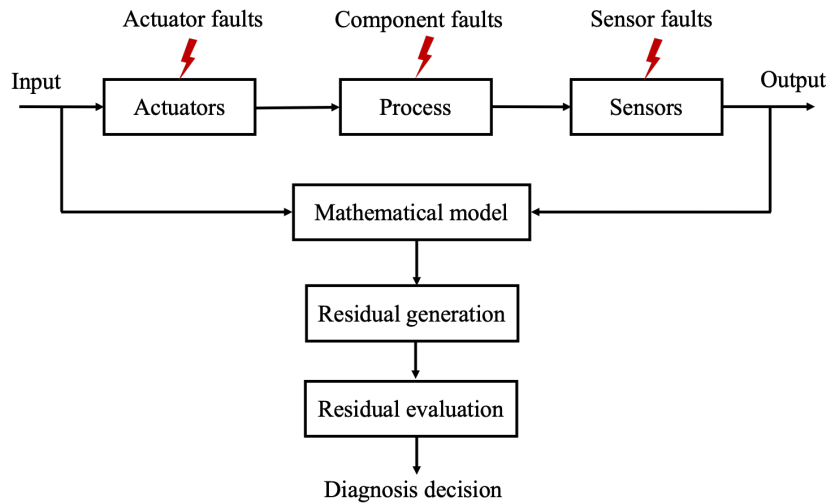


Figure 2.5: Schematic diagram of model-based fault diagnosis

Residual generation method

As described before, residual generation is a procedure for detecting faults in the system. The algorithm (or processor) used to generate residuals is called a residual generator. Well-known model-based approaches for residual generation techniques include observer based techniques, parity space approaches, and parameter estimation approaches. Specifically, observer based techniques have better sensitivity to faults and robustness against disturbances compared with the parity space approach. Moreover, they depend less on the precision of the measured parameters and an explicit correspondence with the physical coefficient than on the parameter estimation methods. As a result, observer based fault diagnosis methods become popular and lead to fruitful results.

(1) Observer based approach

Observers are computational algorithms designed to estimate unmeasured state variables due to the lack of appropriate estimating devices or to replace high priced sensors in a plant. The main idea of observer based residual generation is achieved by comparing measurements from the process with their estimations generated by observers [64]. Then, the weighted estimation error is used as a residual for the purpose of FDD [22]. The residual should be normally zero or close to zero when no fault is present, but it is distinguishably different from zero when a fault occurs. However, due to the presence of disturbance, noise, and model uncertainties, the residual also becomes a nonzero value. Thus, the ideal situation is that the residual is insensitive to noise, disturbance, and model uncertainties, but sensitive to faults. To isolate and identify faults, a bank

of state estimators are usually used where each one is sensitive to a particular fault and insensitive to others.

Observer based method has received high attention for the systems which can be described by ordinary differential equations (ODEs). Compared to the parity space method and parameter estimation method, the fault can be detected quickly. Besides, excitation signal, as well as supplemental conditions or assumptions are not needed. In addition, control engineers are more familiar with the concepts of observer design. In the past few decades, a number of results for observer design have been presented, details are described in Section 4.

(2) Parity space approach

Parity space approach was firstly developed in the early 1980s. The basic idea of the parity space approach is to provide a proper check of the parity (consistency) of the measurements acquired from the monitored system, while the parity equations are derived from the system model or transformed version of the state space model. The parity relation approach can be applied to either time-domain state-space model or frequency-domain input-output model, which is well revisited by [22] [27]. Recently, the parity space method is extended for fault diagnosis for more complex models such as TS fuzzy nonlinear systems and fuzzy tree models, it is also applied to various industrial systems such as aircraft control surface actuators [94] and electromechanical brake systems [61].

Actually, parity space approach and observer based approach are similar as shown in [42] [98], and there exists a one-to-one mapping between the design parameters of observer and parity relation based residual generator. [27] presents two theorems that show how to calculate parity vector corresponding to observer based residual generator and vice versa. Thus, we can design a residual generator in parity space and transform the parity vector into diagnostic observer parameters for online implementation. The implementation of the parity relation based residual generator uses a non-recursive form, while the observer based residual generator represents a recursive form. Thus, it is usual to design in parity space and to realize in observer based structure.

(3) Parameter estimation approach

Parameter estimation approach is a method based on system identification techniques such as least squares (LS), recursive least squares (RLS), extended least squares (ELS), etc. In this approach, the faults are assumed to be reflected in system parameters, and only the model structure is needed to be known. Parameters are firstly estimated on-line by using the input and the output of the system. Then, the estimated parameters are compared with the parameters of the reference model obtained

in fault free condition. If the estimation value deviates from its nominal value, then decisions about fault occurrence are made. This method is well reviewed in the early survey papers [62] [63]. Recent development of this approach can be found in [2] [30]. An advantage of the parameter estimation approach is that with only one input and one output signal, several parameters can be estimated which give a detailed picture on internal process quantities [63]. Another advantage of the method is that it yields the size of the deviations which is important for fault analysis [43]. Parameter estimation based approach is useful for component fault detection, although it can also detect sensor and actuator faults. A disadvantage is that excitation is always needed in order to estimate the parameters that can cause problems if the process is operating at stationary points [43].

As demonstrated in [48], there is a close relationship between the parameter identification based fault detection approach and the observer based fault detection approach. Compared to observer based and parity relation based methods, parameter estimation methods are more flexible in how faults can affect the system. Therefore, parameter estimation methods are more suitable for multiplicative faults detection, especially for multiplicative component fault detection.

Residual evaluation method

Residual evaluation is the second step in a model-based FDD scheme. This is a decision making step that consists of performing appropriate statistical tests on the residuals generated in order to make a decision on the diagnosis of the fault. The proper scheme for residual evaluation plays a significant role in the satisfactory performance of the FDD scheme. For the system affected by unknown input such as disturbance, noise, and model uncertainties, residual evaluation should consider the trade-off between fast and reliable detection.

The residual evaluation block, shown in Figure 2.5, may perform a simple threshold test on the instantaneous values or moving averages of the residuals. On the other hand, it may consist of statistical methods, for example, hypothesis tests on mean, covariance, and whiteness, weighted sum-squared residual (WSSR) test, sequential probability ratio test (SPRT), cumulative sum (CUSUM), generalized likelihood ratio (GLR) test, multiple hypothesis test (MHT). Besides, residual evaluation can be finished by neural network approach and fuzzy logic symptom method [9] [76].

2.2.2 Signal-based approaches

Signal-based methods utilize measured signals rather than explicit input-output models for fault diagnosis. The faults in the process are reflected in the measured signals, whose features are extracted and a diagnostic decision is then made based on the symptom analysis and prior knowledge on the symptoms of the health systems. The schematic diagram is illustrated in Figure. 2.6 to show its methodology.

The feature signals to be extracted for symptom (or pattern) analysis can be either time-domain (e.g., mean, trends, standard deviation, phases, slope, and magnitudes such as peak and root mean square) or frequency-domain (e.g., spectrum). Therefore, signal-based fault diagnosis methods can be classified into time-domain signal-based approach, frequency-domain signal-based approach, and time-frequency signal-based approach.

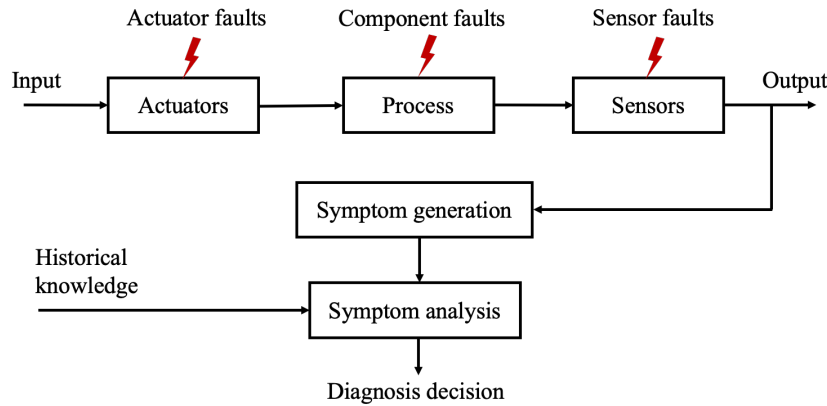


Figure 2.6: Schematic diagram of signal-based fault diagnosis

Time-domain signal-based method

For a continuous dynamical process to be monitored, it is natural to extract time-domain features for fault diagnosis. Thus, time-domain signal-based fault diagnosis utilizes time-domain parameters reflecting component failures such as root-mean-square [21], slope and kurtosis [57] straightforwardly to monitor the dynamics. Besides, the statistical method is also used for the sensor abrupt faults detection in [101], where the covariance of the sensing signals was used for feature extraction.

Different from the approaches for FDD using features of the measured signal in one-dimension domain, a two-dimension signal-based method was proposed in [25], where the vibration signal was translated into an image (two dimensions), and the local features were then extracted from the image using scale invariant feature transform (SIFT)

for FDD under a pattern classification framework. Very recently, a two-dimension approach was reported in [102] for fault diagnosis of induction motors, where time-domain vibration signals acquired from the operating motor were firstly converted into two-dimension gray-scale images, and the discriminating texture features were then extracted from these images utilizing local binary patterns (LBP) technique.

Frequency-domain signal-based method

Frequency-domain signal-based fault diagnosis employs a variety of spectrum analysis tools, such as discrete Fourier transformation (DFT) which can be computed by fast Fourier transformation (FFT) [128] to convert a time-domain waveform into its frequency-domain equivalence for monitoring the systems. One of the most powerful frequency-domain methods for diagnosing motor faults is motor-current signature analysis (MCSA), which utilizes the spectral analysis of the stator current to sense rotor faults associated with broken rotor bars and mechanical balance. Without requiring access to the motor, the MCSA approach has received much attention, which was well reviewed in [11] [92]. Recent development of current based spectrum signature analysis for fault diagnosis can be found in [51] [71].

Time-frequency domain signal-based method

When the measured signals are transient and dynamic under the concerned time section, it is difficult to monitor or detect faults via either a pure time-domain or frequency-domain method. Therefore, time-frequency analysis, which can identify the signal frequency component, and reveal their time variant features, becomes an effective tool for monitoring and fault diagnosis by extracting feature information contained in non-stationary signals. Among the time-frequency methods, short-time Fourier transform (STFT), wavelet transforms (WT), Hilbert-Huang transform (HHT), and Wigner-Ville distribution (WVD) are the most commonly used approaches. For instance, STFT method allows determining signal frequency contents of local sections as the signal changes in time [91]. WT based method can provide a good resolution in time for high-frequency components of a signal and a good resolution in frequency for low-frequency components [53]. Compared to STFT and WT, the HHT method is not constrained by the uncertain limitations, and therefore has shown quite interesting performance in terms of fault severity evaluation [126]. Among the presented methods, the WVD method features a relatively low computational cost and high resolution [110].

2.2.3 Knowledge-based approaches

In contrast to model-based and signal-based diagnosis requiring either mathematical models or extracted signal patterns, a knowledge-based approach relies on a large volume of historic data available to train universal approximations in order to recognize faulty patterns. The underlying knowledge, which implicitly represents the dependency of the variables of the system, is extracted by applying a variety of artificial intelligence techniques to the available historic data. The consistency between the behavior of the operating system and the knowledge base is then checked, and a fault diagnosis decision is made with the help of classifier. The schematic diagram of knowledge-based fault diagnosis is shown in Figure 2.7.

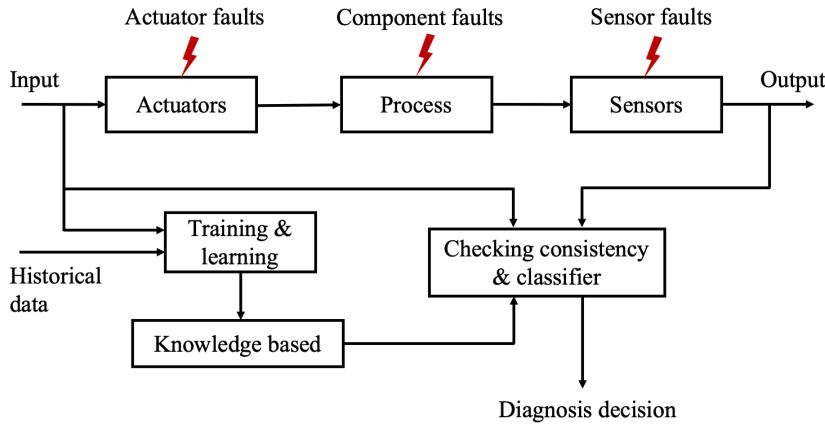


Figure 2.7: Schematic diagram of knowledge-based fault diagnosis

Knowledge-based methods, as well as model-based methods and signal-based methods, have to use real-time data to monitor the operating system and to do online fault diagnosis decisions. However, the knowledge-based approach is the only scheme that needs to employ a large volume of historical data. From this point of view, the knowledge-based method is also referred to data-driven method. The extraction process of the knowledge base can be either qualitative or quantitative. Therefore, knowledge-based fault diagnosis methods can be classified into qualitative methods and quantitative methods.

Qualitative knowledge-based FD method

The expert system based method is one of the most known qualitative fault diagnosis methods. As a branch of artificial intelligence, the expert system emerged in the late 1960s, it is a rule-based system by presenting human's expertise in a set of rules

[26]. The expert system based fault diagnosis was initialized in the 1980s, which was performed based on the evaluation of on-line monitored data in terms of a set of rules, learned by the human experts from experience. Until now, expert system FD methods are still widely used in different industrial systems [18] [32].

The qualitative trend analysis (QTA) method is also a popular data-driven technique to identify the process trends from noisy process data and to associate the extracted trends to fault trends in the database [120]. Recent developments of the QTA have been integrated with other qualitative tools such as signed directed graphs (SDG) to take advantage of the completeness property of SDG and the high diagnostic resolution property of QTA [31] [89].

Quantitative knowledge-based FD method

The quantitative knowledge-based method formulates the diagnostic problem-solving as a pattern recognition problem. Quantitative information (or features) can be either extracted by using statistical or non-statistical methods. Therefore, the quantitative knowledge-based fault diagnosis can be roughly classified into statistical analysis based fault diagnosis and nonstatistical analysis based fault diagnosis.

(1) Statistical-analysis data-driven fault diagnosis

Principle component analysis (PCA), partial least squares (PLS), independent component analysis (ICA), statistical pattern classifiers, and the most recent developed support vector machine (SVM), are commonly used statistical data-driven fault diagnosis techniques. An introduction of these methods and a comparison of their advantages have been shown in [127]. It is evident that the above methods require a large amount of training data to capture the key characteristics of the process by using statistical analysis.

PCA is the most popular statistically-based monitoring technique, which is utilized to find factors with a much lower dimension than the original data set so that the major trends in the original data set can be properly described. PLS is one of the dominant data-driven tools for complex industrial processes. The recent development of the PLS based monitoring and fault diagnosis can be found in [86]. Based on a further decomposition for the obtained PLS structure, an improved structure namely total projection to latent structures (T-PLS), was addressed in [124]. It can well detect quality-relevant faults in industrial processes subjected to a variety of raw materials and changeable control conditions. ICA plays an important role in real-time monitoring and diagnosis for practical industrial processes as it allows latent variables not to follow

Gaussian distribution [134]. Compare to other methods, SVM is a relatively new machine learning technique relying on statistical learning theory, which is capable of achieving high generalization and dealing with problems with low samples and high input features, as addressed in [123]. Associated with appropriate nonlinear kernels tested on the data set, statistical analysis-based methods can achieve more accurate and reliable identifications.

(2) Nonstatistical-analysis data-driven fault diagnosis

Owing to its powerful ability in nonlinear approximation and adaptive learning, neural network (NN) has been the most well-established non-statistical based data-driven fault diagnosis tool. By using unsupervised learning, the knowledge base can be extracted from the historical data to emulate normal system behaviour, which is utilized to check whether the behaviour of the real-time process deviates from the normal system behaviour. By using supervised learning, the knowledge bases for normal systems and faulty conditions are all extracted, which are then utilized for real-time monitoring. Recent developments of the NN can be found in a variety of real-time applications [122] [125].

Fuzzy logic (FL) is an approach of partitioning a feature space into fuzzy sets and utilizing fuzzy rules for reasoning, which essentially provides approximate human reasoning [136]. Recent development has shown an interest in adaptive Neuro-Fuzzy Inference System (ANFIS) to combine these two methods, such that better diagnosis performance can be achieved (e.g. [102]).

2.2.4 Hybrid approaches

Model-based, signal-based, and knowledge-based fault diagnosis methods have their distinctive advantages and various constraints. For instance, Model-based fault diagnosis has the capability to detect unknown types of faults and requires a small amount of online data. However, precise physical models are required. Signal-based approaches and knowledge-based approaches are independent of explicit mathematical models. Nevertheless, without considering system inputs, the performance of signal-based fault diagnosis can be degraded by extra disturbances. Knowledge-based approaches require a vast value of reliable historic data and can be time consuming. In order to leverage the strength of the various fault diagnosis methods, an integration or combination of two or more fault diagnosis methods, called hybrid fault diagnosis approaches, are often exploited for a variety of engineering applications. For example, in [54], signal-based method and data-driven method were hybridized to monitor and diagnose plastic bear-

ing faults. In [103], a hybrid data-driven and model-based fault diagnosis method are proposed for chemical reactors subjected to high nonlinearities and high variability of dynamics.

2.3 Fault tolerant control

A conventional feedback control design for a complex system may result in unsatisfactory performance, or even instability, in the event of malfunctions in actuators, sensors, or other system components. Even though FDD can detect and diagnose the fault when a fault occurs in the industrial system, the original control law, which performs well under fault free cases, cannot make the system maintain its expected performance anymore without the intervene of engineers. To overcome such weaknesses, new approaches to control system design have been developed in order to tolerate component malfunctions while maintaining desirable stability and performance properties. This is particularly important for safety-critical systems, such as aircraft, spacecraft, nuclear power plants, and chemical plants processing hazardous materials, because a minor fault in a system component can be catastrophic in such systems. Therefore, it is necessary to design control systems that are able to tolerate potential faults to improve reliability and availability while providing a desirable performance. These types of control systems are often known as fault tolerant control systems (FTCS).

According to its definition, a FTCS is a closed-loop control system that processes the ability to accommodate component failures automatically and maintain desirable performance and stability properties [16, 135]. More recently, FTC has attracted more and more attention in both industry and academic communities due to increased demands for safety, high system performance, productivity, and operating efficiency in a wider engineering application, not limited to traditional safety-critical systems. Several review papers and books on FTCS have been presented in [15–17, 69, 70, 84, 97, 135].

Generally, FTC can be achieved either passively by the use of a control law designed to be insensitive to some known faults, or actively by an FDI mechanism, and the redesign of a new control law. In a passive approach, once the control system is designed, it will remain fixed during the entire system operation. Contrary to the passive methods, active methods react to the system component failures actively by properly reconfiguring its control actions so that the stability/performance of the entire system can still be acceptable. To achieve a successful control system reconfiguration, this approach relies heavily on a real-time FDD scheme to supervise the behaviors of the

system and present detailed fault information.

2.3.1 Passive FTC

In the passive approach, the controllers are synthesized so that they are robust to certain faults. The main idea is to make the closed-loop system robust to uncertainties and a few specific faults and without the online use of fault information. This approach does not require any FDD scheme or any reconfiguration of the control law. Therefore, the term ‘passive’ indicates that no additional action needs to be taken by the existing control system in response to the design basis faults. As shown in Figure 2.8, a passive FTCS is a control system designed to tolerate system component faults by using the robust controller design. In the passive case, the faulty system continues to operate with the same controller and the same system structure: objectives and performance remain the same as those of the nominal system.

Several approaches have been used in designing passive FTC varies from sliding mode control (SMC) approach [5], adaptive control approach [77] to H_∞ control method [104], Linear Quadratic control [58], fuzzy logic control [129], Lyapunov-based control [12], and control allocation [59]. Such control strategies are commonly less complicated and are popular due to their simplicity in design and application, less lag between fault occurrence and accommodation, and their low computation load [38, 90].

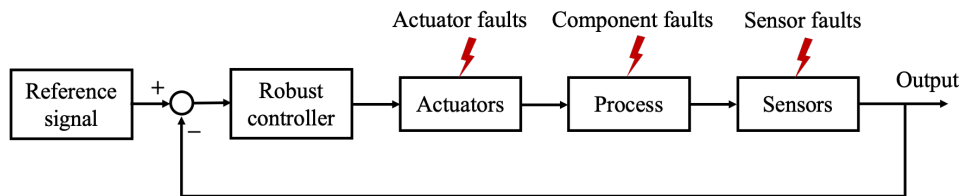


Figure 2.8: Architecture of the passive FTC

2.3.2 Active FTC

An active FTCS reacts to system component malfunctions (including actuators, processes, and sensors) by redesigning the controller based on the real-time information from a FDD scheme. The term ‘active’ represents corrective actions taken actively by the reconfiguration mechanism to adapt the control system in response to the detected system faults. As shown in Figure 2.9, an active FTCS typically consists of a FDD scheme, a redesignable controller, and a controller redesign mechanism. These three

units have to work in harmony to complete successful control tasks. Based on this architecture, the design objectives of an active FTC are:

- develop an effective FDD scheme (as presented in Section 2.2) to provide information about the fault with minimal uncertainties in a timely manner;
- redesign the existing control scheme effectively to achieve stability and acceptable closed-loop system performance;
- commission the reconstructed controller smoothly into the system by minimizing potential switching transients.

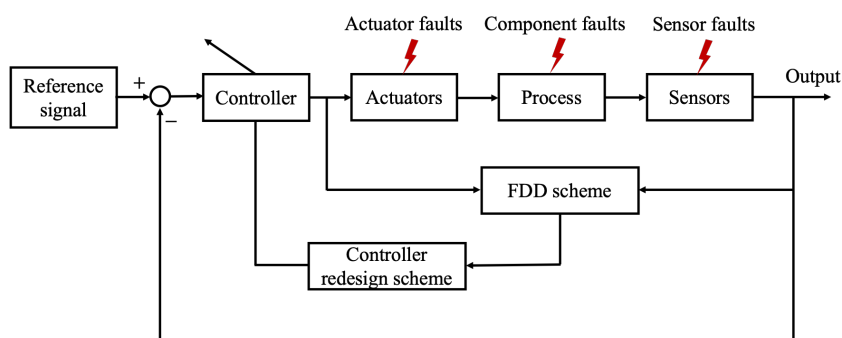


Figure 2.9: Architecture of the active FTC

Two principal ways of controller redesign have to be distinguished, which are fault accommodation and control reconfiguration [16]. Fault accommodation means adapting the controller parameters to the dynamical properties of the faulty plant. The input and output of the plant used in the control loop are not changed, just the same as for fault-free cases. For fault accommodation, one simple but well established way is based on a predesigned controller, each of which has been selected off-line for a specific fault. Then, the redesign step only needs to set the switch among the different laws. This step is quick and can meet strong real-time constraints. However, all possible faults should be considered before the system is put into operation and all resulting controllers have to be stored in the control software. Control reconfiguration is another way to redesign the controller, and it includes the selection of a new control configuration where alternative input and output signals are used. The necessity of control reconfiguration is particularly obvious if sensor or actuator failures are considered. If these components fail completely, the fault will lead to a break-down of the control loop, and there is no possibility to adapt the controller by simply changing its parameters to the faulty situation. Therefore, the control signal should be reconfigured to satisfy the performance of the closed-loop system.

In order to make the closed-loop system can match the reference model even in the presence of a fault, several redesign methods have been developed in [68, 84].

Pseudo-inverse method

The pseudo-inverse method [44] consists of modifying the control law by state feedback so that the dynamic of the failed closed-loop system is approximately equal to that of the nominal closed-loop system by minimizing a given criterion. The main drawback of this method lies in the fact that the optimal control law does not always guarantee the closed-loop stability of the faulty system. To overcome this problem, the modified pseudo-inverse method was developed in [45] by adding additional constraints such that the closed-loop system is stable.

Linear model-following method

The model-following method is an active FTC approach that allows designing a new control law so that the performance of the faulty system under control comes as close as possible to that of a reference model. Most of these methods have been developed for linear systems. For instance, the first one, the perfect model following method [108], uses stabilizing feedback with dynamic compensators. The second one, the adaptive model-following method [19], applies an adaptive feedback control algorithm consisting of state feedback, a reference prefilter and an affine term to the faulty plant. In the eigenstructure assignment method [75], the nominal eigenvalues and eigenvectors are recovered after a fault has occurred.

Multiple model method

The multiple model approach is attracting the attention of many researchers to solve the accommodation problem in nonlinear systems [99, 111]. Indeed, these techniques make it possible to control a nonlinear system over a large operating area broken down into several linearized areas around different operating points. Multiple model approaches deal with fault diagnosis problems in a way to avoid the complicated process of observer and controller design of the real system. However, complexities still exist in integrated controller design for sub-models, especially when the considered system is complex and highly nonlinear.

Optimal control method

Optimal control methods such as linear quadratic (LQ) optimal control, model predictive control (MPC) can also be used for the controller redesign. The basic idea of LQ optimal control is to design a linear time-invariant controller off-line using LQ-optimal design according to the optimization goal. After a fault is identified, a new controller is designed by recalculating the state feedback of the faulty plant and the nominal weights. The main drawback of this method lies in completely discarding the nominal controller. LQ regulator design was used in [82], and more recently in [109].

Model predictive control (MPC) is capable of solving the reconfiguration problem with little extra effort compared with control of the nominal plant [44, 54]. A basic model predictive control scheme generates at each discrete time step an optimal sequence of control inputs for the control horizon with respect to the predicted output error trajectory. The input is calculated to minimize a cost function. To achieve control reconfiguration after fault identification, the internal plant model of the MPC is updated to reflect the faults. Developments on MPC are presented in [85] [66].

2.4 Summary

This chapter introduced the state of arts of the existing FDD and FTC scheme. Definitions of elementary nomenclature such as fault and failure are firstly provided. Different types of faults are then presented from various points of view. Moreover, a classification of FDD (model-based approach, signal-based approach, knowledge-based approach, and hybrid approach) and FTC (passive FTC and active FTC) schemes were presented with the description of each approach.

Chapter 3

Modeling of the Heat-exchanger/Reactor

For the model-based FDD methods, a known mathematical model of the whole process is indispensable. In this chapter, we present the modeling process of an intensified heat-exchanger (HEX) /reactor. First of all, the physical structure of the HEX reactor is briefly introduced. According to its physical structure, this HEX reactor consists of three parts: process plate, utility plate, and plate wall. And then, a cell-based modeling scheme is presented. The HEX reactor is divided into numbers of cells according to its physical structure. And then, the mathematical equations corresponding to each cell are presented.

3.1 Introduction

With the development of process intensification [35] [52] [107] in chemical industries, traditional batch chemical reactors is gradually replaced by novel reactors which combine two or more traditional operations in one hybrid unit. Poor heat exchanging performances of discontinuous reactors may cause the degradation of safety and productivity in whole processes. Therefore, develop new devices based on the coupling of high heat transfer behavior and good mixing performances has been an increasing interest. As a consequence, an intensified HEX reactor, which combines heat-exchanger and chemical reactor together, is developed by French laboratory LGC (Laboratoire de Génie Chimique à Toulouse) in the frame of the RAPIC project [7]. This HEX reactor presents a strong ability of heat and mass transfer and good thermal and hydrodynamic performances [6].

3.2 Physical structure

Based on the concept of plate heat-exchanger in a modular block, the HEX reactor consists of three process plates sandwiched between four utility plates. The process plates, as well as the utility plates, have been engraved by laser machining to obtain 2 mm square cross-section channels. Process and utility channels are presented in 3.1 (a) and (b). Chemical reactions are taken place in process channel, where the single channel offers the longest possible residence time for reactants. Utility fluid (usually is water) flows in parallel zigzag-type channels so as to bring in or take reaction heat away as soon as possible.

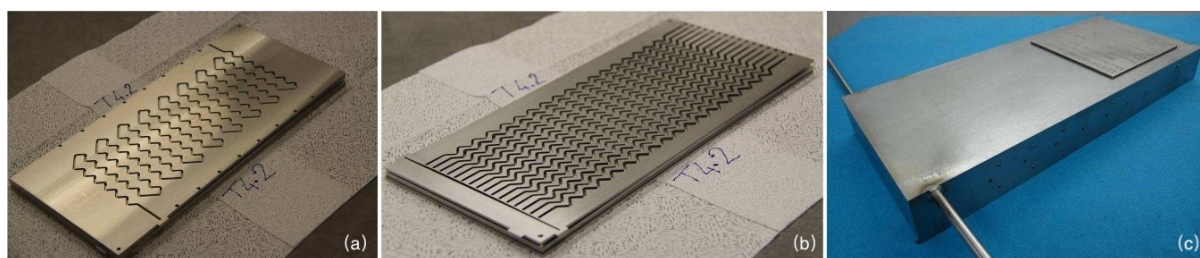


Figure 3.1: Physical structure of the heat exchanger/reactor: (a) Process channel; (b) utility channel; (c) the heat exchanger/reactor after assembly

The reactor material is 316L stainless steel and the different plates have been assembled by hot isostatic pressing (HIP) [7] [115] [116]. After assembly, the reactor has a 32 cm height, a 14 cm width, a 3.26 cm thickness, and a mass of 10.84 kg, which makes

it a very compact HEX reactor. Geometrical parameters such as curvature radius, the straight length between two bends, aspect ratio, and bend angle, which have a great impact on the thermal performances, residence time, and pressure drop distribution, have been studied at lab-scale. More details are described in a previous paper dedicated to the experimental study of the reactor [8].

3.3 Modeling

3.3.1 General Modeling of the Reactor

Figure 3.2 shows a realistic description based on a modular structure of the HEX reactor, it also presents the flow configuration of two different fluids, process fluid, and utility fluid. Three kinds of plates, process plate, utility plate, and plate wall, are represented in different colors, red, blue, and grey, respectively. Two (or several) feeding lines, R1 and R2, ensure that reactants could be introduced in the reactor. Two loops, process fluid, and utility fluid, are in charge of reacting and cooling/heating, respectively. Arrows indicate the inner flow directions of the process fluid and utility fluid.

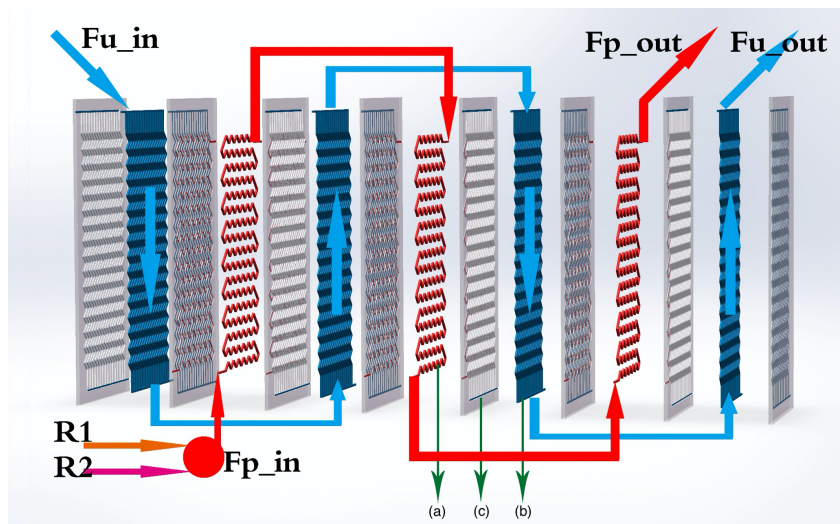


Figure 3.2: Block modeling description, showing (a) process plate, (b) utility plate, and (c) plate wall

The HEX reactor operates as a plug-flow reactor, thus, its modeling is based on the same hypothesis as the one used for the modeling of real continuous reactors [93], which is represented by a series of perfectly stirred tank reactors (called cells). The number of cells is generally defined by the requirement of accuracy. More cells are defined,

the more accurate model we will have, but the calculation cost also increases with the increase of cell numbers. Therefore, in order to find a balance between model accuracy and calculation cost, a modeling scheme that is based on the geometry and physical structure of the process channel is used. As shown in Figure 3.2, there are 17 horizontal lines in each process place, so, 17 computing units are defined, as presented in Figure 3.3. In each unit, there are 15 cells: 3 process cells, 4 utility cells, and 8 plate wall cells, see Figure 3.4. Therefore, the HEX reactor considered in this paper was divided into 255 cells in total. The reaction heat is generated in each process cell, and we assume that the convective heat exchange (bi-directional arrows in Figure 3.4) mainly occurs between neighboring cells in the horizontal direction inside one computing unit. In the vertical direction, it is the fluids inside process channels and utility channels that transfer the heat. Besides, the far-right plate wall, as well as the far-left one is assumed adiabatic since they are covered by low heat transfer materials.

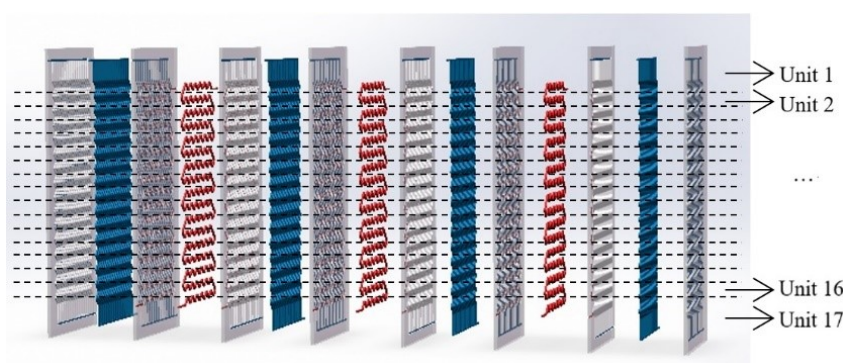


Figure 3.3: Structure of units dividing

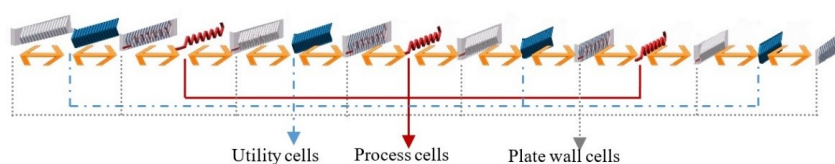


Figure 3.4: Internal description of one computing unit and convective heat exchange

Therefore, the flow configurations of the reactor (co-current, counter-current) are clearly represented. In such a way, the behavior of a cell only depends on the inlet streams and phenomena taking place inside, such as chemical reaction, heat transfer, etc. And for a given cell, its inlets are exactly the outlets of the preceding one. Thus, the configuration of flows can be represented by correct discretization. In addition, this modeling scheme can be easily applied to any HEX reactor by adjusting the corresponding plate number and cell number in the plate.

For each cell, the expression of mass balance, energy balance, and constraint equations are the foundation of the modeling procedure. The constraint equations concern the geometric characteristics of the reactor and the physical properties of the medium mentioned. The relations which concern temperature, mass composition, etc. are described by the balance equation below:

$$\left\{ \begin{array}{c} \textit{Accumulation} \\ \textit{flow} \end{array} \right\} = \left\{ \textit{Inlet} \right\} - \left\{ \textit{Outlet} \right\} + \left\{ \begin{array}{c} \textit{Production} \\ \textit{flow} \end{array} \right\} \quad (3.1)$$

The HEX reactor mentioned in this paper has three main parts, process plate, utility plate, and plate wall. Among these three parts, the process plate is the most complex part, because we should consider both heat transfers and hydrodynamics, especially the hydrodynamics coupled with reactions when chemical reactions are considered. The modeling of utility plate will be the same as that of process plate as long as chemical reactions are not considered. For the rest plate wall, only heat transfer aspect is concerned.

3.3.2 Modeling of process plate

The process plate is sandwiched between two plate walls (right and left), so each process cell is also sandwiched by two plate wall cells. Assume that each process cell is filled with a perfectly stirred homogeneous medium which is homogeneous in characteristic values (temperature, flow rate, composition, etc.), physical properties (density, viscosity, etc.), and chemical phenomena (mixing, reaction, etc.). Besides, the volume of the fluid (reactants) mixture is invariable.

According to the energy balance (W) inside process cell k , the mathematical expression of process cell can be expressed as:

$$\rho_p^k V_p^k C_{p,p}^k \frac{dT_p^k}{dt} = F_p^k \rho_p^k C_{p,p}^k (T_p^{k-1} - T_p^k) + \Delta q_p^k \times V_p^k + h_p^k A_p^k (T_{wL}^k - T_p^k) + h_p^k A_p^k (T_{wR}^k - T_p^k) \quad (3.2)$$

where $\rho_p^k (kg \cdot m^{-3})$, $V_p^k (m^3)$ and $C_{p,p}^k (J \cdot kg^{-1} \cdot K^{-1})$ are density, volume and specific heat of material in process plate cell k , respectively; $F_p^k (m^3 \cdot s^{-1})$ is volume flow rate in process plate cell k ; $T_p^k (K)$ is temperature in process plate cell k ; $\Delta q_p^k (W \cdot m^{-3})$ denotes heat generated by the reactions in process plate cell k ; $h_p^k (W \cdot m^{-2} \cdot K^{-2})$ and $A_p^k (m^2)$ represent heat transfer coefficient and area between process plate and plate wall for cell k , respectively; and $T_{wL}^k (K)$ and $T_{wR}^k (K)$ are temperatures of left and right plate wall cells of the targeting cell k .

3.3.3 Modeling of utility plate and plate wall

To represent the reactor structure precisely, all the different heat transfer zones must be considered. Therefore, elements involved in the heat balance described by the model are utility plate and plate wall. But we should pay attention that, there are two kinds of plate wall, one is the plate wall sandwiched between the process plate and utility plate, the other is the two far-left and far-right plate wall that only have contact with utility process in one side. And these two special pieces are called adiabatic plates because we assume that there is no heat exchange between the reactor and environment.

As shown in Figure 3.4, a utility plate cell is sandwiched between two plate wall cells (right and left), and the description of heat transfer based on energy balance of utility fluid (W) is as follows:

$$\rho_u^k V_u^k C_{p,u}^k \frac{dT_u^k}{dt} = F_u^k \rho_u^k C_p u^k (T_u^{k-1} - T_u^k) + h_u^k A_u^k (T_{wL}^k - T_u^k) + h_u^k A_u^k (T_{wR}^k - T_u^k) \quad (3.3)$$

where $\rho_u^k (kg \cdot m^{-3})$, $V_u^k (m^3)$ and $C_{p,u}^k (J \cdot kg^{-1} \cdot K^{-1})$ are density, volume, and specific heat of material in utility plate cell k respectively; $F_u^k (m^3 \cdot s^{-1})$ is volume flow rate in utility plate cell k ; $T_u^k (K)$ is temperature in utility plate cell k ; $h_u^k (W \cdot m^{-2} \cdot K^{-1})$ and $A_u^k (m^2)$ represent heat transfer coefficient and area between utility plate and plate wall for cell k , respectively.

A plate wall cell (except the adiabatic plate) is always sandwiched between a process plate cell and a utility plate cell, between which only heat transfer is considered, as presented in Figure 3.4.

Energy balance on the plate wall (W):

$$\rho_w^k V_w^k C_{p,w}^k \frac{dT_w^k}{dt} = h_p^k A_p^k (T_p^k - T_w^k) + h_u^k A_u^k (T_u^k - T_w^k) \quad (3.4)$$

where $\rho_w^k (kg \cdot m^{-3})$, $V_w^k (m^3)$ and $C_{p,w}^k (J \cdot kg^{-1} \cdot K^{-1})$ are density, volume, and specific heat of plate wall cell k respectively; $T_w^k (K)$ is temperature of plate wall cell k .

Adiabatic plates assembled on both sides of the HEX reactor are special plate walls, for which heat transfer is taking place between utility plate and environment. However, in our case, it is assumed that the adiabatic plates are heat-insulated, i.e. there is no heat transfer between adiabatic plates and the environment.

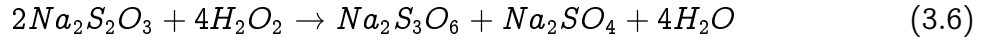
Energy balance on the adiabatic plate (W):

$$\rho_w^k V_w^k C_{p,w}^k \frac{dT_w^k}{dt} = h_u^k A_u^k (T_u^k - T_w^k) \quad (3.5)$$

According to the energy balance and mass balance, the mathematical model of each cell has been clearly expressed. Then, these cells are connected to construct the model of the HEX reactor.

3.3.4 Reaction modeling

To improve the mathematical modeling of the HEX reactor, chemical reactions must be considered. In [112], experiments were carried out step by step. First, only water is injected into both process channel and utility channel to verify the thermal description of the reactor. And then, the reaction of sodium thiosulfate oxidation by hydrogen peroxide is carried out in the reactor in the second step. The reaction takes place in a homogeneous liquid phase and shows the following characteristics: irreversibility, fast kinetics, and very strong exothermicity. These features make it an ideal example for validation of the thermal and kinetic aspects of the HEX reactor and its model. So, the following part gives the modeling information when this reaction is considered.



As the reaction goes, the concentrations of the reactants (C_i^k) gradually decrease, and this decrease of reactant concentration indicates the speed of the reaction. Therefore, the production rate of a given constituent (Δn_i^k), the total production rate (Δn^k), and the heat generated (Δq^k) by this reaction can be estimated according to the known reaction speed.

These estimations, which are used within the mass and energy balance of the cell, are based on the following relations:

The production rate of constituent i in cell k :

$$\Delta n^k = \sum \tau_i r^k \quad (3.7)$$

where τ_i represents stoichiometric coefficient of constituent i in the given reaction.

Total production rate:

$$\Delta n^k = \sum_i \Delta n_i^k \quad (3.8)$$

Heat generated:

$$\Delta q^k = \sum (\Delta Hr \times r^k) \quad (3.9)$$

where ΔHr is the heat of the given reaction ($J \cdot mol^{-1}$).

In our case, the kinetic constant of the reaction is assumed to be governed by an Arrhenius law, which makes it possible to estimate the evolution of the constant as a function of temperature:

$$k_c = k_c^0 \exp\left(-\frac{E^a}{RT}\right) \quad (3.10)$$

where k_c^0 ($m^3 \cdot mol^{-1} \cdot s^{-1}$) is the pre-exponential factor; E^a ($J \cdot mol^{-1}$) is activation energy; and R ($J \cdot mol^{-1} \cdot K^{-1}$) is the perfect gas constant. Each chemical reaction has

Table 3.1: Characteristics of the reaction of sodium thiosulfate oxidation by hydrogen peroxide [6]

Item	Value
heat of reaction ΔHr ($J \cdot mol^{-1}$)	-5.86×10^5
pre-exponential factor k_c^0 ($m^3 \cdot mol^{-1} \cdot s^{-1}$)	8.13×10^8
activation energy E^a ($J \cdot mol^{-1}$)	7.6123×10^4
perfect gas constant R ($J \cdot mol^{-1} \cdot K^{-1}$)	8.314

its corresponding pre-exponential factor and activation energy. For the reaction of sodium thiosulfate oxidation by hydrogen peroxide, these values are presented in Table 3.1.

Considering the stoichiometric scheme of the reactions and Equations (3.7) to (3.10), the concentration of each reactant in a cell behaves according to the following relationships:

$$\frac{dC_{Na_2S_2O_3}^k}{dt} = \frac{F_{Na_2S_2O_3}}{V_p^k} C_{Na_2S_2O_3}^{k-1} - \frac{F_{Na_2S_2O_3}}{V_p^k} C_{Na_2S_2O_3}^k - 2r^k \quad (3.11)$$

$$\frac{dC_{H_2O_2}^k}{dt} = \frac{F_{H_2O_2}}{V_p^k} C_{H_2O_2}^{k-1} - \frac{F_{H_2O_2}}{V_p^k} C_{H_2O_2}^k - 4r^k \quad (3.12)$$

where $C_{Na_2S_2O_3}^k$ and $C_{H_2O_2}^k$ ($mol \cdot m^{-3}$) are the concentrations of $Na_2S_2O_3$ and H_2O_2 in process cell k , respectively; and r^k is the speed of the reaction taking place in cell k . It is expressed as a function of the concentrations of the reactants, as follows:

$$r^k = k_c C_{Na_2S_2O_3}^k C_{H_2O_2}^k \quad (3.13)$$

where k_c ($m^3 \cdot mol^{-1} \cdot s^{-1}$) is the kinetic constant of the reaction and is given in Equation (3.10).

3.3.5 Simulation result

The system was modeled and simulated in Simulink. As described before, it is composed of 17 units, in each unit, there are three plate cells, four utility cells, and eight plate wall cells. Every cell is named as a calculation module, and it is expressed by several hybrid differential and algebraic equations (DAE). For example, mass balance, and energy balance are expressed by ordinary differential equations (ODE) (3.2) (3.3) (3.4) (3.5), while constraints and physical properties of the reactor are expressed by algebraic equation (AE). Different equations are applied to express the behaviors of

different cells, for instance, the process plate cells should consider both mass and energy balance equations to evaluate the temperature and concentration of the fluid, and energy balance equations are enough to express the utility cells and plate wall cells.

During the modeling process, the order of connection is restricted to that presented in Figure 3.2 and Figure 3.3, the order of units is in the vertical direction, while the order of cells in one given unit is in the horizontal direction. These connections maximize the heat transfer efficiency, it makes the heat generated by reactions can be rapidly taken away by utility fluid. According to the manner of the connection, heat exchange mostly takes place in the horizontal direction, i.e. between different kinds of cells inside a unit, and in the vertical direction, the heat is transferred by the flowing of fluid.

In order to investigate the accuracy of the model proposed in this chapter, the same situations as in [112] are used in the simulations. And the chemical reaction of sodium thiosulfate oxidation by hydrogen peroxide is considered. Firstly, by injecting water into both channels, the reactor reaches a balanced state for the heat exchange procedure without reaction. Then, reactants (sodium thiosulfate $Na_2S_2O_3$ and hydrogen peroxide H_2O_2 with a concentration of 9% in mass) are injected into the reactor and the reaction begins.

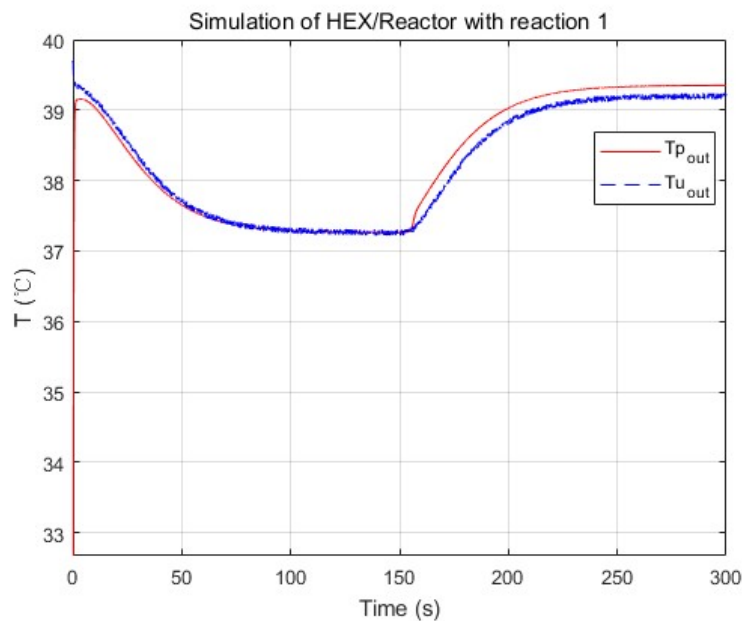


Figure 3.5: Simulated temperature profiles for experiment 1 (reaction was introduced at 150 s)

The dynamic procedure of the simulation with reaction is shown in Figure 3.5. As

described before, water is injected into both process channel (with the flow rate of $F_p = 14 \text{ L} \cdot \text{h}^{-1}$ at temperature $T_{p,in} = 17.6 \text{ }^\circ\text{C}$) and utility channel (with the flow rate of $F_u = 113 \text{ L} \cdot \text{h}^{-1}$ at temperature $T_{u,in} = 39.7 \text{ }^\circ\text{C}$) until the reactor reaches a steady state (at about 100 s). Then, reactants are introduced at time $t = 100 \text{ s}$ with the same temperature $T_{p,in} = 17.6 \text{ }^\circ\text{C}$ as before. The flow rate of the reactants sodium thiosulfate $\text{Na}_2\text{S}_2\text{O}_3$ and hydrogen peroxide H_2O_2 are $F_{p1} = 9.3 \text{ L} \cdot \text{h}^{-1}$ and $F_{p2} = 4.7 \text{ L} \cdot \text{h}^{-1}$, respectively. At the same time, the utility fluid keeps injecting with the flow rate of $F_u = 113 \text{ L} \cdot \text{h}^{-1}$ at $39.7 \text{ }^\circ\text{C}$. After a residence time, the output temperature starts to increase because of the heat generated by the reaction. And this trend is consistent with the experiment presented in Figure 16 of [112].

More simulation results and the comparison between simulation and experimental data are presented in [55]. The comparison is lunched by two steps, which is the same as that in real case [112]. First, only heat exchange part is considered, i.e. only water is used for both process channel and utility channel to verify the heat transfer procedure. At the second step, the reaction of sodium thiosulfate oxidation by hydrogen peroxide is carried out to the constructed model.

Overall, from the comparisons between experiments and simulations in each step, it could be deduced that the model proposed in this paper is generally valid to the HEX reactor for both the heat exchange and reaction parts.

3.4 Summary

This chapter presents the modeling process of the intensified HEX reactor. First of all, the physical structure of the HEX reactor is introduced. Due to its physical structure, the continuous process is discretized into cells. Consequently, each cell is expressed by mathematical equations according to the properties of heat exchange, fluid movement, and chemical reaction. In the following step, the cell-based HEX reactor model is constructed in the general simulation platform Matlab/Simulink. The dynamic of the proposed model obtained by simulation is shortly presented when the chemical reaction is considered. Detailed comparisons between simulation and experimental data are presented in [55], and the simulation results are quite consistent with the experiments.

The purpose of modeling the HEX reactor is for further control use. With the developed model, internal states are easily obtained by simulation. In the following chapter, controller and model-based observer are designed for the proposed model to diagnose and tolerant the possible faults.

Chapter 4

Observer based FDD schemes and their applications for the Heat-exchanger/Reactor

In this chapter, two kinds of observer based FDD schemes are presented and applied to the intensified HEX reactor. First, an overview of the recent nonlinear observers is introduced. Then, some special forms of system representation and basic properties of nonlinear systems are presented. Besides, the mathematical expression of the dynamic and sensor faulty model is also given. In the following, we introduce the structure of two kinds of observers, adaptive observer, and interval observer, which focus not only on the internal states but also on the system parameters. The FDD schemes based on these two observers are also presented. Moreover, the intensified HEX reactor presented in Section 3 is used to validate the effectiveness of the FDD schemes. Both dynamic fault and sensor fault are considered in this chapter.

4.1 Introduction

In general, for a given system, we cannot use as many sensors as signals of interest characterizing the system behavior (for cost reasons, technological constraints, etc.). The only quantities accessible to the system are the input and output variables in most cases, but they are not enough for the modeling (identification) monitoring (fault detection), or driving (control) of the system. Therefore, there is a need for internal information to keep the given system under control. The state observers, which use the structure of the real system and a minimum set of measurements, are then constructed to provide the estimation of the actual states of the system in real time. As presented in Figure 4.1, observer acts as the heart of a general control problem [14].

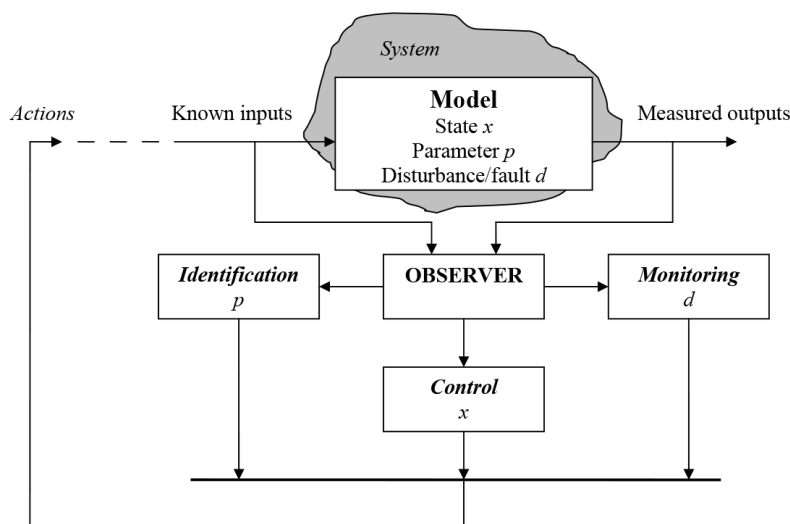


Figure 4.1: Observer as the heart of control systems [14]

4.2 Classification of nonlinear observers

Luenberger [83] and Kalman [72] introduced the basic concepts of state observers and Kalman Filter (KF) in the 1960s, and then, research in the design of observers has become popular over the years. Survey papers such as [3] [29] [37] [78] has reviewed the developed observers in linear and nonlinear systems since the year 2000. Due to the variety of methodologies in observer design for nonlinear systems, combining and classifying them into several different groups would be highly useful to serve as guidelines to select and then design the appropriate observers for a specific application. In [3], observers are classified into six major classes based on the review of the recent

observers applied to chemical process systems. These classes are the Luenberger-based observers, finite-dimensional system observers, Bayesian estimators, disturbances and fault detection observers, artificial intelligence-based observers, and hybrid observers. Table 4.1 sorts the specific observers into their respective classes.

Table 4.1: Recent observers categorized under different classes

<i>Class</i>					
Luenberger-based observers	Finite-dimensional system observers	Bayesian estimators	Disturbance and fault detection observers	Artificial intelligence-based observers	Hybrid observers
<i>Specific observer</i>					
1. Extended Luenberger observer		1. Particle filter	1. Disturbance observer		1. Extended Luenberger-asymptotic observer
2. Sliding mode observer		2. Extended Kalman filter	2. Modified disturbance observer		2. Proportional-integral observer
3. Adaptive observer	1. Reduced-order observer	3. Unscented Kalman filter	3. Fractional-order disturbance observer	1. Fuzzy Kalman filter	3. Proportional-SMO observer
4. High gain observer	2. Low-order observer	4. Ensemble Kalman filter	4. Bode-ideal cut-off observer	2. Augmented fuzzy Kalman filter	4. Continuous-discrete observer
5. Zeitz nonlinear observer	3. High gain observer	5. Steady state Kalman filter	5. Unknown input observer	3. Differential neural network observer	5. Continuous-discrete-interval observer
6. Discrete-time nonlinear recursive observer	4. Asymptotic observer	6. Adaptive fading Kalman filtering	6. Nonlinear unknown input observer	4. EKF with neural network model	6. Continuous-discrete-EKF
7. Geometric observer	5. Exponential observer	7. Moving horizon estimator	7. Extended unknown input observer		7. Continuous-discrete-high gain observer
8. Backstepping observer	6. Integral observer	8. Generic observer	8. Modified proportional observer		
	7. Interval observer	9. Specific observer			

The first category is the Luenberger-based observers, which involves the extended versions of the classical Luenberger observer itself [29]. This type of observer is famous for its simple computation, but it is always based on the perfect knowledge of system parameters. It is useful for crucial state and parameter estimation.

The category of finite-dimensional system observers is the second class. They have simple formulation and are easily implemented to the system with less kinetic information. However, the accuracy of the convergence rate is uncertain. It is worth noting that asymptotic/exponential and interval observers can also be extended to infinite dimensional systems (i.e., distributed parameter systems) such as for tubular reactors and plug flow reactors [28].

The third category is the Bayesian estimators [36], which uses probability distribution and mathematical inference of the system. Internal states can be estimated rapidly based on the prediction-correction method and versatile estimators. But the complexity of their computational method is sometimes infeasible for high dimensional systems.

The fourth class is the disturbance and fault detection observers, which are mostly applied to estimate irregularities in the system, either through disturbances or faults [95]. Examples of disturbance and fault detection observers are the disturbance ob-

server (DOB), the modified disturbance observer (MDOB), the unknown input observer (UIO), and the nonlinear unknown input observer (NUIO). These are highly specific types of observers and focus only on disturbances or fault detection related variables during the estimation process.

The fifth category is the artificial intelligence (AI)-based observers [96] [105], which is based on AI technologies such as fuzzy logic, artificial neural networks (ANN), expert systems are genetic algorithms. AI-based observers can overcome the limitations of single observers and are suitable for systems with incomplete model structures and information. However, it may be difficult and time consuming for online implementation compared to other hybrid observers in some systems.

The sixth class is the hybrid observers that combine more than one observer to obtain improved estimation results. For example, the combination of extended Luenberger observer and asymptotic observer in [60], the combination of fuzzy logic and sliding mode observer in [4]. Normally, this class of observer is suitable for conditions where the single observer is not accurate enough for the process systems.

The author of [3] also gives the detailed applications of various observers under these six classes and the general guideline for selecting observers. In our case, the principles of observer selection are easy implementation and less complex computation.

A great number of work concerning the development of observers for all types of systems has been carried out since the founding work of Luenberger and the model-based FDI has benefited from this. For linear systems, the first case corresponds to the Luenberger observers [83], in the deterministic framework, for linear time invariant (LTI) systems. While the second concerns the Kalman observers [72], in the stochastic framework, for the linear time variant (LTV) systems. For nonlinear systems, as presented in the former section, the structure of observers varies a lot. Some of them are based on the linearization of the model, some of them are based on the probability distribution theory, and some of them are based on the artificial intelligent algorithm. In the following part, different structures of observers are presented for linear and nonlinear systems.

4.3 Nonlinear model under consideration

Systems can be classified into three categories: continuous time systems, discrete systems, and hybrid systems. In this chapter, we will focus on the first one, continuous time systems. For continuous systems, the model of the dynamic systems can be linear

or nonlinear systems [100]. In chemical engineering, most of the systems are nonlinear. So, we will investigate the mathematical expression of the nonlinear system and its properties.

4.3.1 Expressions of nonlinear system

The system under consideration can be described by a state-space representation generally of the following form:

$$\begin{cases} \dot{x}(t) = f(x(t), u(t)) \\ y(t) = h(x(t), u(t)) \end{cases} \quad (4.1)$$

where x is the state vector ($x \in X \subset \mathcal{R}^n$), u is the external input vector ($u \in U \subset \mathcal{R}^m$), y is the measured output vector ($y \in Y \subset \mathcal{R}^p$). Functions $f(\cdot)$ and $h(\cdot)$ are assumed to be C^∞ [14].

Generally, the dynamics might explicitly depend on time via $f(x(t), u(t), t)$, while y might further directly depend on input u and even time t , via $h(x(t), u(t), t)$. Such an explicitly time-dependent system is usually called 'time-varying' and generalizes (4.1) into:

$$\begin{cases} \dot{x}(t) = f(x(t), u(t), t) \\ y(t) = h(x(t), u(t), t) \end{cases} \quad (4.2)$$

As described in [14], an observer can be defined as follows:

Definition 4.1 (Observer):

Considering a system 4.1, an observer is given by an auxiliary system:

$$\dot{\hat{x}}(t) = f(\hat{x}(t), u(t)) + k(t, h(\hat{x}(t)) - y(t)), \quad \text{with } k(t, 0) = 0 \quad (4.3)$$

such that:

- (i) $\hat{x}(0) = x(0) \Rightarrow \hat{x}(t) = x(t), \quad \forall t \geq 0;$
- (ii) $\|\hat{x}(t) - x(t)\| \rightarrow 0$ as $t \rightarrow \infty;$

If (ii) holds for any $x(0), \hat{x}(0)$, the observer is global.

If (ii) holds with exponential convergence, the observer is exponential.

If (ii) holds with a convergence rate which can be tuned, the observer is tunable.

where \hat{x} represents the estimated state vector, $k(\cdot)$ is called observer gain.

Notice that the difference $\hat{x}(t) - x(t)$ is called *observer error*, it is usually denoted by $\tilde{x}(t)$, the term $\chi_u(t, x_0)$ represent the solution of equation (4.1) when we apply the input u in time interval $[0, t]$.

4.3.2 Properties of nonlinear system

For a nonlinear observer, one must be able to recover the information on the state via the output measured from the initial time, i.e., the notion of observability is based on the possibility of distinguishing various initial conditions, or equivalently, one cannot admit *indistinguishable* states. More details can be found in the work of [50] [56] and [14].

Definition 4.2 (Indistinguishability):

A paire $(x_0, x'_0) \subset \mathcal{R}^n \times \mathcal{R}^n$ is *indistinguishable* for a system (4.1) if:

$$\forall u \in U, \forall t \geq 0, h(\chi_u(t, x_0)) = h(\chi_u(t, x'_0)) \quad (4.4)$$

A state x is *indistinguishable* from x_0 if the pair (x, x_0) is *indistinguishable*.

From this, observability can be defined:

Definition 4.3 (Observability [resp. at x_0]):

A system (4.1) is *observable* [resp. *at x_0*] if it does not admit any *indistinguishable* paire [resp. *any state indistinguishable from x_0*].

This definition is quite general for practical use, since one might be mainly interested in distinguishing states from their neighbors. For example, consider the following system:

$$\dot{x} = u, \quad y = \sin(x) \quad (4.5)$$

Clearly, output y cannot help distinguishing between $[x_0, x_0 + 2k\pi]$, and thus the system is not observable. It is yet clear that y allows to distinguish states of $[-\frac{\pi}{2}, \frac{\pi}{2}]$. This brings to consider a weaker notion of observability.

Definition 4.4 (Weak observability [resp. at x_0]):

A system (4.1) is *weakly observable* [resp. *at x_0*] if there exists a neighborhood V of any x [resp. of x_0] such that there is no *indistinguishable* state from x [resp. x_0] in V .

Definition 4.5 (Local weak observability [resp. at x_0]):

A system (4.1) is *locally weakly observable* [resp. *at x_0*] if there exists a neighborhood V of any x [resp. of x_0] such that for any neighborhood W of x [resp. x_0] contained in V , there is no *indistinguishable* state from x [resp. x_0] in W when considering time intervals for which trajectories remain in W .

This roughly means that one can distinguish every state from its neighbors without "going too far". Such a condition relies on the notion of *observation space* roughly corresponding to the space of all observable states:

Definition 4.6 (Observation space):

The observation space for a system (4.1) is defined as the smallest real vector space (denoted by $\mathcal{O}(h)$) of C^∞ functions containing the components of h and closed under Lie derivation along $f_u := f(\cdot, u)$ for any constant $u \in \mathcal{R}^m$ (namely such that for any $\varphi \in \mathcal{O}(h)$, $L_{f_u}\varphi \in \mathcal{O}(h)$, where $L_{f_u}\varphi(x) = \frac{\partial \varphi}{\partial x} f(x, u)$).

Definition 4.7 (Observability rank condition [resp. at x_0]):

A system (4.1) is said to satisfy the observability rank condition [resp. at x_0] if:

$$\forall x, \quad \dim(d\mathcal{O}(h))|_x = n \quad [\text{resp.} \quad \dim(d\mathcal{O}(h))|_{x_0} = n] \quad (4.6)$$

where $d\mathcal{O}(h)|_x$ is the set of $d\varphi(x)$ with $\varphi \in \mathcal{O}(h)$.

Theorem 4.1:

A system (4.1) satisfying the observability rank condition at x_0 is locally weakly observable at x_0 .

More generally a system (4.1) satisfying the observability rank condition is locally weakly observable.

Conversely, a system (4.1) locally weakly observable satisfies the observability rank condition in an open dense subset of X .

However, the observability of a nonlinear system sometimes is not sufficient for the design of observer, we have to take into account the problem of inputs. Hence, it is important to study the characteristics of the inputs for such a system to build an observer. The notions of *universal inputs* and *uniform observability* for systems (4.1) are first introduced in [20] and they are cited below.

Definition 4.8 (Universal inputs [resp. on $[0, t]$]):

An input u is universal (resp. on $[0, t]$) for system (4.1) if $\forall x_0 \neq x'_0, \exists \tau \geq 0$ (resp. $\exists \tau \in [0, t]$) s.t. $h(\chi_u(\tau, x_0)) \neq h(\chi_u(\tau, x'_0))$.

An input u is a singular input if it is not universal.

Definition 4.9 (Universal observable systems [resp. locally]):

A system is uniformly observable (UO) if every input is universal (resp. on $[0, t]$).

4.3.3 Dynamic and sensor faulty model

According to the location of fault occurrence, the fault can be divided into component fault (dynamic fault), actuator fault, and sensor fault. In closed-loop, the actuator fault could be compensated automatically by the controller. So, in our case, we will mainly

focus on the FDD and FTC of the dynamic fault and sensor fault. The expression of the system which is interrupted by dynamic fault or sensor fault is presented in the following.

Considering the following nonlinear model:

$$\begin{cases} \dot{x} = f(x) + g(x)u + p(x)\theta \\ y = Cx \end{cases} \quad (4.7)$$

where $f(x) \in \mathcal{R}^n$ is a nonlinear vector function, $g(x) \in \mathcal{R}^{n \times k}$, $p(x) \in \mathcal{R}^{n \times m}$ are matrix functions with nonlinear elements, $C \in \mathcal{R}^{q \times n}$ is a constant matrix. $x \in \mathcal{R}^n$, $u \in \mathbf{R}^k$, $y \in \mathcal{R}^q$ represent the state vector, input vector and system output vector, respectively. $\theta \in \mathcal{R}^m$ is a vector composed of possible faulty parameters, its nominal value is denoted by θ^0 and it is known. Assume that $f(x)$ and $g(x)$ are both Lipchitz.

Dynamic fault refers to the variations of the process parameter. If a fault occurs at the j th parameter, then we have $\theta_j^f(t) = \theta_j^0(t) + f_{pj} = \beta_{pj}(t)$ for $t \geq t_f$, $j = 1, 2, \dots, m$, and $\lim_{t \rightarrow \infty} |\theta_j^0(t) - \beta_{pj}(t)| \neq 0$. Here, the constant f_{pj} is the j th element of the parameter fault vector f_p . $\theta_j^f(t)$ is the actual value of the j th parameter when it is faulty, while $\theta_j^0(t)$ is the expected value when it is healthy.

The corresponding dynamic fault model for nonlinear system (4.7) is:

$$\begin{cases} \dot{x} = f(x) + g(x)u + \sum_{l \neq j} p_l(x)\theta_l + p_j(x)\theta_j^f, \quad l \in 1, 2, \dots, m \\ y = Cx \end{cases} \quad (4.8)$$

where $p(x) = [p_1(x) \ \dots \ p_m(x)]$.

The sensor fault can be modeled in the same way as the dynamic fault, except that the unknown fault item is added to the output equation. If the j th sensor is faulty, we have $y_j^f(t) = y_j(t) + f_{sj} = \beta_{sj}(t)$ for $t \geq t_f$, $j = 1, 2, \dots, q$, and $\lim_{t \rightarrow \infty} |y_j(t) - \beta_{sj}(t)| \neq 0$, where f_{sj} is a constant as well as the j th element of the sensor fault vector f_s . $y_j^f(t)$ is the actual faulty output for the j th sensor, while $y_j(t)$ is the expected healthy output.

Then, the sensor fault model becomes:

$$\begin{cases} \dot{x} = f(x) + g(x)u + p(x)\theta \\ y = Cx + f_s \end{cases} \quad (4.9)$$

where $C = [c_1 \ \dots \ c_q]^T$.

In our case, both fault vectors f_p and f_s are limited signals, i.e. $\|f_p\| \leq M_p$, and $\|f_s\| \leq M_s$ (M_p and M_s are positive known constants).

In reality, the considered HEX reactor may be affected by unexpected dynamic fault or sensor fault, and a single fault may cause the degradation of its performance. As introduced in former section, the HEX reactor is a high intensified device, so it cannot be opened for cleaning once the assembly is finished. According to the functions of process channels and utility channels, the chemical reaction is taken place in process channels, so, the accumulation of products may cause the fouling of the process channel. In the contrast, the utility channel is less affected by the fouling compared to the process channel, because the fluid injected into the utility channel is usually water. The fouling in process channels will directly influence the performance of heat exchange between the process channel and plate wall, i.e. the decrease of the heat transfer coefficient h_p . Besides, the temperature of the inlet fluid $T_{p,in}$ and $T_{u,in}$ may change due to various reasons, such as environmental change, malfunction of the thermocouples installed in the injection pipes. Except for the possible faults presented before, output temperature sensors, which are used to measure not only the output temperatures of process fluid and utility fluid, but also the temperature of the plate wall, may also be bothered with an unexpected fault. These two kinds of faults are mainly treated in the process of fault diagnosis and fault tolerant control design.

In order to detect and diagnose the dynamic fault or sensor fault of the the system, two kinds of observers, adaptive observers and interval observers, will be introduced in the following part. Because they focus on both states and parameters compared to other kinds of observers. Besides, dynamic or sensor fault diagnosis schemes based on these two types of observers will also be presented and applied to the considered HEX reactor.

4.4 Adaptive observer

The adaptive observer is a well-known robust observer which can estimate the system states under the parameter uncertainties and modeling errors. One of the advantages of AO is that it can estimate the state and the unknown parameter at the same time, which is quite useful for obtain the details of faulty parameters. The design of AO is based on online adaption for joint estimation of state and some of the parameters (or for state estimation only, despite the presence of some unknown parameters) [132]. Early works on adaptive observers for linear systems can be traced back to the 70s. And the design for the nonlinear cases started from the early 90s. Nonlinear adaptive observer can be achieved for the nonlinear systems whose dynamics can be linearized

by coordinate change and output injection [87], or it can also be accomplished by some Lyapunov functions satisfying particular conditions instead of linearization [13]. Then, adaptive observers are widely used in actuator, sensor, and process fault diagnosis [23] [40] [100].

4.4.1 Structure of adaptive observer

Consider a nonlinear system described in [13]:

$$\begin{cases} \dot{x} = f(x, u) + g(x, u)\theta \\ y = h(x) \end{cases} \quad (4.10)$$

where x , y and u are state vector, output vector and measurable bounded input vector, θ is a vector of unknown constant parameters.

The adaptive observer design are divided into two steps, the first one is to transform the system into nonlinear adaptive observer form:

$$\begin{cases} \dot{y} = \alpha(y, z, u) + \beta(y, z, u)\theta \\ \dot{z} = \gamma(y, z, u) \end{cases} \quad (4.11)$$

where y is the output vector of the system which is also the measurable states, z is the vector of the unmeasurable states. $\alpha(\cdot)$ and $\beta(\cdot)$ are globally Lipschitz functions with respect to z , and uniformly with respect to (y, u) . $\beta(\cdot)$ is globally bounded.

And then, an adaptive observer in the following form is design in the second step:

$$\begin{cases} \dot{\hat{y}} = \alpha(y, \hat{z}, u) + \beta(y, \hat{z}, u)\hat{\theta} - k_y(\hat{y} - y) \\ \dot{\hat{z}} = \gamma(y, \hat{z}, u) \\ \dot{\hat{\theta}} = -k_\theta\beta^T(y, \hat{z}, u)(\hat{y} - y) \end{cases} \quad (4.12)$$

where $k_y > 0$ and $k_\theta > 0$ are the observer gains. However, it is recommended to take $k_y < k_\theta$, such that for any $\hat{y}(0)$, $\hat{z}(0)$, any $y(0)$, $z(0)$ and measurable bounded u , the estimation errors $\|\hat{y}(t) - y(t)\|$ and $\|\hat{z}(t) - z(t)\|$ asymptotically go to zero when t tends to infinity, while $\|\hat{\theta}(t) - \theta\|$ remains bounded. Moreover, if $\beta^T(y, \hat{z}, u)$ is persistently exciting, and its time derivative is bounded, then $\|\hat{\theta}(t) - \theta\|_{t \rightarrow \infty} \rightarrow 0$.

If all the states can be measured, a reduced order asymptotic state observer is obtained by:

$$\begin{cases} \dot{\hat{y}} = \alpha(y, u) + \beta(y, u)\hat{\theta} - k_y(\hat{y} - y) \\ \dot{\hat{\theta}} = -k_\theta\beta^T(y, u)(\hat{y} - y) \end{cases} \quad (4.13)$$

4.4.2 Adaptive observer based FDD scheme

FDD for dynamic fault

In order to detect, isolate and identify the faulty parameter, the author of [23] [39] [133] proposed a FDD method based on a bank of adaptive observers, where each observer is specified for one faulty parameter. These observers are state-based observers, which assumes that the system states are available. The number of the observers is equal to the number of the possible faulty parameters m . For the faulty model (4.8), the structure of this observer are given as follows:

$$1 \leq i \leq m, \quad \begin{cases} \dot{\hat{x}}^{(i)} = f(\hat{x}^{(i)}) + g(\hat{x}^{(i)})u + \sum_{l \neq i} p_l(\hat{x}^{(i)})\theta_l + p_i(\hat{x}^{(i)})\hat{\beta}^{(p_i)} + H_i(\hat{y}^{(i)} - x) \\ \dot{\hat{\beta}}^{(p_i)} = -2\gamma_i(\hat{x}^{(i)} - x)^T S_i p_i(\hat{x}^{(i)}) \\ \hat{y}^{(i)} = \hat{x}^{(i)} \end{cases} \quad (4.14)$$

where $\hat{x}^{(i)}$, and $\hat{y}^{(i)}$ are the estimated state vector and output vector, $\hat{\beta}^{(p_i)}$ is the fault estimation of the i th observer, $p_i(\hat{x}^{(i)})$ is the i th column of matrix $p(\hat{x}^{(i)})$. H_i is a Hurwitz matrix that can be chosen freely with a goal to increase as much as possible the dynamic of the observer, γ_i is a design constant, and S_i is a positive definite matrix. $S^{(i)}$ can be calculated with the help of (4.15), where Q_i is a positive definite matrix that can be chosen freely:

$$H_i^T S_i + S_i H_i = -Q_i \quad (4.15)$$

Each observer gives an estimation of one particular parameter, and we have to choose the appropriate gain matrices H_i , S_i , as well as gain constant γ_i to have a good fault estimation performance. Details about the observer used can be found in [23] [39].

Once the fault occurs at the j th dynamic parameter, it can be detected and isolated using the following residual:

$$r_i = \|\hat{y}^{(i)} - y\|, \quad i \in 1, \dots, m. \quad (4.16)$$

where $\hat{y}^{(i)}$ and y represent the output vector of the i th observer and the output vector of the system, respectively.

These residuals are designed to be insensitive to the fault of a particular parameter while being sensitive to others, i.e. if the j th parameter is faulty, then the j th residual converges to zero and the other $m - 1$ residuals converge to a nonzero constant. Thus, the fault is isolated.

When the fault on the j th parameter is isolated, we can obtain the faulty value according to the parameter estimation of the corresponding adaptive observer:

$$\hat{f}_{pj} = \hat{\beta}^{(pj)} - \theta_j^0 \quad (4.17)$$

FDD for sensor fault

A healthy sensor is one of the most important tools to obtain the output of the system in real-time, especially for the closed-loop systems. In the closed-loop system, the measured output are used to calculate the control law. So, a single sensor fault affects all of the system variables. To supervise the performances of sensors, a similar FDD scheme is applied for the sensors. A bank of adaptive observers in the following form are constructed for the faulty model (4.9) [24] [39]:

$$1 \leq i \leq q, \quad \begin{cases} \dot{\hat{x}}^{(i)} = f(\hat{x}^{(i)}) + g(\hat{x}^{(i)})u + H^{(i)}(\hat{y}^{(i)} - x) \\ \hat{y}_l^{(i)} = \hat{x}_l^{(i)}, \quad l = 1, \dots, i-1, i+1, \dots, n \\ \dot{\hat{y}}_i^{(i)} = -2\gamma_i(\hat{y}^{(i)} - x)^T S_i c_i \end{cases} \quad (4.18)$$

where c_i is the i th row vector of the n dimensional unit matrix C . The gain matrices H_i , S_i , and constant γ_i is chosen as the same manners as that in dynamic fault case. The number of the observers is equal to the number of the sensors q .

Then, residuals of the form (4.16) are calculated to detect and isolate the fault. The isolation idea is the same as we presented in dynamic fault case. The residuals are insensitive to the faulty sensor, but they are sensitive to others. That is to say, if the j th parameter is faulty, then the j th residual converges to zero while the other $p-1$ residuals converge to a nonzero constant. And then, the estimation of the faulty value can be calculated by:

$$\hat{f}_{sj} = \hat{y}_j^{(j)} - \hat{x}_j^{(j)} \quad (4.19)$$

4.4.3 Application to HEX reactor: adaptive observer based FDD scheme

In this part, we will apply the presented adaptive observer based FDD scheme for the considered HEX reactor in open-loop. For simplicity, only the heat exchange part is considered in this section. Water with different temperatures ($T_{p,in}$, $T_{u,in}$) is injected into process channel and utility channel respectively. And the flow rate of utility fluid is the only input signal $u = F_u$. Define the state vector as $x = [T_p \quad T_u \quad T_w]^T$, all

these temperatures are measurable. According to the energy balance equation, the mathematical model of the HEX reactor is:

$$\begin{cases} \dot{T}_p = \frac{F_p}{V_p}(T_{p,in} - T_p) + \frac{h_p A_p}{\rho_p V_p C_{p,p}}(T_w - T_p) \\ \dot{T}_u = \frac{F_u}{V_u}(T_{u,in} - T_u) + \frac{h_u A_u}{\rho_u V_u C_{p,u}}(T_w - T_u) \\ \dot{T}_w = \frac{h_p A_p}{\rho_w V_w C_{p,w}}(T_p - T_w) + \frac{h_u A_u}{\rho_w V_w C_{p,w}}(T_u - T_w) \end{cases} \quad (4.20)$$

where the subscript p , u and w represent the process fluid, utility fluid and plate wall, the subscript in represents the inlet fluid.

The model above is just for one cell, which may cause slight differences in the dynamic behavior of the real reactor. However, the application of the FDD scheme will not be affected. Table 4.2 gives the nominal values of the operating conditions used in the simulation. Further details about the studied system could be found in [112].

Table 4.2: Physical data of the pilot

Constant	Value	Units
V_p	2.68×10^{-5}	m^3
ρ_p, ρ_u	10^3	$kg \cdot m^{-3}$
$C_{p,p}, C_{p,u}$	4.186×10^3	$J \cdot kg^{-1} \cdot K^{-1}$
h_p	7.5975×10^3	$W \cdot m^2 \cdot K^{-1}$
A_p	2.68×10^{-2}	m^2
V_u	1.141×10^{-4}	m^3
h_u	7.5833×10^2	$W \cdot m^2 \cdot K^{-1}$
A_u	4.564×10^{-1}	m^2
V_w	1.355×10^{-3}	m^3
ρ_w	8×10^3	$kg \cdot m^{-3}$
$C_{p,w}$	5×10^2	$J \cdot kg^{-1} \cdot K^{-1}$

To start, the utility fluid is injected into the utility channel with a flow rate $F_u = 62.2 L \cdot h^{-1}$ and a fixed temperature $T_{u,in} = 15.6 \text{ }^\circ C$. When they reach a steady state, the process fluid is injected into the process channel with a constant flow rate $F_p = 10 L \cdot h^{-1}$ and a constant temperature $T_{p,in} = 77 \text{ }^\circ C$. That is to say, the initial temperatures of process channel, utility channel and plate wall are $x(0) = [T_p(0) \ T_u(0) \ T_w(0)]^T = [77 \ 15.6 \ 15.6]^T$. After a period of time, the fault is introduced. Since the fault is introduced in the open-loop, so the input signal will be a constant other than a variable.

Simulation with dynamic fault

we consider the two possible faulty parameters caused by the fouling in process channels, and the inlet fluid temperature change, respectively. The first one is the heat transfer coefficient between the process channel and the plate wall h_p . The second one is the inlet process fluid temperature $T_{p,in}$. As can be seen from the model (4.20), the inlet temperature change in utility fluid $T_{u,in}$ can be compensated directly by increasing or decreasing the utility fluid flow rate F_u . We will focus on the parameter which can not be compensated automatically when it is faulty. Therefore, our possible fault vector $\beta = [h_p \ T_{p,in}]^T$. Their nominal values are $\beta = [7.5975 \times 10^3 \ 77]^T$.

Then, similar to (4.7), the mathematical model of the HEX reactor can be rewritten into the following form:

$$\dot{x} = f(x) + g(x)F_u + p(x) \begin{bmatrix} h_p \\ T_{p,in} \end{bmatrix} \quad (4.21)$$

where $x = [T_p \ T_u \ T_w]^T$,

$$f(x) = \begin{bmatrix} -\frac{F_p}{V_p} T_p \\ \frac{h_u A_u}{\rho_u V_u C_{p,u}} (T_w - T_u) \\ \frac{h_u A_u}{\rho_w V_w C_{p,w}} (T_u - T_w) \end{bmatrix}$$

$$g(x) = \begin{bmatrix} 0 \\ \frac{T_{u,in} - T_u}{V_u} \\ 0 \end{bmatrix}$$

$$p(x) = \begin{bmatrix} \frac{A_p}{\rho_p V_p C_{p,p}} (T_w - T_p) & \frac{F_p}{V_p} \\ 0 & 0 \\ \frac{A_p}{\rho_w V_w C_{p,w}} (T_p - T_w) & 0 \end{bmatrix}$$

Thus, two adaptive observers (4.22) (4.23) are constructed to detect and diagnose the possible dynamic fault.

$$\begin{cases} \dot{\hat{x}}^{(1)} = f(\hat{x}^{(1)}) + g(\hat{x}^{(1)})F_u + p(\hat{x}^{(1)}) \begin{bmatrix} \hat{h}_p^{(1)} \\ T_{p,in} \end{bmatrix} + H_1(\hat{x}^{(1)} - x) \\ \dot{\hat{h}}_p^{(1)} = -2\gamma_1(\hat{x}^{(1)} - x)S_1 p_1(\hat{x}^{(1)}) \\ \hat{y}^{(1)} = \hat{x}^{(1)} \end{cases} \quad (4.22)$$

$$\begin{cases} \dot{\hat{x}}^{(2)} = f(\hat{x}^{(2)}) + g(\hat{x}^{(2)})F_u + p(\hat{x}^{(2)}) \begin{bmatrix} h_p \\ \hat{T}_{p,in}^{(2)} \end{bmatrix} + H_2(\hat{x}^{(2)} - x) \\ \dot{\hat{T}}_{p,in}^{(2)} = -2\gamma_2(\hat{x}^{(2)} - x)S_2p_2(\hat{x}^{(2)}) \\ \hat{y}^{(2)} = \hat{x}^{(2)} \end{cases} \quad (4.23)$$

First of all, we suppose that the process channel is fouled at $t_f = 400s$, which causes a decrease of the heat transfer coefficient h_p to 85% of its nominal value h_p^0 (i.e. $f_{p1} = -1.1393 \times 10^3 \text{ W} \cdot \text{m}^2 \cdot \text{K}^{-1}$). Then the heat transfer coefficient in faulty case becomes $h_p^f = h_p^0 + f_{p1} = 6.4852 \times 10^3 \text{ W} \cdot \text{m}^2 \cdot \text{K}^{-1}$.

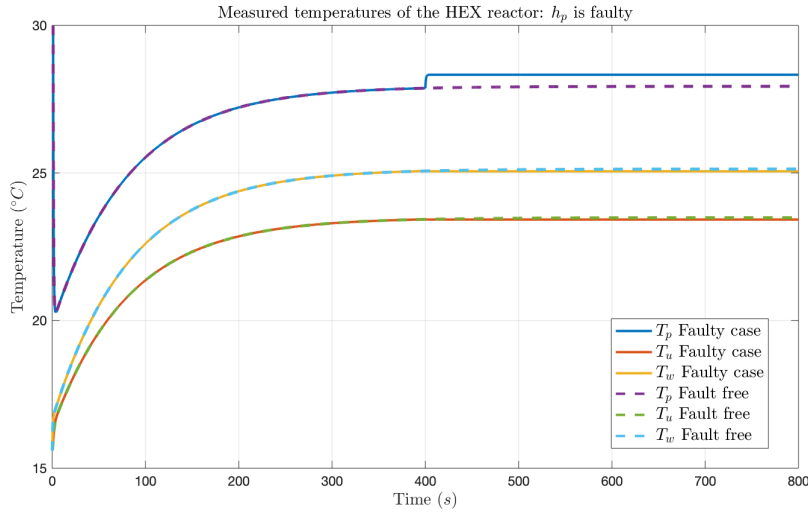


Figure 4.2: Temperature performances of the HEX reactor: dynamic h_p is faulty at 400s

Figure 4.2 presents the performances of the measured temperatures of process fluid, utility fluid, and plate wall. The dot lines represent temperatures in fault free case, and the solid line represents the real performance of the HEX reactor. According to the initial values of both fluid, the utility fluid is used to cool down the process fluid. So the temperature of process fluid T_p drops greatly at the beginning. And then, it reaches at a steady state about 27.93°C . At 400s, the heat transfer coefficient h_p drops to 85% of its nominal value, that means the heat is gathered in process channel and cannot be taken away as quickly as before. As a consequence, the temperature of utility fluid T_u and the temperature of plate wall T_w all change slightly.

The residuals of both observers are shown in Figure 4.3. The residuals leave zero at 400s, that means there is a fault in the system. After a few second, the first residual r_1 corresponding to the first observer comes back to zero while the second residual r_2 stays at a nonzero value. According to our isolation principle, the fault is isolated

in the first element of the possible faulty parameter, i.e. h_p . Moreover, the adaptive observer gives the estimation of the fault, as presented in Figure 4.4. The estimated value \hat{f}_{p1} is the same as the fault we applied.

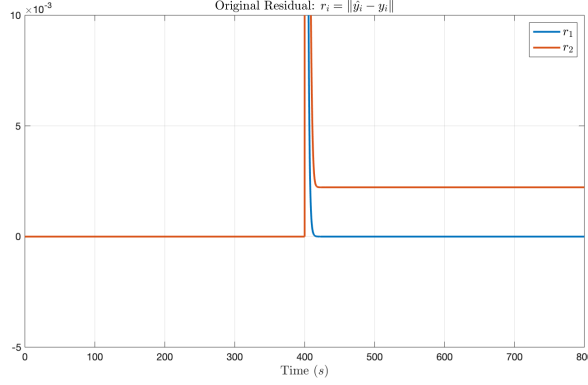


Figure 4.3: Residuals of both adaptive observers: dynamic h_p is faulty at 400s

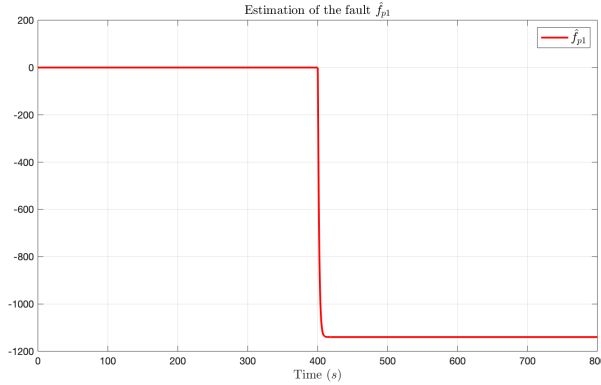


Figure 4.4: Estimated fault value \hat{f}_{p1} : dynamic h_p is faulty at 400s

In the second case, we introduce a fault $f_{p2} = -5 \text{ }^\circ\text{C}$ in the second parameter $T_{p,in}$, the temperature of the inlet process fluid, at $t_f = 400\text{s}$. Then, $T_{p,in}$ drops to the faulty case $T_{p,in}^f = T_{p,in} + f_{p2} = 72 \text{ }^\circ\text{C}$. The performance of the HEX reactor is given in Figure 4.5. The dot line represents the fault free case, while the solid line represents the faulty case.

As presented in Figure 4.5, the decrease of inlet process fluid temperature $T_{p,in}$ causes the temperature decrease of the whole HEX reactor. The residuals are presented in Figure 4.6. It is obvious that both residuals change at 400s, which indicates the occurrence of fault. After a period of time, the second residual r_2 converges to zero, while the first residual r_1 converges to a nonzero value. Then, we can judge that

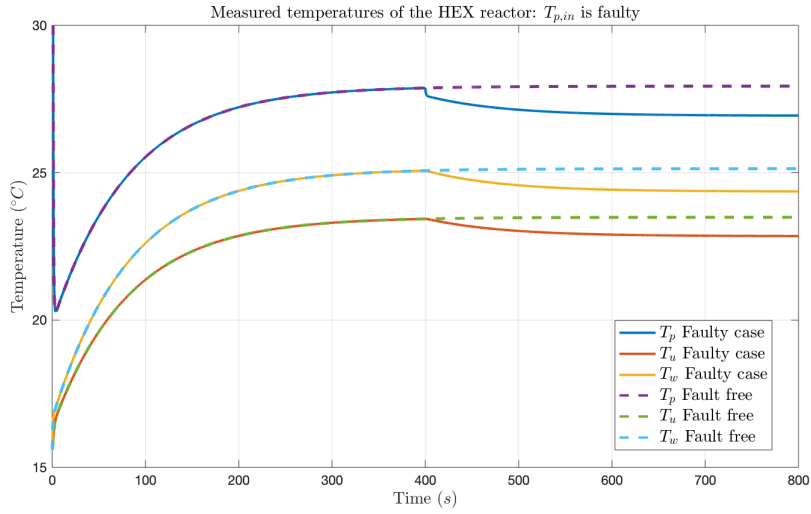


Figure 4.5: Temperature performances of the HEX reactor: dynamic $T_{p,in}$ is faulty at 400s

the fault occurs at the second parameter $T_{p,in}$. Besides, the second observer gives the estimation of the faulty value $\hat{f}_{p2} = -5$, it equals the faulty value we introduced.

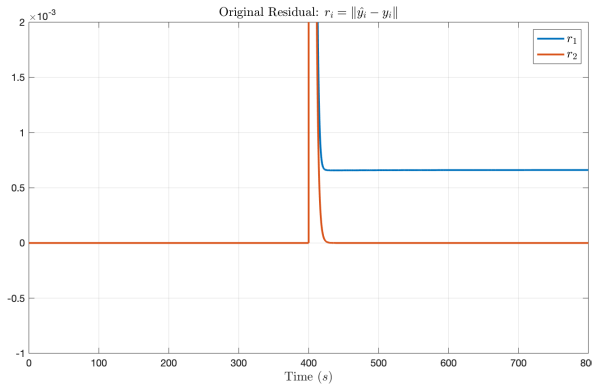


Figure 4.6: Residuals of both adaptive observers: dynamic $T_{p,in}$ is faulty at 400s

Simulation with sensor fault

For the considered HEX reactor, we mainly focus on the temperature of process fluid and utility fluid, because the plate wall is a heat transfer media whose temperature varies according to the temperatures of both flowing fluid. So, we mainly focus on the sensor of process fluid temperature and the sensor of utility fluid. Normally, the measured output should equal the real output of the system, i.e. $y_{mea} = y_{sys}$. When the j th sensor is faulty, then, $y_{j,mea} = y_{j,sys} + f_{sj}$, while other elements of measured

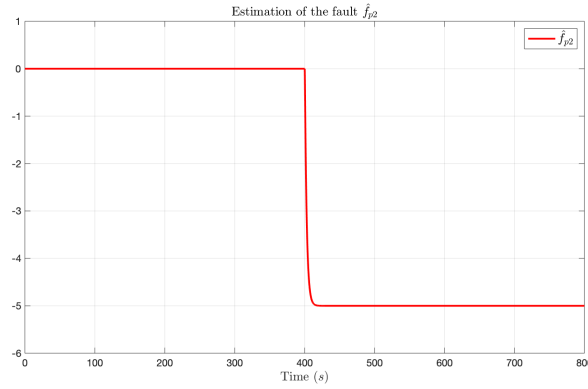


Figure 4.7: Estimated fault value \hat{f}_{p2} : dynamic $T_{p,in}$ is faulty at 400s

output still equal to the output of the system. To detect and isolate the fault, two observers are constructed in form (4.18) are constructed.

First, we consider a temperature sensor fault $f_{s1} = 3 \text{ }^\circ\text{C}$ occurring at the process fluid temperature sensor s_1 at 400s. So the output of the faulty sensor is $y_1^f = y_1 + f_{s1}$.

Simulation results are presented in Figure 4.8. The real output of the system $T_{p,sys}$ is presented in blue dot line, and the measured value (the output of the sensor) $T_{p,mea}$ is represented by the red line. The black dot line represents the desired process fluid temperature T_{pd} .

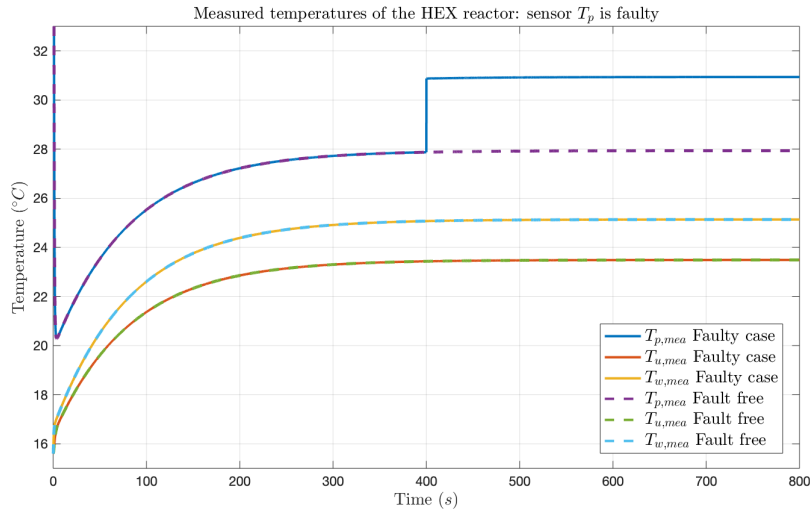


Figure 4.8: Temperature performances of the HEX reactor: sensor T_p is faulty at 400s

Since the fault f_{s1} is introduced in open-loop, so one sensor fault will not affect all the other measured output but only the faulty one. In Figure 4.8, the first sensor is faulty, so the measured process fluid temperature $T_{p,mea}$ no longer equals to the fault

free case. And, the measured temperature of utility fluid $T_{u,mea}$, and the measured temperature of plate wall $T_{w,mea}$ still equal to their value under fault free case.

Residuals of each observers are given in Figure 4.9. Obviously, the residuals do not stay at zero at 400s. Then, the first residual goes back to zero while the second one stays at a nonzero value. That is to say, the fault occurs at the first sensor. And the faulty value is presented in Figure 4.10. The estimated faulty value \hat{f}_{s1} equals to the real faulty value $f_{s1} = 3 \text{ }^\circ\text{C}$.

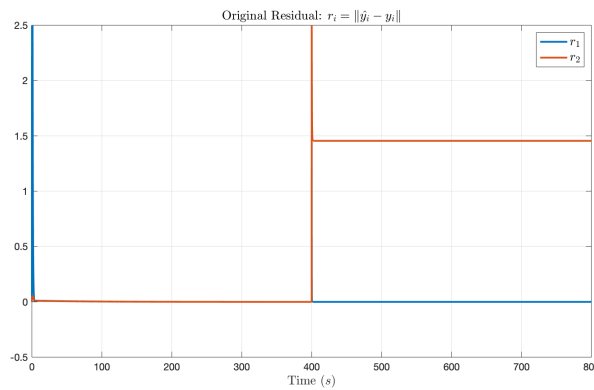


Figure 4.9: Residuals of both adaptive observers: sensor T_p is faulty at 400s

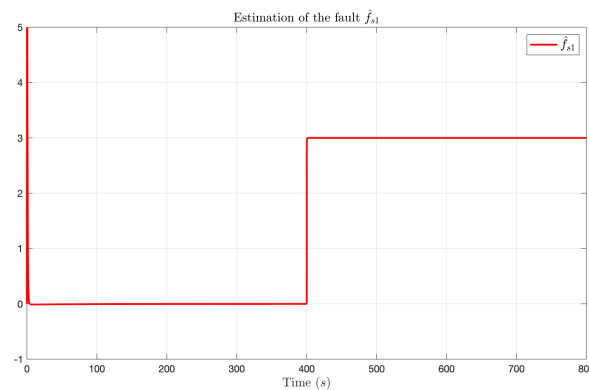


Figure 4.10: Estimated fault value \hat{f}_{s1} : sensor T_p is faulty at 400s

In the next, a fault $f_{s2} = 7 \text{ }^\circ\text{C}$ is applied to the utility fluid temperature sensor s_2 at 400s. Then, the faulty temperature measurement is $y_2^f = y_2 + f_{s2}$. The measured temperatures of the HEX reactor is presented in Figure 4.11. After 400s, the measured utility fluid temperature changes greatly because of the interruption of sensor fault. And the other measurements stays at its healthy value since the fault is introduced in open-loop.

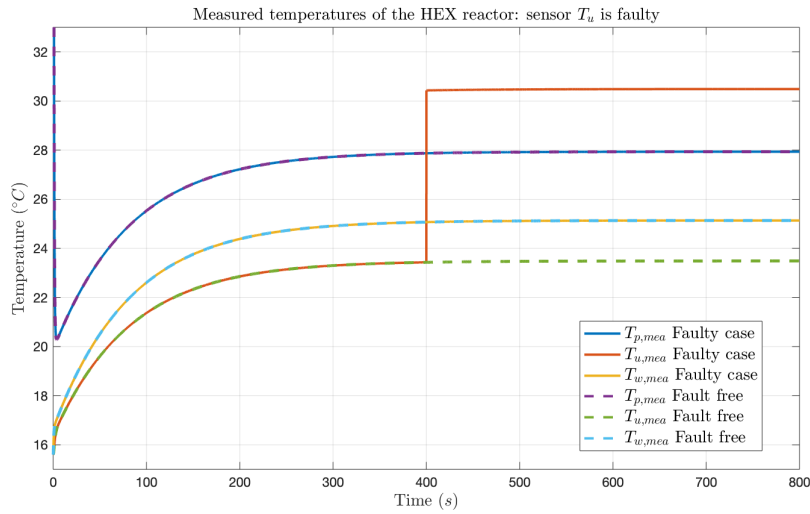


Figure 4.11: Temperature performances of the HEX reactor: sensor T_u is faulty at 400s

Figure 4.12 shows the performance of residuals. At 400s, the variations of residual indicate the occurrence of fault. After a few seconds, the second residual returns to zero and the first residual stays at a nonzero value. Thus, the fault is isolated according to our isolation principle. The estimated faulty value is shown in 4.13. The fault f_{s2} that we applied to the second sensor is well estimated by the second observer.

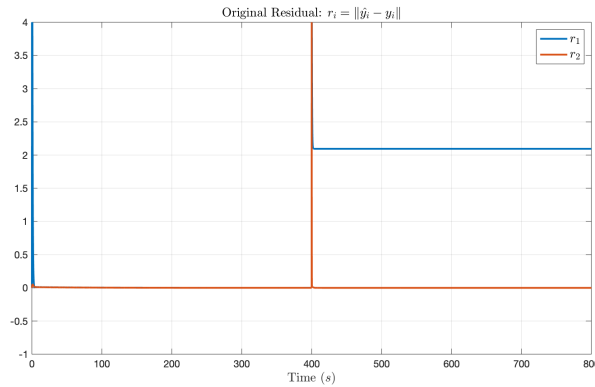


Figure 4.12: Residuals of both adaptive observers: sensor T_u is faulty at 400s

Simulation results show that the adaptive observer based FDD scheme can well detect, isolate, and identify the dynamic fault, and sensor fault.

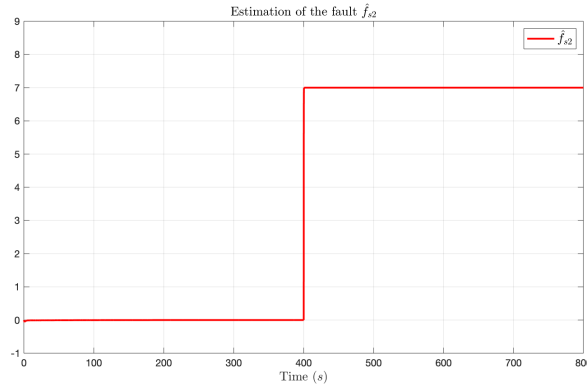


Figure 4.13: Estimated fault value \hat{f}_{s1} : sensor T_u is faulty at 400s

4.5 Interval observer

Interval observer is a kind of observer that focuses on the speed of fault isolation and identification. It is firstly proposed in [80], and then applied to numbers of nonlinear systems [81] [100] [131]. The main idea of this method is to divide the practical domain of the value of each system parameter into a certain number of intervals. After verifying all the intervals whether or not one of them contains the faulty parameter value of the system, the faulty parameter value is found, the fault is therefore isolated and identified. The principle of the verification is based on the local monotonous characteristic of the observer prediction error, i.e. residual. The only condition for the application of this method is that the system dynamic is a monotonous function with respect to the considered parameter. Therefore, it fits many kinds of nonlinear systems.

4.5.1 Structure of interval observer

For the considered nonlinear system:

$$\begin{cases} \dot{x} = f(x, \theta, u) \\ y = Cx \end{cases} \quad (4.24)$$

where $x \in \mathcal{R}^n$ is the state vector, $\theta \in \mathcal{R}^m$ is the possible faulty parameter vector, $y \in \mathcal{R}^q$ is the measurable output vector $C \in \mathcal{R}^{q \times n}$ is the output matrix. $f(x, \theta, u)$ is a nonlinear vector function, and its first partial derivatives on x and θ are continuous, bounded, Lipschitz in x and θ . The nominal value of the parameter vector θ is denoted by θ^0 and is known.

Once the parameter vector difference $\Delta\theta = \theta - \theta^0$ is great, it will cause a great

dynamic difference between the system (4.24) and its nominal model $\dot{x} = f(x, \theta^0, u)$:

$$\Delta(x, \theta, \theta^0, u) = f(x, \theta, u) - f(x, \theta^0, u) \quad (4.25)$$

and this is defined as a fault. The faulty parameter vector is denoted by θ^f .

Then considered observer is given by:

$$\begin{cases} \dot{\hat{x}} = f(\hat{x}, \theta^{ob}, u) + H(\hat{y} - y) \\ \hat{y} = C\hat{x} \\ e_{y,h} = \hat{y}_h - y_h \end{cases} \quad (4.26)$$

where y_h is the h th element of the output vector y . θ^{ob} is the observer parameter vector, and $\theta^{ob} = \theta^0$ for $t < t_f$. t_f is the fault occurrence time. H is the observer gain matrix.

At t_f , the s th parameter changes due to the fault, and then, to isolate the fault, the j th parameter is switched to a preselected value by the isolation procedure once the fault is detected:

$$\begin{cases} \theta_s^f = \theta_s^0 + \Delta^f, \\ \theta_l^f = \theta_l^0, \quad l \neq s, \end{cases} \quad t \geq t_f, \quad \begin{cases} \theta_j^{ob} = \theta_j^0 + \Delta^{ob}, \\ \theta_l^{ob} = \theta_l^0, \quad l \neq j, \end{cases} \quad t \geq t_f \quad (4.27)$$

where Δ^f , Δ^{ob} are real numbers. Δ^f is the value change caused by the fault, $\theta_j^0 + \Delta^{ob}$ is the preselected value of the observer, which is a bound of a parameter interval of j th system parameter. For each interval bounds, there are two particular cases of the isolation observer:

$$\begin{cases} \dot{\hat{x}}^a = f(\hat{x}^a, \theta^{oba}, u) + H(\hat{y}^a - y) \\ \hat{y}^a = C\hat{x}^a \\ e_y^a = \hat{y}^a - y \end{cases} \quad (4.28)$$

$$\begin{cases} \dot{\hat{x}}^b = f(\hat{x}^b, \theta^{obb}, u) + H(\hat{y}^b - y) \\ \hat{y}^b = C\hat{x}^b \\ e_y^b = \hat{y}^b - y \end{cases} \quad (4.29)$$

where

$$\theta_j^{oba} = \begin{cases} \theta_j^0, & t < t_f \\ \theta_j^a, & t \geq t_f \end{cases} \quad \theta_l^{oba} = \theta_l^0 \quad \forall t, \quad l \neq j$$

$$\theta_j^{obb} = \begin{cases} \theta_j^0, & t < t_f \\ \theta_j^b, & t \geq t_f \end{cases} \quad \theta_l^{obb} = \theta_l^0 \quad \forall t, \quad l \neq j$$

where θ_j^a and θ_j^b are two bounds of the parameter interval $[\theta_j^a \quad \theta_j^b]$ of the j th parameter. θ_l^0 is the nominal value of the l th parameter.

The isolation principles are presented by the following theorems.

Theorem 4.2:

It is assumed that the parameter changes of the system and of the observers are at the same parameter, that is to say, $s = j$. Two bounds of a considered parameter interval are noted by θ_j^a and θ_j^b , respectively. The interval is smaller than a certain size which will be mentioned later. The residuals $e_y^a(t)$ and $e_y^b(t)$ correspond to the two interval bounds while $e_y(t)$ represents residual in general case.

(1) If $\theta_j^f \in [\theta_j^a \ \theta_j^b]$, then, $\text{sgn}(e_y^a(t)) = -\text{sgn}(e_y^b(t)) \forall t$, and $e_y(t)$ is a monotonous function of the parameter difference $\delta\theta_j = \theta^{ob} - \theta^f|_{t \geq t_f}$ when $\theta_j^{ob} \in [\theta_j^a \ \theta_j^b]$. Specially, $\lim_{\delta\theta \rightarrow 0} e_y(t) = 0 \forall t \geq t_f$.

(2) If $\theta_j^f \notin [\theta_j^a \ \theta_j^b]$, then, at the period beginning after the fault occurrence, the equality $\text{sgn}(e_y^a(t)) = \text{sgn}(e_y^b(t))$ is satisfied.

Theorem 4.3:

It is assumed that after the fault occurrence the parameter changes of the system and of the observers are not at the same parameter, i.e. $s \neq j$. If the parameter interval $[\theta_j^a \ \theta_j^b]$ is small enough, then the time t_e exists that $\text{sgn}(e_y^a(t_e)) = \text{sgn}(e_y^b(t_e))$.

The proofs of these theorems can be found in [81].

According to Theorem 4.2 and Theorem 4.3, we can conclude that: for the parameter interval $[\theta_j^a \ \theta_j^b]$ which is small enough, if the faulty parameter value is not contained in this interval, the isolation index:

$$v(t) = \text{sgn}(e_y^a(t))\text{sgn}(e_y^b(t)) \quad (4.30)$$

will be '1' some time after the fault occurrence. If the parameter interval contains the faulty parameter value, the isolation index $v(t)$ will be maintained as '-1' all the time.

4.5.2 Interval observer based FDD scheme

FDD for dynamic fault

First of all, the practical domain of each possible faulty parameter is divided into a certain number of intervals. For instance, parameter θ_j is partitioned into n intervals, their bounds are $\theta_j^{(0)}, \theta_j^{(1)}, \dots, \theta_j^{(i)}, \dots, \theta_j^{(n)}$. The bounds of i th interval are $\theta_j^{(i-1)}$ and $\theta_j^{(i)}$, they are also noted as $\theta_j^{a(ij)}$ and $\theta_j^{b(ij)}$.

To detect and isolate the faulty parameter, each bound of parameter intervals is used as a parameter to build an isolation observer. For n intervals in series, there are $(n + 1)$ bounds, so, $(n + 1)$ observers are constructed. On the other hand, each isolation

observer serves two neighboring intervals. And the interval which contains a parameter nominal value is unable to contain the faulty parameter value.

Therefore, for the i th interval, the isolation observers corresponding to each bound are given below:

$$\begin{cases} \dot{\hat{x}}^{a(ij)} = f(\hat{x}^{a(ij)}, \theta^{oba(ij)}(t), u) + H(\hat{y}^{a(ij)} - y) \\ \hat{y}^{a(ij)} = C\hat{x}^{a(ij)} \\ e_y^{a(ij)} = \hat{y}^{a(ij)} - y \end{cases} \quad (4.31)$$

$$\begin{cases} \dot{\hat{x}}^{b(ij)} = f(\hat{x}^{b(ij)}, \theta^{obb(ij)}(t), u) + H(\hat{y}^{b(ij)} - y) \\ \hat{y}^{b(ij)} = C\hat{x}^{b(ij)} \\ e_y^{b(ij)} = \hat{y}^{b(ij)} - y \end{cases} \quad (4.32)$$

where

$$\theta_j^{oba(ij)}(t) = \begin{cases} \theta_j^0, & t < t_f \\ \theta_j^{i-1}, & t \geq t_f \end{cases} \quad \theta_l^{oba(ij)}(t) = \theta_l^0 \quad \forall t, \quad l \neq j$$

$$\theta_j^{obb(ij)}(t) = \begin{cases} \theta_j^0, & t < t_f \\ \theta_j^i, & t \geq t_f \end{cases} \quad \theta_l^{obb(ij)}(t) = \theta_l^0 \quad \forall t, \quad l \neq j$$

To detect the fault, we will use the residuals presented in (4.16). Once the residuals leave zero, that indicates the occurrence of fault. And the parameter of the observer is changed to the preselected value. To isolate the fault, we calculate the isolation index of each interval by:

$$v^{(ij)}(t) = \text{sgn}(e_y^{a(ij)}(t))\text{sgn}(e_y^{b(ij)}(t)) \quad (4.33)$$

$v^{(ij)}(t) = 1$ indicates that this interval does not contain the faulty parameter value. In the contrast, $v^{(ij)}(t) = -1$ indicates that the faulty parameter value is located in this interval.

Assume that the i th interval of j th parameter contains the faulty parameter, the fault value can be obtained by the following:

$$\hat{\theta}_j^f = \frac{1}{2}(\theta_j^{a(ij)} + \theta_j^{b(ij)}) \quad (4.34)$$

This estimation of the faulty parameter value and the obtained parameter bounds do not rely on classic parameter identification methods but rely on the proposed fault isolation method. As soon as the fault is isolated, they are obtained.

FDD for sensor fault

A similar idea can be used for sensor fault isolation and identification. In this case, the system parameters are all in nominal condition, while the measured output is malfunction. Since the sensor fault will affect the calculation of the input signal, which will cause an unexpected performance of the whole closed-loop system, we still have to find the fault as soon as possible.

At t_f , the s th sensor of the system is faulty, then, the j th sensor of the observer is switched to a preselected value to isolate the fault:

$$\begin{cases} y_{s,mea}^f = y_{s,sys} + f_{s,s}, \\ y_{l,mea}^f = y_{l,sys}, \quad l \neq s, \end{cases} \quad t \geq t_f, \quad \begin{cases} y_{j,mea}^{ob} = y_{j,sys}^{ob} + \Delta^{ob}, \\ y_{l,mea}^{ob} = y_{l,sys}^{ob}, \quad l \neq j, \end{cases} \quad t \geq t_f \quad (4.35)$$

where $y_{s,sys}$ and $y_{l,sys}$ represent the s th and l th output of the real system, which can be calculated by $y_{s,sys} = c_s x$, $y_{l,sys} = c_l x$. $y_{j,sys}^{ob}$ and $y_{l,sys}^{ob}$ are the j th and l th output of the observer, they can be calculated in the similar way $y_{j,sys}^{ob} = c_j x^{ob}$, $y_{l,sys}^{ob} = c_l x^{ob}$. c_s and c_l are the s th and l th row of the output matrix C . $f_{s,s}$ is the sensor s value change caused by the fault, Δ^{ob} is the preselected value of the observer, which represent the possible variation of the sensor. Thus, $c_j x + \Delta^{ob}$ is a bound of j th sensor's interval.

Firstly, each variation range of possible faulty sensor are divided into several intervals. For example, the variation Δ_j of j th measured output $y_{j,mea}$ can divided into m intervals according to different variations: $\Delta_j^{(0)}$, $\Delta_j^{(1)}$, \dots , $\Delta_j^{(m)}$. Thus, the measured output $y_{j,mea}$ are changed into m intervals: $y_{j,sys} + \Delta_j^{(0)}$, $y_{j,sys} + \Delta_j^{(1)}$, \dots , $y_{j,sys} + \Delta_j^{(m)}$. For simplicity, we will discuss the intervals of sensor variations. The bounds of i th interval are $\Delta_j^{(i-1)}$ and $\Delta_j^{(i)}$, which are also noted as $\Delta_j^{a(ij)}$ and $\Delta_j^{b(ij)}$.

Therefore, similar to the dynamic fault case, $(m + 1)$ observers corresponding to $(m + 1)$ bounds are constructed for m intervals in the second step. For the i th interval, the isolation observers are shown as follows:

$$\begin{cases} \dot{\hat{x}}^{a(ij)} = f(\hat{x}^{a(ij)}, \theta^0, u) + H(\hat{y}^{a(ij)} - y) \\ \hat{y}^{a(ij)} = [c_1 \hat{x}^{a(ij)} \quad \dots \quad \hat{y}^{oba(ij)}(t) \quad \dots \quad c_q \hat{x}^{a(ij)}]^T \\ e_y^{a(ij)} = \hat{y}^{a(ij)} - y \end{cases} \quad (4.36)$$

$$\begin{cases} \dot{\hat{x}}^{b(ij)} = f(\hat{x}^{b(ij)}, \theta^0, u) + H(\hat{y}^{b(ij)} - y) \\ \hat{y}^{b(ij)} = [c_1 \hat{x}^{b(ij)} \quad \dots \quad \hat{y}^{obb(ij)}(t) \quad \dots \quad c_q \hat{x}^{b(ij)}]^T \\ e_y^{b(ij)} = \hat{y}^{b(ij)} - y \end{cases} \quad (4.37)$$

where

$$\hat{y}_j^{oba(ij)}(t) = \begin{cases} c_j \hat{x}^{a(ij)}, & t < t_f \\ c_j \hat{x}^{a(ij)} + \Delta_j^{a(ij)}, & t \geq t_f \end{cases} \quad \hat{y}_l^{oba(ij)}(t) = c_l \hat{x}^{a(ij)} \quad \forall t, \quad l \neq j$$

$$\hat{y}_j^{obb(ij)}(t) = \begin{cases} c_j \hat{x}^{b(ij)}, & t < t_f \\ c_j \hat{x}^{b(ij)} + \Delta_j^{b(ij)}, & t \geq t_f \end{cases} \quad \hat{y}_l^{obb(ij)}(t) = c_l \hat{x}^{b(ij)} \quad \forall t, \quad l \neq j$$

The fault detection is the same with that used in dynamic fault case. Once the fault is detected, the performance of estimation error between the observers and real system e_y are analyzed. And then, the isolation index of each interval is calculated:

$$v^{(ij)}(t) = \text{sgn}(e_y^{a(ij)}(t)) \text{sgn}(e_y^{b(ij)}(t)) \quad (4.38)$$

The principle to isolate the fault is the same as the one we used before. If the faulty parameter value is contained in this interval, then $v^{(ij)}(t) = 1$. Otherwise, $v^{(ij)}(t) = -1$.

Since the faulty measured output is easily got, what we need to do in the identification part is to find out the faulty variance value Δ^f . Suppose that the fault has been isolated in the i th interval of j th sensor, the fault value can be identified at the same time:

$$\hat{f}_{s_j} = \frac{1}{2}(\Delta_j^{a(ij)} + \Delta_j^{b(ij)}) \quad (4.39)$$

4.5.3 Application to HEX reactor: interval observer based FDD scheme

The interval observer based FDD scheme is applied to the HEX reactor (4.20). The same initial values are given to the considered HEX reactor model. The same faulty situation is used as the former section, dynamic fault and sensor fault are introduced respectively.

Simulation with dynamic fault

The dynamic fault vector considered is $[h_p \quad T_{p,in}]^T$, and their nominal values are $[h_p^0 \quad T_{p,in}^0]^T = [7.5975 \times 10^3 \quad 77]^T$. Both parameters are divided into five intervals, the bounds of each interval are given in Table 4.3 and Table 4.4. The interval diving of h_p is different percentages of its nominal value h_p^0 .

Once the fault is detected, the parameter of observers will changes to the preselected value, i.e. every observer will use the parameter value corresponds to each bound. In

Table 4.3: The value of interval bounds for h_p

No. of interval	1	2	3	4	5
$h_p^{(a)}$	100%	90%	80%	70%	60%
$h_p^{(b)}$	90%	80%	70%	60%	50%

Table 4.4: The value of interval bounds for $T_{p,in}$

No. of interval	1	2	3	4	5
$T_{p,in}^{(a)}$	81	79	77	75	73
$T_{p,in}^{(b)}$	79	77	75	73	71

our case, both possible faulty parameters are divided into five intervals with six bounds. So, twelve observers are constructed in total.

In this part, the same dynamic faults, $f_{p1} = -15\%h_p^0$, $f_{p2} = -5$ in heat transfer coefficient h_p and the inlet process fluid temperature $T_{p,in}$, are applied to the considered HEX reactor (4.20). The performances of the reactor in presence of fault have been presented in the former section Figure 4.2 and Figure 4.5. So, we will focus on the fault isolation and identification part.

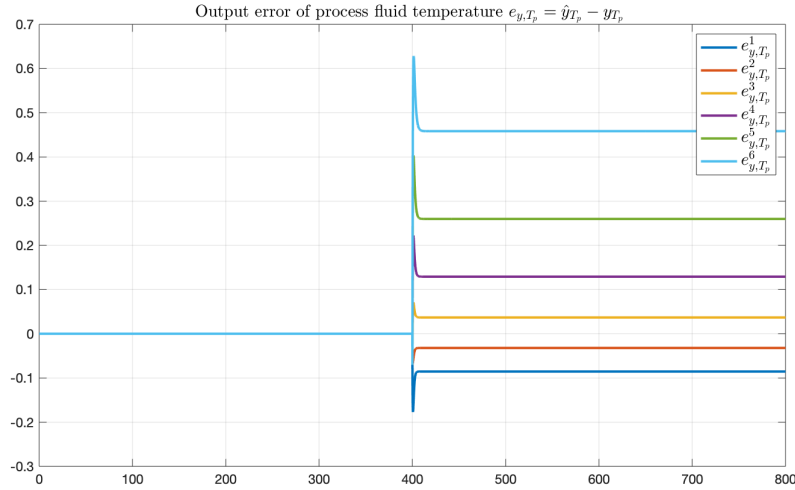


Figure 4.14: Output errors e_{y,T_p} correspond to intervals of h_p when dynamic h_p is faulty at 400s

First of all, the fault is introduced in the first parameter h_p at 400s, it decreases to 85% of its nominal value. To isolate the fault, we verify the performances of output errors shown in Figure 4.14 and Figure 4.15. We can easily find that the sign of the

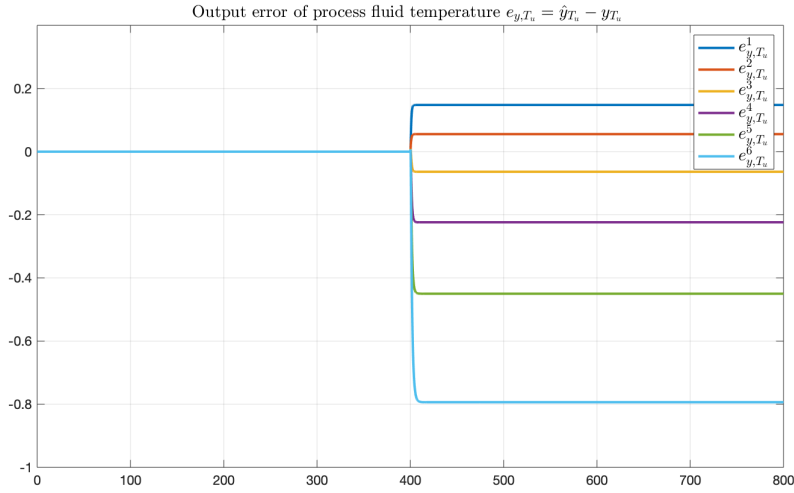


Figure 4.15: Output errors e_{y,T_u} correspond to intervals of h_p when dynamic h_p is faulty at 400s

second output error and third output error are different after $t = 400s$. They lie on both sides of zero. After checking the interval bounds value in Table 4.3, they correspond to the second bound and third bound of h_p interval. That means the fault is located in this interval [80%, 90%] of parameter h_p . Thus, the fault is isolated.

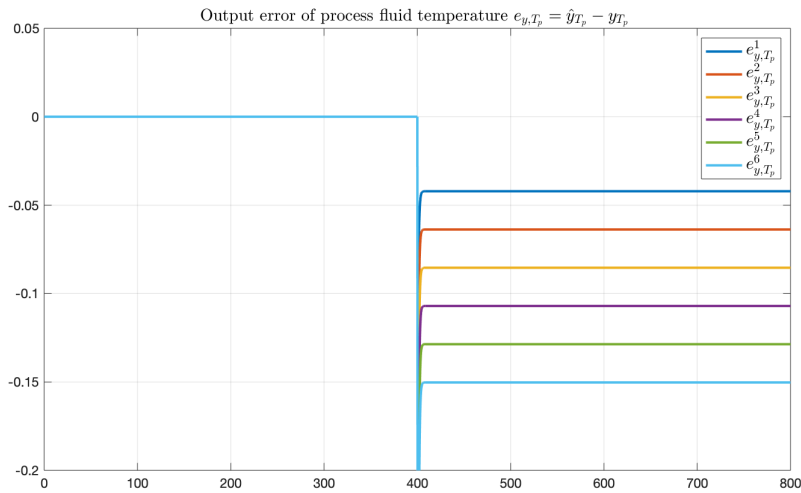


Figure 4.16: Output errors e_{y,T_p} correspond to intervals of $T_{p,in}$ when dynamic h_p is faulty at 400s

We should pay attention that both output errors e_{y,T_p} and e_{y,T_u} should be considered. For instance, in Figure 4.14, $e_{y,T_p}^{(2)}$ and $e_{y,T_p}^{(3)}$ lie in different sides of zero. Only if we make sure that the output error $e_{y,T_u}^{(2)}$ and $e_{y,T_u}^{(3)}$ also locate in different sides of zero, can

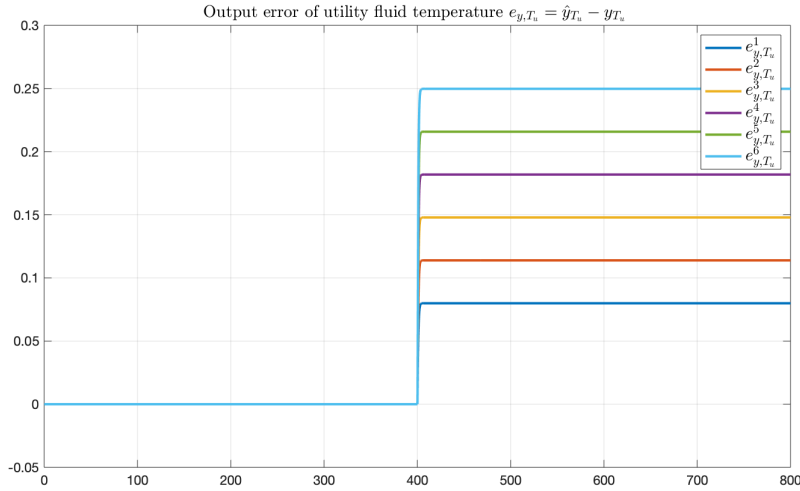


Figure 4.17: Output errors e_{y,T_u} correspond to intervals of $T_{p,in}$ when dynamic h_p is faulty at 400s

we judge that the faulty parameter is contained in the second interval. Otherwise, if $e_{y,T_p}^{(2)}$ and $e_{y,T_p}^{(3)}$ stay in different sides of zero, while $e_{y,T_u}^{(2)}$ and $e_{y,T_u}^{(3)}$ lie in the same side of zero, then, the fault is not contained in the second interval.

However, we should not forget that, there are several observers whose parameters are changed to the preselected bounds correspond to the second parameter $T_{p,in}$ once the fault is detected. The output errors between the interval observers corresponding to $T_{p,in}$ and real system are shown in Figure 4.16 and Figure 4.17. For both output error of process fluid temperature e_{y,T_p} and output error of utility fluid temperature e_{y,T_u} , they all stay on the same side of zero, either the negative side or the positive side. That is to say, the fault is not located in the intervals of $T_{p,in}$.

Therefore, the fault is isolated in the second interval of parameter h_p , and its identification can be obtained easily by the following:

$$\begin{aligned}
 \hat{h}_p^f &= \frac{1}{2}(h_p^{(2)} + h_p^{(3)}) \\
 &= \frac{1}{2}(90\%h_p^0 + 80\%h_p^0) \\
 &= 85\%h_p^0
 \end{aligned} \tag{4.40}$$

In the second case, the fault is introduced at the second parameter $T_{p,in}$, the inlet temperature of process fluid decrease to $72^\circ C$ from its nominal value $T_{p,in}^0 = 77^\circ C$ at 400s. Once the fault is detected, the observer parameter changes to the preselected value. The bounds of intervals corresponding to each parameter are the same as in Table 4.3 and Table 4.4.

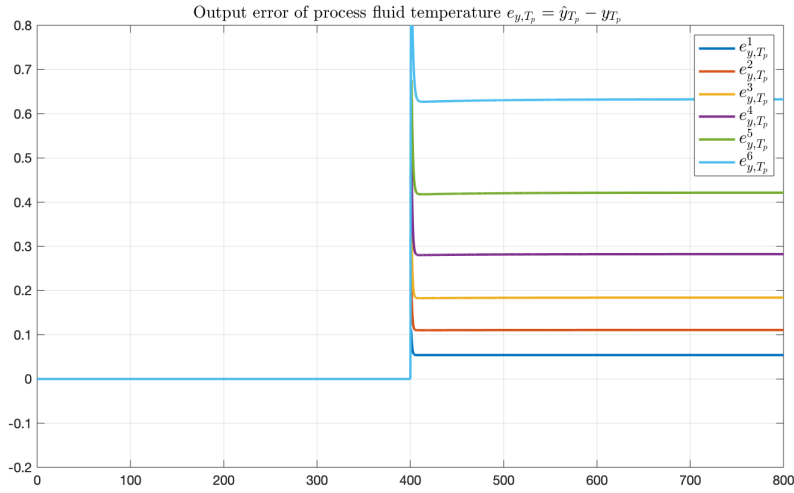


Figure 4.18: Output errors e_{y,T_p} correspond to intervals of h_p when dynamic $T_{p,in}$ is faulty at 400s

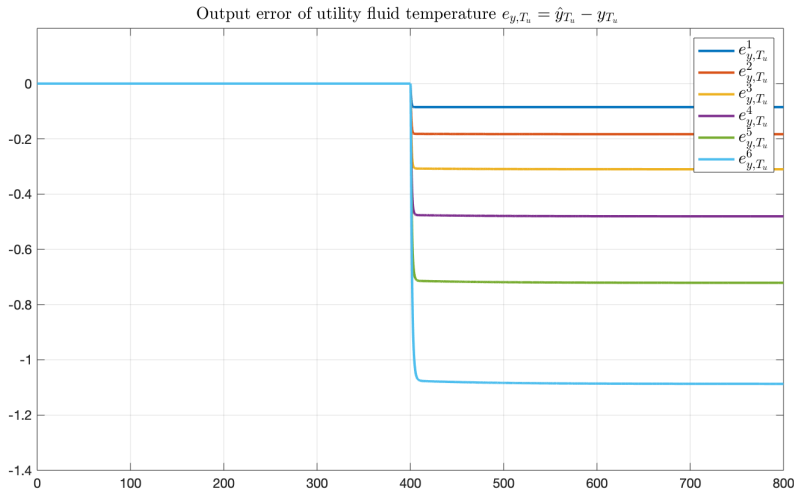


Figure 4.19: Output errors e_{y,T_u} correspond to intervals of h_p when dynamic $T_{p,in}$ is faulty at 400s

Figure 4.18 and Figure 4.19 present the output error e_{y,T_p} and e_{y,T_u} corresponding to the interval of h_p . All the output error e_{y,T_p} between h_p interval observers and real system stay in the upper side of zero, while e_{y,T_u} stay under zero. That means the faulty parameter does not lie in the interval of h_p .

Then, we check the performances of the observer whose parameter is changed at $T_{p,in}$. The output errors of process fluid temperature e_{y,T_p} between $T_{p,in}$ interval observers and real system are presented in Figure 4.20. We can find that the error

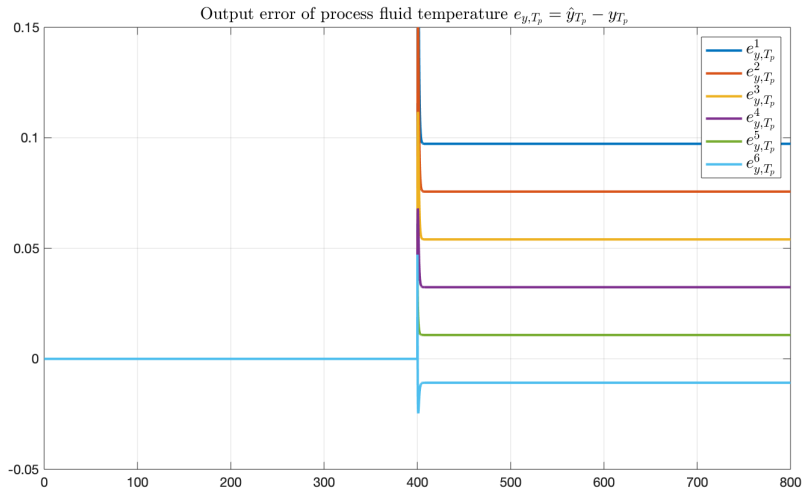


Figure 4.20: Output errors e_{y,T_p} correspond to intervals of $T_{p,in}$ when dynamic $T_{p,in}$ is faulty at 400s

corresponding to the sixth bound of $T_{p,in}$ interval lies under zero, while the fifth bound of $T_{p,in}$ interval locates in the upper side of zero.

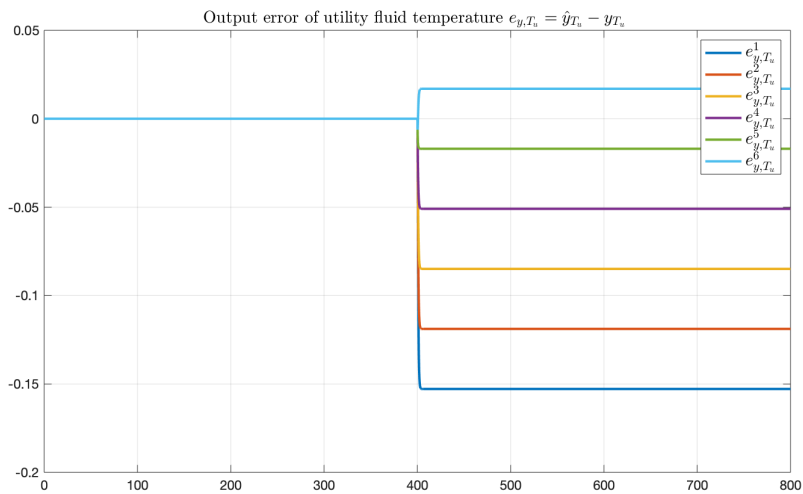


Figure 4.21: Output errors e_{y,T_u} correspond to intervals of $T_{p,in}$ when dynamic $T_{p,in}$ is faulty at 400s

Figure 4.21 shows the output error of utility fluid temperature e_{y,T_u} between $T_{p,in}$ interval observers and real system. It has the same phenomenon that the fifth bound and the sixth bound of $T_{p,in}$ interval stay in different sides of zero. Therefore, we can conclude that the faulty parameter is contained in the fifth interval $[71, 73]$ of $T_{p,in}$ parameters.

Therefore, we can calculate the estimation of faulty value by calculating the average value of the interval bounds:

$$\begin{aligned}
\hat{T}_{p,in}^f &= \frac{1}{2}(T_{p,in}^{(5)} + T_{p,in}^{(6)}) \\
&= \frac{1}{2}(71 + 73) \\
&= 72
\end{aligned} \tag{4.41}$$

Simulation with sensor fault

In this part, sensor faults $f_{s1} = 3 \text{ } ^\circ\text{C}$, $f_{s2} = 7 \text{ } ^\circ\text{C}$ are introduced to the sensor of process fluid temperature T_p and the sensor of the utility fluid temperature T_u . The performances of the faulty reactor have been shown in Figure 4.8 and Figure 4.11.

To isolate and identify the fault, the possible variation of each sensor is divided into four intervals with five bounds. They are presented in Table 4.5 and Table 4.6. Once the fault is detected, the measured output of the observer will vary in the way expressed in (4.35). In our case, we consider two possible faulty sensors, and each possible variation range is divided into four intervals with five bounds. Thus, ten observers are constructed in total.

Table 4.5: The value of variation Δ_{T_p} interval bounds for sensor T_p

No. of interval	1	2	3	4
$\Delta_{T_p}^{(a)}$	0	2	4	6
$\Delta_{T_p}^{(b)}$	2	4	6	8

Table 4.6: The value of variation Δ_{T_u} interval bounds for sensor T_u

No. of interval	1	2	3	4
$\Delta_{T_u}^{(a)}$	0	2	4	6
$\Delta_{T_u}^{(b)}$	2	4	6	8

At the beginning, we will consider the fault $f_{s1} = 3 \text{ } ^\circ\text{C}$ in the first sensor, the process fluid temperature sensor $s1$. Once the fault is detected, the measured output of each observer varies to different values in Table 4.5 and Table 4.6.

Figure 4.22 and Figure 4.23 shows the performances of measured output error between the measurements of observers with Δ_{T_p} variations and the measurements of the system (the output of sensor). In Figure 4.22, the sign of the second measured output error e_{y,mea,T_p}^2 are different from the sign of the third measured output error e_{y,mea,T_p}^3 .

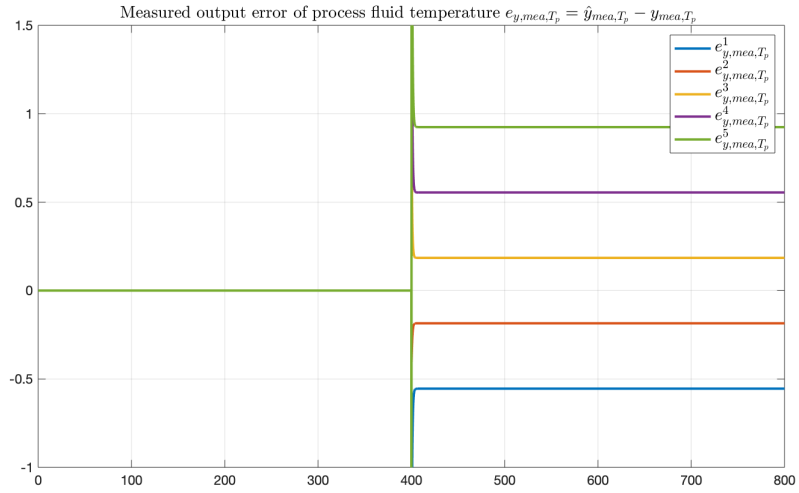


Figure 4.22: Output errors e_{y,mea,T_p} correspond to variation intervals of Δ_{T_p} when sensor T_p is faulty at 400s

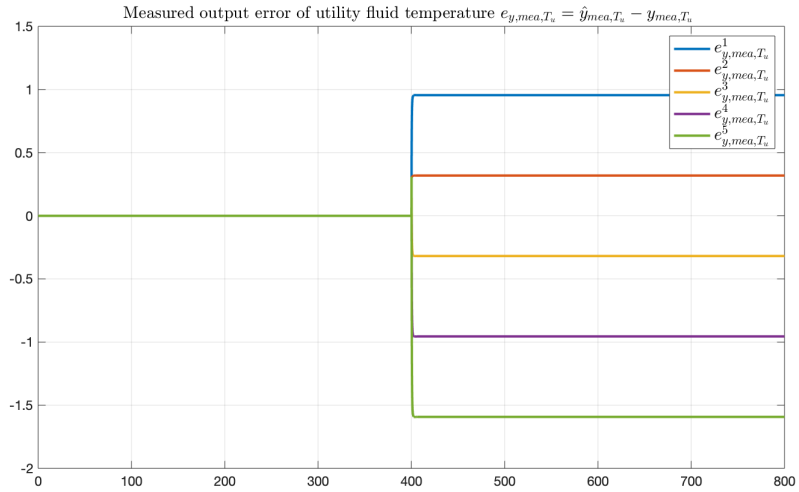


Figure 4.23: Output errors e_{y,mea,T_u} correspond to variation intervals of Δ_{T_p} when sensor T_p is faulty at 400s

Figure 4.23 shows the same phenomena, the zero is sandwiched by the second measured output error e_{y,mea,T_u}^2 and the third measured output error e_{y,mea,T_u}^3 . That indicates the faulty value is located in the second interval $[2, 4]$ of variation Δ_{T_p} .

To make sure we have isolated the faulty parameter correctly, we need to check the performance of other observers who has the parameter change in the second sensor Δ_{T_u} . Once the fault is detected, the second element of measured output of observers y_{T_u} are changed according to Table 4.6. The measurement error between these observers and

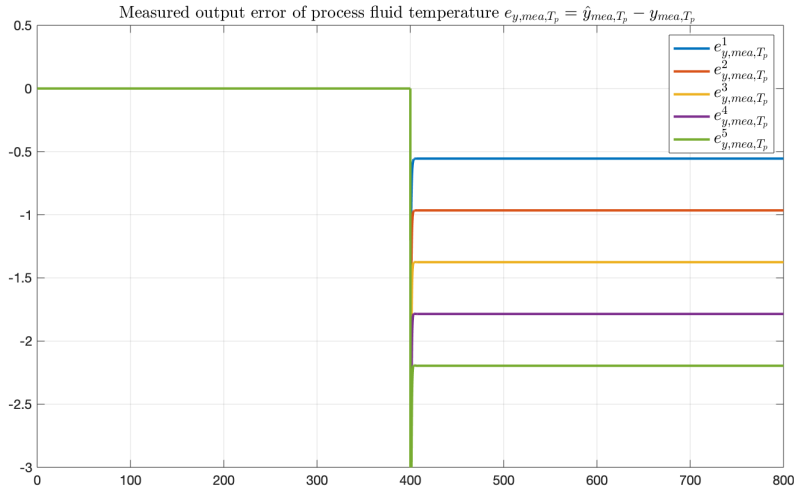


Figure 4.24: Output errors e_{y,mea,T_p} correspond to variation intervals of ΔT_u when sensor T_p is faulty at 400s

the measurement of the real system is presented in Figure 4.24 and Figure 4.25. It is obvious that measured output error between the interval observer corresponding to ΔT_u variation and the measurement of the real system are located on the same side of zero, either the upper side for e_{y,mea,T_p} or the lower side for e_{y,mea,T_u} . According to our isolation principle, the same sign means the fault is not located in these intervals of ΔT_u variation.

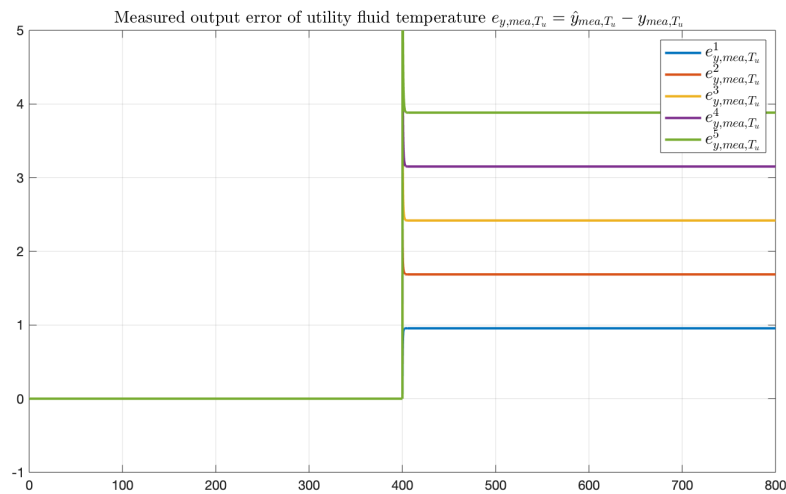


Figure 4.25: Output errors e_{y,mea,T_u} correspond to variation intervals of ΔT_u when sensor T_p is faulty at 400s

Thus, the estimation of the faulty value can be calculated by using the bounds value

of the first interval:

$$\begin{aligned}
 \hat{f}_{s1} &= \frac{1}{2}(\Delta_{T_p}^{(2)} + \Delta_{T_p}^{(3)}) \\
 &= \frac{1}{2}(2 + 4) \\
 &= 3
 \end{aligned} \tag{4.42}$$

and the value is the same as the fault we introduced.

In the second case, the sensor fault $f_{s2} = 7 \text{ }^\circ\text{C}$ is introduced in the utility fluid temperature sensor $s2$ at 400s . Then, the faulty output of sensor (the measurement of the system) is $y_2^f = y_2 + f_{s2}$.

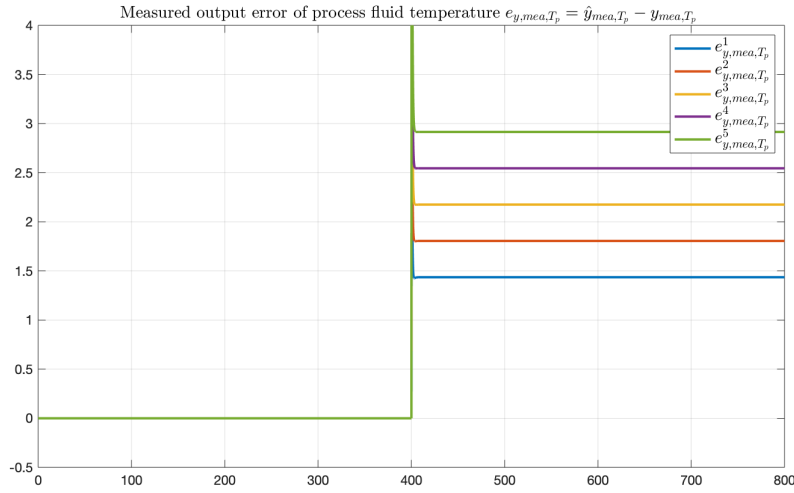


Figure 4.26: Output errors e_{y,mea,T_p} correspond to variation intervals of Δ_{T_p} when sensor T_u is faulty at 400s

The measured output errors $e_{y,mea}$ between the variation Δ_{T_p} interval observers and the measurement of the system are presented in Figure 4.26 and Figure 4.27. It is obvious that all the measured output errors e_{y,mea,T_p} stay on the same side of zero. And all the e_{y,mea,T_u} perform in the same way, they all lie under zero. So, the faulty value is not contained in any of the preselected intervals.

Then, we check the performance of the observers whose measured output changes at Δ_{T_u} . The measured output error $e_{y,mea}$ between these observers and the measurement of the system are presented in Figure 4.28 and Figure 4.29. We can find that in Figure 4.28, the performances of e_{y,mea,T_p}^4 and e_{y,mea,T_p}^5 lie in different sides of zero. That may indicate the existence of faulty value. Then, we have to check if the fourth measured output error of utility temperature e_{y,mea,T_u}^4 and the fifth measured output error of utility temperature e_{y,mea,T_u}^5 has the same trend in Figure 4.29. We can easily find that

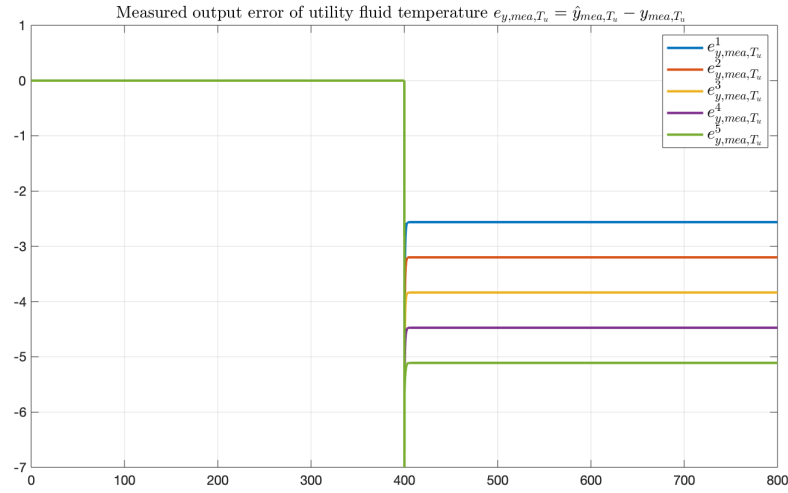


Figure 4.27: Output errors e_{y,mea,T_u} correspond to variation intervals of Δ_{T_p} when sensor T_u is faulty at 400s

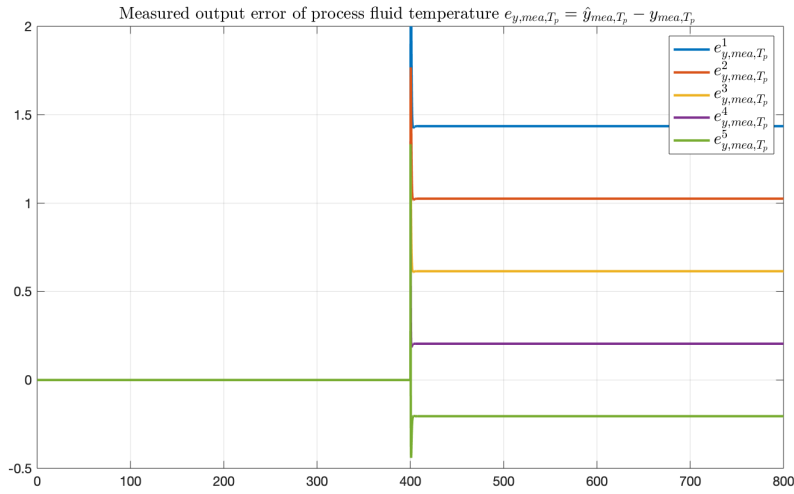


Figure 4.28: Output errors e_{y,mea,T_p} correspond to variation intervals of Δ_{T_u} when sensor T_u is faulty at 400s

the zero is sandwiched by these two lines e_{y,mea,T_u}^4 and e_{y,mea,T_u}^5 . And they correspond to the fourth bound and fifth bound of variance Δ_{T_u} interval. Therefore, we can conclude that the faulty value is contained in the fourth interval $[6, 8]$ of Δ_{T_u} .

Finally, the sensor fault is isolated in the second sensor s_2 . Since we have bounded

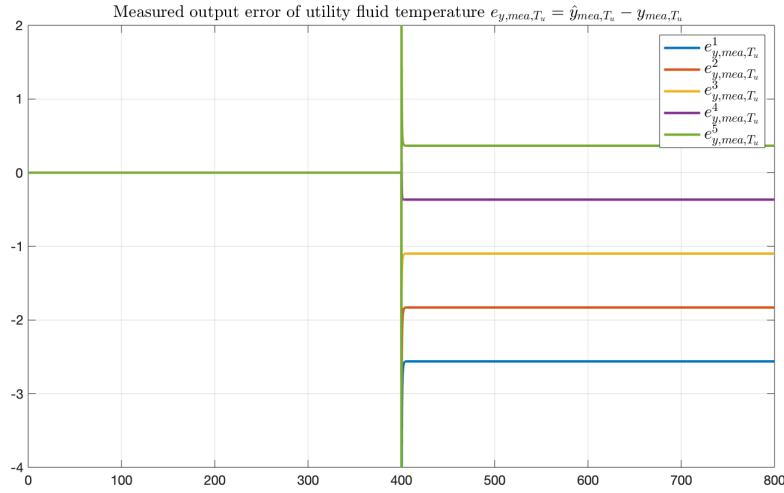


Figure 4.29: Output errors e_{y,mea,T_u} correspond to variation intervals of Δ_{T_u} when sensor T_u is faulty at 400s

the faulty value in one small interval, then it can be easily calculated:

$$\begin{aligned}
 \hat{f}_{s2} &= \frac{1}{2}(\Delta_{T_u}^{(4)} + \Delta_{T_u}^{(5)}) \\
 &= \frac{1}{2}(6 + 8) \\
 &= 7
 \end{aligned} \tag{4.43}$$

According to the simulation results, we can conclude that both dynamic fault and sensor fault are well detected and diagnosed by the presented interval observer based FDD scheme.

4.6 Summary

This chapter started from an overview of the existing observers in the past decades. Basic properties of nonlinear systems, such as indistinguishability, observability, etc have been introduced firstly. Besides, the dynamic and sensor faulty model were also constructed. Then, we mainly focused on the introduction of two kinds of observers, adaptive observer and interval observers. Their structures, as well as the FDD schemes based on these two observers were all presented. Both observer based FDD schemes were applied to the HEX reactor to validate their effectiveness. According to the simulation results, not only the dynamic fault but also the sensor fault could be well detected, isolated and identified.

Chapter 5

Backstepping controller design for the Heat-exchanger/Reactor

Backstepping [74] [79] is a recursive procedure that breaks a controller design problem for the full system into a sequence of design problems for lower order systems. In this chapter, a backstepping controller is designed for the nonlinear HEX reactor. Firstly, various backstepping design techniques, including integrator backstepping, backstepping for strict-feedback systems, adaptive backstepping, and robust backstepping, for nonlinear systems are reviewed. And then, the recursive backstepping controller design procedure is presented for the considered HEX reactor. Finally, simulation results are presented to prove the control ability of the designed controller.

5.1 Backstepping design

In this section, the backstepping design is introduced. The key idea of backstepping is to start with a system which is stabilizable with a known feedback law for a known Lyapunov function, and then to add to its input an integrator [74]. First, the backstepping procedure for scalar systems which are extended with a single integrator is given. Then, using this integrator backstepping approach, a recursive design procedure for strict feedback systems is defined. Besides, the adaptive backstepping and the robust backstepping design procedures for a class of nonlinear systems with uncertainties are also presented.

5.1.1 Integrator backstepping

Integrator backstepping as a design tool is based on the following assumption.

Assumption 5.1:

Consider a system

$$\dot{x} = f(x) + g(x)u, \quad f(0) = 0 \quad (5.1)$$

where $x \in \mathcal{R}^n$ is the state, and $u \in \mathcal{R}$ is the control input. There exist a continuously differentiable feedback control law

$$u = \alpha(x), \quad \alpha(0) = 0 \quad (5.2)$$

and a smooth, positive definite, radially unbounded function $V : \mathcal{R}^n \rightarrow \mathcal{R}_+$ such that

$$\frac{\partial V}{\partial x}(x) [f(x) + g(x)\alpha(x)] \leq -W(x) \leq 0, \quad \forall x \in \mathcal{R}^n \quad (5.3)$$

where $W : \mathcal{R}^n \rightarrow \mathcal{R}$ is positive semidefinite.

Under this assumption, the control signal (5.2) applied to the system (5.1) guarantees global boundedness of $x(t)$, and via the LaSalle-Yoshizawa theorem [79], the regulation of $W(x(t))$:

$$\lim_{t \rightarrow \infty} W(x(t)) = 0 \quad (5.4)$$

The result of integrator backstepping is summarized in the following lemma.

Lemma 5.1 (Integrator Backstepping [79]):

Let the system 5.1 be augmented with an integrator

$$\dot{x}_1 = f(x_1) + g(x_1)x_2 \quad (5.5a)$$

$$\dot{x}_2 = u \quad (5.5b)$$

and suppose that (5.5a) satisfies assumption 5.1 with $x_2 \in \mathcal{R}$ as its control.

- If $W(x_1)$ is positive definite, then

$$V_a(x_1, x_2) = V(x_1) + \frac{1}{2} [x_2 - \alpha(x_1)]^2 \quad (5.6)$$

is a control Lyapunov function (CLF) for the full system (5.5), that is, there exists a feedback control $u = \alpha_a(x_1, x_2)$ which renders $x_1 = 0, x_2 = 0$ the global asymptotically stable (GAS) equilibrium of (5.5). one such control is

$$u = -c(x_2 - \alpha(x_1)) + \frac{\partial \alpha}{\partial x_1}(x_1) [f(x_1) + g(x_1)x_2] - \frac{\partial V}{\partial x_1}(x_1)g(x_1), \quad c > 0 \quad (5.7)$$

- If $W(x_1)$ is only positive semidefinite, then there exists a feedback control which renders $\dot{V}_a \leq -W_a(x_1, x_2) \leq 0$, such that $W_a(x_1, x_2) > 0$ whenever $W(x_1) > 0$ or $x_2 \neq \alpha(x_1)$. This guarantees global boundedness and convergence of $\begin{bmatrix} x_1(t) \\ x_2(t) \end{bmatrix}$ to the largest invariant set M_a contained in the set

$$E_a = \left\{ \begin{bmatrix} x_1 \\ x_2 \end{bmatrix} \in \mathcal{R}^{n+1} \mid W(x_1) = 0, \quad x_2 = \alpha(x_1) \right\}$$

The proof is given in chapter 2 of [79].

5.1.2 Backstepping for strict-feedback systems

Based on the recursive implementation of the integrator backstepping methodology, the same controller design procedure can be applied recursively to a strict feedback system of a higher order. The only difference is that there are more "virtual states" to step through. The method starts with the state separated from the actual control input by the largest number of integrators, and at each step, the backstepping technique can be divided into three parts [118].

Firstly, a virtual control signal and error state variable are introduced. And then, the current state equation can be rewritten in terms of these variables. Secondly, we choose a CLF for the system, treat it as if it were the final stage. Thirdly, a stabilizing feedback term is chosen for the virtual control signal to make the CLF stabilizable.

Consider the following nonlinear strict-feedback systems:

$$\begin{cases} \dot{x}_1 = f_1(x_1) + g_1(x_1)x_2 \\ \dot{x}_2 = f_2(x_1, x_2) + g_2(x_1, x_2)x_3 \\ \dots \\ \dot{x}_i = f_i(x_1, x_2, \dots, x_i) + g_i(x_1, x_2, \dots, x_i)x_{i+1} \\ \dots \\ \dot{x}_n = f_n(x_1, x_2, \dots, x_n) + g_n(x_1, x_2, \dots, x_n)u \end{cases} \quad (5.8)$$

where $x_j \in \mathcal{R}$, $u \in \mathcal{R}$ and $g_j \neq 0 \forall x$. The control objective is to let $y = x_1$ asymptotically track a reference signal $y_{ref}(t)$ whose first n derivatives are assumed known and bounded. The backstepping starts by defining the tracking errors:

$$z_i = x_i - \alpha_{i-1} \quad (5.9)$$

where $\alpha_0 = y_{ref}$, and rewrite the dynamics of the error system as:

$$\dot{z}_i = f_i(x_1, \dots, x_i) + g_i(x_1, \dots, x_i)x_{i+1} - \dot{\alpha}_{i-1} \quad (5.10)$$

where $x_{n+1} = u$.

Then, for each subsystem, a CLF function $V_i(z_1, \dots, z_i)$ is constructed as:

$$\dot{V}_i(z_1, \dots, z_i) = V_{i-1}(z_1, \dots, z_{i-1}) + \frac{1}{2}z_i^T z_i \quad (5.11)$$

where α_i is a stabilizing feedback law that satisfies (5.3) for the x_{i-1} -subsystem. Such intermediate control laws are called stabilizing functions or virtual control laws.

Now, the derivative of V_i with respect to time has to be made non-positive when $x_{i+1} = \alpha_i$. Thus, a possible feedback control law is obtained:

$$\alpha_i(x_1, \dots, x_i) = g_i^{-1}(-c_i z_i - f_i + \dot{\alpha}_{i-1} - g_{i-1}^T z_{i-1}) \quad (5.12)$$

with gains $c_i > 0$.

Theorem 5.1 (Recursive backstepping design for tracking):

If V_n is radially unbounded and $g_i \neq 0$ holds globally, then the closed-loop system consisting of the tracking error dynamics (5.10) and the feedback control laws (5.12) has a globally asymptotic equilibrium at $(z_1, \dots, z_n) = 0$, and $z_i \rightarrow 0$ as $t \rightarrow \infty$. Since the tracking errors go to zero, this means that global asymptotic tracking is achieved:

$$\lim_{t \rightarrow \infty} z_1 = \lim_{t \rightarrow \infty} (x_1 - y_{ref}) = 0 \quad (5.13)$$

5.1.3 Adaptive backstepping

In the previous two subsections, the backstepping designs for nonlinear systems satisfying certain structured properties are presented. When there are unknown parameters in the system, the former backstepping methods cannot be used. However, an adaptive backstepping design is suitable for this kind of situation. Examples in [79] [74] present the procedure of the adaptive backstepping design clearly. As shown in [118], this approach can be divided into adaptive integrator backstepping and recursive adaptive backstepping according to different forms of the nonlinear systems.

Adaptive integrator backstepping

Even though the integrator backstepping design cannot be applied to the system with unknown parameters, its main idea can still be used. The adaptive backstepping is based on the following assumption:

Assumption 5.2:

Consider the system

$$\dot{x} = f(x) + F(x)\theta + g(x)u \quad (5.14)$$

where $x \in \mathcal{R}^n$ is the state vector, $\theta \in \mathcal{R}^p$ is a vector of unknown constant parameters, and $u \in \mathcal{R}$ is the control input. There exist an adaptive controller

$$\begin{aligned} u &= \alpha(x, \hat{\theta}_1) \\ \dot{\hat{\theta}}_1 &= T(x, \hat{\theta}_1) \end{aligned} \quad (5.15)$$

where $\hat{\theta}_1 \in \mathcal{R}^q$ is the parameter estimation, and a smooth function $V(x, \hat{\theta}_1) : \mathcal{R}^{n+q} \rightarrow \mathcal{R}$ which is positive definite and radially unbounded in the variables $(x, \hat{\theta}_1 - \theta)$ such that for all $(x, \hat{\theta}_1) \in \mathcal{R}^{n+q}$:

$$\frac{\partial V}{\partial x}(x, \hat{\theta}_1) [f(x) + F(x)\theta + g(x)\alpha(x, \hat{\theta}_1)] + \frac{\partial V}{\partial \hat{\theta}_1}(x, \hat{\theta}_1)T(x, \hat{\theta}_1) \leq -W(x, \hat{\theta}_1) \leq 0 \quad (5.16)$$

where $W : \mathcal{R}^{n+q} \rightarrow \mathcal{R}$ is positive semidefinite.

Under this assumption, the control signal (5.15), which is applied to the system (5.14), guarantees global boundedness of $x(t)$, $\hat{\theta}_1$, and, by the LaSalle-Yoshizawa theorem [79], regulation of $W(x(t), \hat{\theta}_1)$ converges to zero as $t \rightarrow \infty$. Besides, adaptive integrator backstepping allows us to achieve the same properties for the augmented system.

Lemma 5.2 (Adaptive integrator backstepping):

Let the system (5.14) be augmented by an integrator,

$$\dot{x}_1 = f(x_1) + F(x_1)\theta + g(x_1)x_2 \quad (5.17a)$$

$$\dot{x}_2 = u \quad (5.17b)$$

where $x_2 \in \mathcal{R}$.

Consider for this system the dynamic feedback controller

$$u = -c(x_2 - \alpha(x_1, \hat{\theta}_1)) + \frac{\partial \alpha}{\partial x_1}(x_1, \hat{\theta}_1) [f(x_1) + F(x_1)\hat{\theta}_2 + g(x_1)x_2] + \frac{\partial \alpha}{\partial \hat{\theta}_1}(x_1, \hat{\theta}_1)T(x_1, \hat{\theta}_1) - \frac{\partial V}{\partial x_1}(x_1, \hat{\theta}_1)g(x_1), \quad c > 0 \quad (5.18a)$$

$$\dot{\hat{\theta}}_1 = T(x_1, \hat{\theta}_1) \quad (5.18b)$$

$$\dot{\hat{\theta}}_2 = -\Gamma \left[\frac{\partial \alpha}{\partial x_1}(x_1, \hat{\theta}_1)F(x_1) \right]^T (x_2 - \alpha(x_1, \hat{\theta}_1)) \quad (5.18c)$$

where $\hat{\theta}_2$ is a new estimate of θ , $\Gamma = \Gamma^T > 0$ is the adaptation gain matrix. Under Assumption 5.2, this adaptive controller guarantees global boundedness of $x_1(t)$, $x_2(t)$, $\hat{\theta}_1$, $\hat{\theta}_2$, and the regulation of $W(x_1(t), \hat{\theta}_1)$ and $(x_2(t) - \alpha(x_1(t), \hat{\theta}_1))$ go to zero as $t \rightarrow \infty$. These properties can be established with the Lyapunov function:

$$V_a(x_1, x_2, \hat{\theta}_1, \hat{\theta}_2) = V(x_1, \hat{\theta}_1) + \frac{1}{2} [x_2 - \alpha(x_1, \hat{\theta}_1)]^2 + \frac{1}{2} (\theta - \hat{\theta}_2)^T \Gamma^{-1} (\theta - \hat{\theta}_2) \quad (5.19)$$

The proof in detail can be found in chapter 3 of [79].

Recursive adaptive backstepping for strict-feedback systems

The same controller design procedure can be applied repeatedly to the nonlinear systems which can be transformed through a diffeomorphism into parametric strict-feedback form [118]:

$$\begin{cases} \dot{x}_1 = x_2 + f_1(x_1) + \varphi_1^T(x_1)\theta \\ \dot{x}_2 = x_3 + f_2(x_1, x_2) + \varphi_2^T(x_1, x_2)\theta \\ \dots \\ \dot{x}_{n-1} = x_n + f_{n-1}(x_1, \dots, x_{n-1}) + \varphi_{n-1}^T(x_1, \dots, x_{n-1})\theta \\ \dot{x}_n = f_n(x) + g(x)u + \varphi_n^T(x_1, \dots, x_n)\theta \end{cases} \quad (5.20)$$

where $g(x) \neq 0$ for all $x \in \mathcal{R}^n$, f represents the known dynamics, and $\theta \in \mathcal{R}^p$ is the unknown constant parameter vector. For these systems, n design steps are required

which is equal to the relative degree of the system. At each step, an error variable z_i , a stabilizing function α_i , and a parameter estimation θ_i are generated. Therefore, if a system has p unknown parameters, the controller has to estimate $p \times n$ parameter estimations.

A controller for the system (5.20) can be designed which achieves tracking of a differentiable reference signal y_{ref} . Introduce the tracking errors:

$$z_i = x_i - \alpha_{i-1}(x_1, \dots, x_{i-1}, y_{ref}, \dots, y_{ref}^{i-1}, \hat{\theta}_1, \dots, \hat{\theta}_{i-1}) \quad (5.21)$$

with $\alpha_0 = y_{ref}$, $z_0 = 0$. Then, the stabilizing functions α_i are defined by:

$$\begin{aligned} \alpha_i = & -c_i z_i - z_{i-1} - f_i - \left(\varphi_i - \sum_{j=1}^{i-1} \frac{\partial \alpha_{i-1}}{\partial x_j} \varphi_j \right)^T \hat{\theta}_i \\ & + \sum_{j=1}^{i-1} \left[\frac{\partial \alpha_{i-1}}{\partial x_j} (x_{j+1} + f_{j+1}) + \frac{\partial \alpha_{i-1}}{\partial \hat{\theta}_j} \Gamma_j \left(\varphi_j - \sum_{k=1}^{j-1} \frac{\partial \alpha_{j-1}}{\partial x_k} \varphi_k \right) z_j \right] \end{aligned} \quad (5.22)$$

The control law for u and parameter update laws for each θ_i are defined by:

$$\begin{aligned} u = & g^{-1}(x) \alpha_n(x, y_{ref}, \dots, y_{ref}^n, \hat{\theta}_1, \dots, \hat{\theta}_n) \\ \dot{\hat{\theta}}_i = & \Gamma_i \left(\varphi_i - \sum_{j=1}^{i-1} \frac{\partial \alpha_{i-1}}{\partial x_j} \varphi_j \right) z_i \end{aligned} \quad (5.23)$$

where $\Gamma_i = \Gamma_i^T > 0$ is the adaptation gain matrix, $c_i > 0$ are the controller gains. The controller design (5.22) (5.23) guarantee global boundedness of $x(t)$, $\hat{\theta}_1(t)$, \dots , $\hat{\theta}_n(t)$, and regulation of $z(t)$ to zero. Consider then simple quadratic Lyapunov function:

$$V_n(z_1, \dots, z_n, \hat{\theta}_1, \dots, \hat{\theta}_n) = \frac{1}{2} \sum_{i=1}^n \left[z_i^2 + (\theta - \hat{\theta}_i)^T \Gamma_i^{-1} (\theta - \hat{\theta}_i) \right] \quad (5.24)$$

to prove this. Its derivative using the adaptive backstepping control design is:

$$\dot{V}_n = - \sum_{i=1}^n z_i^T c_i z_i \quad (5.25)$$

Thus, convergence of the parameter estimates $\hat{\theta}_i$ is guaranteed, yet they do not necessarily converge to the true value θ .

5.1.4 Robust backstepping

The adaptive backstepping controller is useful for the nonlinear system with an unknown constant. For the system with uncertain nonlinearities, the robust backstepping controller becomes a suitable choice. By adding a nonlinear damping term to the control law, the boundedness of the state vector can be guaranteed.

The robust backstepping design is based on the Assumption 5.3:

Assumption 5.3:

Consider the system:

$$\dot{x} = f(x) + g(x) + F(x)\Delta_1(x, u, t) \quad (5.26)$$

where $x \in \mathcal{R}^n$, $u \in \mathcal{R}$ are state vector and input vector respectively. $F(x)$ is a $n \times q$ matrix of known smooth nonlinear function, and $\Delta_1(x, u, t)$ is a $q \times 1$ vector of uncertain nonlinearities which is uniformly bounded for all values of x, u, t .

Suppose that there exists a feedback control $u = \alpha(x)$ that renders $x(t)$ globally uniformly bounded, and that this is established via positive definite and radially unbounded functions $V(x)$, $W(x)$ and a constant b , such that

$$\frac{\partial V}{\partial x}(x) [f(x) + g(x)\alpha(x) + F(x)\Delta_1(x, u, t)] \leq -W(x) + b \quad (5.27)$$

The results of robust backstepping is presented in the following lemma.

Lemma 5.3 (Boundedness via backstepping):

Consider the augmented system:

$$\begin{cases} \dot{x}_1 = f(x_1) + g(x_1)x_2 + \varphi_1^T(x_1)\Delta_1(x_1, u, t) \\ \dot{x}_2 = u + \varphi_2^T(x_1, x_2)\Delta_2(x_1, x_2, u, t) \end{cases} \quad (5.28)$$

where $\varphi_1(x_1)$ and $\varphi_2(x_1, x_2)$ are vectors of known, smooth nonlinear functions, $\Delta_1(x_1, u, t)$ and $\Delta_2(x_1, x_2, u, t)$ are uncertain nonlinearities vectors which are uniformly bounded for all values x_1, x_2, u and t .

For this system (5.28), the feedback control:

$$u = -c_2(x_2 - \alpha_1) + \frac{\partial \alpha_1}{\partial x_1}(f_1 + g_1 x_2) - g_1^T \frac{\partial V}{\partial x_1} - \left(\varphi_2^T \kappa_2 \varphi_2 + \left(\frac{\partial \alpha_1}{\partial x_1} \varphi_1 \right)^T \mu_2 \frac{\partial \alpha_1}{\partial x_1} \varphi_1 \right) (x_2 - \alpha_1) \quad (5.29)$$

guarantees global uniform boundedness of $x_1(t)$ and $x_2(t)$ with any $c_2 > 0$, $\kappa > 0$, and $\mu_2 > 0$.

Details of proof is presented in chapter 2 of [79].

Then, we consider the class of strict-feedback systems with uncertainties:

$$\begin{cases} \dot{x}_1 = f_1(x_1) + g_1(x_1)x_2 + \varphi_1^T(x_1)\Delta_1(x, u, t) \\ \dot{x}_2 = f_2(x_1, x_2) + g_2(x_1, x_2)x_3 + \varphi_2^T(x_1, x_2)\Delta_2(x, u, t) \\ \dots \\ \dot{x}_n = f_n(x_1, \dots, x_n) + g_n(x_1, \dots, x_n)u + \varphi_n^T(x, u, t) \end{cases} \quad (5.30)$$

where $g_i \neq 0, \forall x \in \mathcal{R}^n$, and $\varphi_i(x_1, \dots, x_i)$ is a $p \times 1$ vector of known smooth nonlinear functions, and $\Delta(x, u, t)$ is a $p \times 1$ vector of uncertain nonlinearities which are uniformly bounded for all values x, u and t .

Then, the state $x(t)$ of system (5.30) is globally, uniformly bounded if the control signal is chosen as:

$$\begin{aligned}
z_i &= x_i - \alpha_{i-1} \\
\alpha_i &= g_i^{-1} \left(-c_i z_i - f_i + \sum_{k=1}^{i-1} \frac{\partial \alpha_{i-1}}{\partial x_k} (f_k + g_k x_{k+1}) - g_{i-1}^T z_{i-1} \right. \\
&\quad + \sum_{k=1}^{i-1} \frac{\partial \alpha_{i-1}}{\partial y_{ref}^{(k-1)}} y_{ref}^{(k)} - \varphi_i^T \kappa_i \varphi_i z_i \\
&\quad \left. - \left(\sum_{j=1}^{i-1} \frac{\partial \alpha_{i-1}}{\partial x_j} \varphi_j \right)^T \mu_i \left(\sum_{j=1}^{i-1} \frac{\partial \alpha_{i-1}}{\partial x_j} \varphi_j \right) \right)
\end{aligned} \tag{5.31}$$

with $\alpha_0 = y_{ref}$, $u = \alpha_n$, $x_{n+1} = u$ and c_i, κ_i, μ_i are positive definite design matrices.

Using the derivative of the Lyapunov function, it can be shown that $z(t)$ is globally uniformly bounded, and that the tracking errors z converge to the compact set

$$\sum_{i=1}^n z_i^T c_i z_i \leq \frac{1}{4} \sum_{i=1}^n \Delta^T \kappa_i^{-1} \Delta + \frac{1}{4} \sum_{i=1}^n \dot{\Delta}^T \mu_i^{-1} \dot{\Delta} \tag{5.32}$$

Examples of robust backstepping design can be found in [118] [74].

5.2 Backstepping controller design for the considered HEX reactor

In chemical processes, temperature control is a principal problem. To guarantee the safety of the whole process, as well as the productivity and efficiencies of the reaction, the temperature of the reactor is usually kept at a proper stable temperature. In this section, we will design a backstepping controller for the considered HEX reactor.

According to the physical structure of the HEX reactor described in Section 3, reactants are injected into the process channel and the chemical reaction is taken place there, while water is injected into the utility channel to heat or take away the reaction heat. So, our control objective is to make the temperature of the process fluid T_p follows the desired value T_{pd} by adjusting the flowrate of utility fluid F_u .

To start, only the heat exchange part is considered in this section, i.e. water with different temperatures is injected into both process channel and utility channel respectively. According to the energy balance equation, the mathematical model of the HEX

reactor is given below in its entirety:

$$\begin{cases} \dot{T}_p = \frac{F_p}{V_p}(T_{p,in} - T_p) + \frac{h_p A_p}{\rho_p V_p C_{p,p}}(T_w - T_p) \\ \dot{T}_u = \frac{F_u}{V_u}(T_{u,in} - T_u) + \frac{h_u A_u}{\rho_u V_u C_{p,u}}(T_w - T_u) \\ \dot{T}_w = \frac{h_p A_p}{\rho_w V_w C_{p,w}}(T_p - T_w) + \frac{h_u A_u}{\rho_w V_w C_{p,w}}(T_u - T_w) \end{cases} \quad (5.33)$$

where the state vector and the measurable output vector are $x^T = [T_p \ T_u \ T_w]$, $y^T = [T_p \ T_u]$ respectively. $T(^{\circ}C)$ represents the temperature, and the subscript p , u and w represent the process fluid, utility fluid and plate wall. $T_{p,in}$ and $T_{u,in}$ are the temperature of the inlet process and utility fluid. The physical data of the HEX reactor has been given in Table 4.2.

In our case, the flow rate of utility fluid F_u is set as the only input to control the temperature of the process fluid T_p , since the inputs of reactants F_p would generally have a fixed optimal proportion and flow rate to have high productive resultants.

5.2.1 Controller design procedure

For the system (5.33), it satisfies the form of strict-feedback systems (5.8). Therefore, the controller design is based on the recursive backstepping for strict-feedback systems, which has been presented in the former section, and the desired process fluid temperature is represented by T_{pd} .

As can be seen from its mathematical model (5.33), the change in the flow rate of utility fluid F_u will firstly result in the temperature change of utility fluid T_u , then, the temperature of plate wall T_w will be influenced in the second step. Finally, the temperature of process fluid T_p will change. To make the process fluid temperature follows the desired value T_{pd} , we have to ‘step back’ until we get the expression of utility fluid flow rate F_u .

Define the process fluid temperature tracking error z_{T_p} between the actual value T_p and desired temperature T_{pd} as:

$$z_{T_p} = T_{pd} - T_p \quad (5.34)$$

The dynamic of z_{T_p} is:

$$\begin{aligned} \dot{z}_{T_p} &= \dot{T}_{pd} - \dot{T}_p \\ &= \dot{T}_{pd} - \frac{F_p}{V_p}(T_{p,in} - T_p) - \frac{h_p A_p}{\rho_p V_p C_{p,p}}(T_w - T_p) \end{aligned} \quad (5.35)$$

And then, a CLF is defined as:

$$V_{T_p} = \frac{1}{2} z_{T_p}^2 \quad (5.36)$$

By deriving (5.36), we obtain:

$$\dot{V}_{T_p} = z_{T_p} \dot{z}_{T_p} = z_{T_p} (\dot{T}_{pd} - \frac{F_p}{V_p} (T_{p,in} - T_p) - \frac{h_p A_p}{\rho_p V_p C_{p,p}} (T_w - T_p)) \quad (5.37)$$

To make \dot{V}_{T_p} negative definite, the temperature of plate wall T_w is chosen as the first virtual element of control to make the tracking error z_{T_p} converge to zero, its desired value T_{wd} is defined as:

$$T_{wd} = \frac{\rho_p V_p C_{p,p}}{h_p A_p} \left[\dot{T}_{pd} + k_1 z_{T_p} - \frac{F_p}{V_p} (T_{p,in} - T_p) \right] + T_p \quad (5.38)$$

where k_1 is a positive design parameter.

By setting $T_w = T_{wd}$ in (5.37), we get:

$$\dot{V}_{T_p} = -k_1 z_{T_p}^2 \leq 0 \quad (5.39)$$

Then, the stability of the tracking error system z_{T_p} is guaranteed.

However, only one step is not enough to get the expression of the backstepping controller F_u . In the next step, we define a tracking error z_{T_w} as:

$$z_{T_w} = T_{wd} - T_w \quad (5.40)$$

and its dynamic is calculated by:

$$\begin{aligned} \dot{z}_{T_w} &= \dot{T}_{wd} - \dot{T}_w \\ &= \frac{\rho_p V_p C_{p,p}}{h_p A_p} (\ddot{T}_{pd} + k_1 \dot{z}_{T_p} + \frac{F_p}{V_p} \dot{T}_p) + \dot{T}_p - \frac{h_p A_p}{\rho_w V_w C_{p,w}} (T_p - T_w) - \frac{h_u A_u}{\rho_w V_w C_{p,w}} (T_u - T_w) \end{aligned} \quad (5.41)$$

In order to guarantee the stability of tracking error system z_{T_w} , we define a CLF:

$$\begin{aligned} V_{T_w} &= \frac{1}{2} z_{T_p}^2 + \frac{1}{2} z_{T_w}^2 \\ &= V_{T_p} + \frac{1}{2} z_{T_w}^2 \end{aligned} \quad (5.42)$$

The dynamic of (5.42) is:

$$\dot{V}_{T_w} = \dot{V}_{T_p} + z_{T_w} \dot{z}_{T_w} \quad (5.43)$$

To make \dot{V}_{T_w} negative definite, the temperature of utility fluid T_u is chosen as the second element of virtual control to stabilizing z_{T_w} , its desired value T_{ud} is defined as:

$$\begin{aligned} T_{ud} &= \frac{\rho_w V_w C_{p,w}}{h_u A_u} \left[\frac{h_p A_p}{\rho_p V_p C_{p,p}} z_{T_p} + \frac{\rho_p V_p C_{p,p}}{h_p A_p} (\ddot{T}_{pd} + k_1 \dot{z}_{T_p} + \frac{F_p}{V_p} \dot{T}_p) + \dot{T}_p \right. \\ &\quad \left. - \frac{h_p A_p}{\rho_w V_w C_{p,w}} (T_p - T_w) + k_2 z_{T_w} \right] + T_w \end{aligned} \quad (5.44)$$

where k_2 is a positive design parameter.

By setting $T_u = T_{ud}$ and substituting (5.41) in (5.43), we obtain that:

$$\dot{V}_{T_w} = -k_1 z_{T_p}^2 - k_2 z_{T_w}^2 \leq 0 \quad (5.45)$$

i.e. the tracking error system z_{T_w} is stable.

To get the final expression of controller F_u , just like what we did in the former steps, a tracking error z_{T_u} is defined in the third step:

$$z_{T_u} = T_{ud} - T_u \quad (5.46)$$

and its dynamic is easily obtained:

$$\dot{z}_{T_u} = \dot{T}_{ud} - \dot{T}_u \quad (5.47)$$

Our goal is to make the tracking error system z_{T_u} also converge to zero. So, a third CLF is defined:

$$\begin{aligned} V_{T_u} &= \frac{1}{2} z_{T_p}^2 + \frac{1}{2} z_{T_w}^2 + \frac{1}{2} z_{T_u}^2 \\ &= V_{T_w} + \frac{1}{2} z_{T_u}^2 \end{aligned} \quad (5.48)$$

and its derivative is calculated:

$$\dot{V}_{T_u} = \dot{V}_{T_w} + z_{T_u} \dot{z}_{T_u} \quad (5.49)$$

In order to make \dot{V}_{T_u} negative definite, we can finally obtain the expression of the real control law F_u :

$$\begin{aligned} F_u &= \frac{V_u}{T_{u,in} - T_u} \left\{ \frac{h_u A_u}{\rho_w V_w C_{p,w}} (T_{wd} - T_w) + \frac{\rho_w V_w C_{p,w}}{h_u A_u} \left[\frac{h_p A_p}{\rho_p V_p C_{p,p}} (\dot{T}_{pd} - \dot{T}_p) + \frac{\rho_p V_p C_{p,p}}{h_p A_p} (\ddot{T}_{pd} \right. \right. \\ &\quad \left. \left. + k_1 (\ddot{T}_{pd} - \ddot{T}_p) + \frac{F_p}{V_p} \ddot{T}_p \right) + \ddot{T}_p - \frac{h_p A_p}{\rho_w V_w C_{p,w}} (\dot{T}_p - \dot{T}_w) + k_2 (\dot{T}_{wd} - \dot{T}_w) \right] + \frac{h_p A_p}{\rho_w V_w C_{p,w}} (T_p - T_w) \\ &\quad \left. + \frac{h_u A_u}{\rho_w V_w C_{p,w}} (T_u - T_w) - \frac{h_u A_u}{\rho_u V_u C_{p,u}} (T_w - T_u) + k_3 (T_{ud} - T_u) \right\} \end{aligned} \quad (5.50)$$

where k_3 is a positive design parameter.

Substituting (5.47) and (5.50) to (5.49), the dynamic of the CLF (5.48) \dot{V}_{T_u} becomes:

$$\dot{V}_{T_u} = -k_1 z_{T_p}^2 - k_2 z_{T_w}^2 - k_3 z_{T_u}^2 \leq 0 \quad (5.51)$$

this implies that the tracking error system z_{T_u} is stable.

After the ‘step back’ deduction, the control law F_u for this HEX reactor in nominal case is obtained in (5.50). And the closed-loop tracking system is globally asymptotically stable since each tracking subsystem is stable during the design procedure.

5.2.2 Simulation result

In this section, the obtained control signal (5.50) is applied to the reactor system (5.33) to verify the tracking performance of process fluid temperature. In this part, only the heat exchange procedure is considered. The initial values are chosen the same as the experimental data presented in Table 3 of [112]. The flow rate of process fluid F_p is set at $10 \text{ kg} \cdot \text{h}^{-1}$ with a temperature of $77 \text{ }^\circ\text{C}$. The initial flow rate of the utility fluid F_u is set as $62.2 \text{ kg} \cdot \text{h}^{-1}$ with a temperature of $15.6 \text{ }^\circ\text{C}$. Due to the physical limitation of the pump, the flow rate of both fluids has a range from 0 to $150 \text{ kg} \cdot \text{h}^{-1}$. In this case, the utility fluid is used to cool down the process fluid temperature. In the beginning, water is injected into the utility channel first to make the plate wall has the same temperature as the utility fluid. Then, the process fluid is injected. The desired temperature T_{pd} is fixed at $27 \text{ }^\circ\text{C}$, and then changed to $25 \text{ }^\circ\text{C}$ at $t = 400\text{s}$. As presented in (5.50), the third derivative, the second derivative, and the first derivative of the desired temperature T_{pd} are used to calculate the control signal. To get a smoothing input signal, a filter is applied to the reference signal. Therefore, start from $t = 400\text{s}$, the desired temperature T_{pd} changes smoothly until it reaches the new desired value $25 \text{ }^\circ\text{C}$. The dynamics of process fluid temperature T_p and utility fluid flow rate F_u are presented in Figure 5.1.

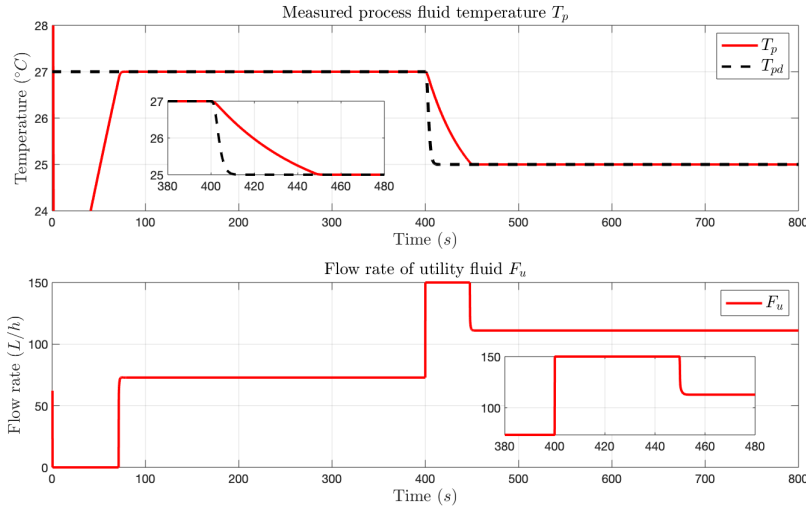


Figure 5.1: Without chemical reaction case: measured process fluid temperature T_p and utility fluid flow rate F_u

In Figure 5.1, the desired temperature T_{pd} is represented by the black dot line, while the measured process fluid temperature is presented by the red line. With the help of control signal (5.50), the temperature of process fluid T_p can well follow the desired value T_{pd} . At $t = 400\text{s}$, the desired temperature decreases to $25 \text{ }^\circ\text{C}$, in order to cool

down the process fluid, the flow rate of utility fluid increases, since the utility fluid has a lower temperature of $15\text{ }^{\circ}\text{C}$. For the considered HEX reactor, there is a quite huge thermal inertia due to the existence of plate wall. To track the desired temperature as fast as possible, the flow rate of utility fluid is quickly set either the minimum value $0\text{ kg}\cdot\text{h}^{-1}$ or the maximum value $150\text{ kg}\cdot\text{h}^{-1}$ until the process fluid T_p converges to the desired value. Simulation result shows that the control law obtained in the former section works. The desired temperature is well tracked by the output temperature.

5.3 Summary

In this chapter, a control law based on the backstepping technique has been proposed for the considered HEX reactor. In the first section, four kinds of backstepping design methods have been introduced, integrator backstepping, backstepping for strict-feedback systems, adaptive backstepping, and robust backstepping. Then, the backstepping design procedure was presented for the HEX reactor. Besides, simulation has been done to validate the control effect of the obtained control law. The control objective is to make the temperature of the process fluid follow the desired value. Finally, the simulation result proved that the obtained backstepping control law can make the temperature of the process fluid well track the desired temperature.

Chapter 6

Backstpping fault tolerant control for the Heat-exchanger/Reactor based on different observers

Based on the backstepping controller obtained in the Chapter 5 and the presented observer based FDD scheme in Chapter 4, a backstepping fault tolerant control system is designed for the considered HEX reactor in this chapter. The fault is firstly detected and diagnosed by the observer based FDD scheme. Then, the backstepping controller is redesigned according to the estimated fault information. In this chapter, both dynamic fault and sensor fault are considered. The proposed FTC strategies are applied to the HEX reactor, and the simulation results are presented to prove their effectiveness. Besides, the performances of each FTC strategy are compared.

6.1 Backstepping fault tolerant control based on observers

As introduced in Chapter 2, FTC can be divided into passive FTC and active FTC according to the construction of control law. The passive approach depends on a fixed controller which is insensitive to some known faults, while the active approach is based on the redesigning of the controller according to the real-time faulty information from a FDD scheme.

In Chapter 4, two FDD schemes based on the adaptive observer and interval observer have been presented. By combining the FDD scheme and the proposed backstepping controller in Chapter 5, two active FTC strategies based on the adaptive observer and interval observer are obtained. The main idea of the proposed active FTC strategies is controller reconfiguration. The fault is firstly detected and diagnosed by the observer based FDD scheme. Then, the control law is reconstructed according to the details of the fault. With the help of FTC strategy, the performance of the system can be guaranteed even in the presence of a fault.

6.1.1 Dynamic FTC design

Normally, the control law is constructed with the nominal value of parameter vector θ^0 . When the fault occurs in the plant, the j th parameter will change to an unexpected value $\theta^f = \theta^0 + f_p$. But, the controller design is still based on the nominal value of the parameter. So, we have to compensate the influence of the unexpected change f_p .

Here, we use a short expression (6.1) to represent the nominal backstepping control law (5.50) obtained in Chapter 5.

$$F_u = \varphi(T_{pd}, y, \theta^0, k) \quad (6.1)$$

where φ is the nonlinear function expressed in (5.50), θ^0 represents the nominal value of the parameter vector, and $k = [k_1, k_2, k_3]$ is the controller gain matrix. Assume that the fault occurs in the j th parameter, after the fault detection and isolation, the faulty value can be estimated \hat{f}_{pj} , then, a new control law is redesigned by using the estimated faulty value:

$$F_u = \varphi(T_{pd}, y, \theta_l^0, \theta_j^0 + \hat{f}_{pj}, k), \quad l = 1, \dots, j-1, j+1, \dots, m \quad (6.2)$$

where the faulty parameter is compensated.

6.1.2 Sensor FTC design

Generally, the measurements of the system are used for the control law design in closed-loop. So, a sensor fault will cause the performance degradation of the entire system. That is the reason why we also need to find out the sensor fault and redesign the controller as the dynamic fault case.

For the obtained backstepping control law (6.1), y represents the measurements of the system. If the fault occurs in j th sensor, then the control law becomes:

$$F_u = \varphi(T_{pd}, y_l, y_j^f, \theta^0, k), \quad l = 1, \dots, j-1, j+1, \dots, q \quad (6.3)$$

where $y_j^f = y_j + f_{sj}$, y_j represents the output of j th sensor when it is healthy, y_j^f represents the output of j th sensor when it is faulty.

To eliminate the effect of sensor fault, the estimated faulty value \hat{f}_{sj} offered by the FDD scheme is used to redesign the control signal:

$$F_u = \varphi(T_{pd}, y_l, y_j^f - \hat{f}_{sj}, \theta_j^0, k), \quad l = 1, \dots, j-1, j+1, \dots, q \quad (6.4)$$

where φ is the nonlinear function expressed in (5.50).

6.2 Application to the HEX reactor

In this part, the FTC strategies based on different observers are applied to the HEX reactor (4.20). The objective is the same as that we proposed in the backstepping controller design part: guarantee the temperature of the process fluid T_p stay at the desired value T_{pd} , even though with the interruption of an unexpected fault.

6.2.1 Backstepping fault tolerant control based on adaptive observers

Method presentation

In the first step, the adaptive observer based FDD scheme presented in Chapter 4.4 is used to detect and isolate the fault. A bank of observers are constructed, where each one gives an estimation of the possible faulty parameter/sensor. Residuals (4.16) are calculated to detect the state change.

However, in the closed-loop system, these residuals are easily affected by the change of the input signal, which makes it difficult to identify the reason for the residual change, the change is caused by the occurrence of a fault or by the variance of the input signal.

Even though the input signal change may also be caused by the actuator fault, in our case, only dynamic fault and sensor fault are considered. So, we suppose that all the actuators are in nominal condition, and the input change comes from the adjustment of the control signal.

To identify the reason of residual variance, auxiliary residuals calculated by (6.5) are used in the fault isolation procedure:

$$Dr_i = \frac{d\|\hat{y}^{(i)} - y\|}{dt}, \quad i \in 1, \dots, m. \quad (6.5)$$

Then, we name the residual r_i calculated by (4.16) as original residual. When the original residuals r_i leave zero, it indicates the detection of the state change. In order to make sure the reason for this state change (the occurrence of a fault or the input change), we must analyze the stable values of each residual r_i . Then, the auxiliary residuals Dr_i are used to check the stability of the original residuals. When one of the residual is stable (i.e. the corresponding Dr_i go back under the threshold), the final value of the original residual is verified. The procedure is not finished until all the original residuals are stable and their values are checked. If all the original residuals lie under the threshold, we can judge that the state variation is caused by the change of input signal. However, if only one original residual goes under the threshold while the rest stay at a nonzero value, we can know that a fault occurs. Besides, the residual that returns to zero corresponds to the faulty parameter.

Once the fault is isolated and identified, the control law is redesigned as (6.2) or (6.4).

Simulation results: fault free case

To validate the effectiveness of the proposed FTC scheme, numerical simulations were performed using the MATLAB. In these simulations, dynamic faults and sensor faults are considered. The objective is to make the measured process fluid temperature T_p follows the desired value T_{pd} in presence of different kinds of fault. For simplicity, only the heat exchange part is considered. The mathematical model of the HEX reactor is presented in (4.20).

The initial values of the HEX reactor is settled the same as in Chapter 4.4. The process fluid is injected into the process channel with a constant flow rate $F_p = 10 \text{ L} \cdot \text{h}^{-1}$ and a constant temperature $T_{p,in} = 77 \text{ }^\circ\text{C}$, while the utility fluid is injected into the utility channel with a initial flow rate $F_u(0) = 62.2 \text{ L} \cdot \text{h}^{-1}$ and a fixed temperature $T_{u,in} = 15.6 \text{ }^\circ\text{C}$. The flow rates of the both fluids have a range from 0 to 150

$L \cdot h^{-1}$ because of the physical limitation of the pumps. The initial temperatures of process channel, utility channel and plate wall are $x(0) = [T_p(0) \ T_u(0) \ T_w(0)]^T = [77 \ 15.6 \ 15.6]^T$. The desired temperature T_{pd} is firstly settled at $27^\circ C$ and then resettled at $25^\circ C$ at $400s$.

Figure 6.1 shows the measured temperature of process fluid T_p and the variable control input utility fluid flow rate F_u in fault free case. The temperature of process fluid T_p in red can follow the desired temperature T_{pd} in the black dot line, even the desired value changes at $400s$.

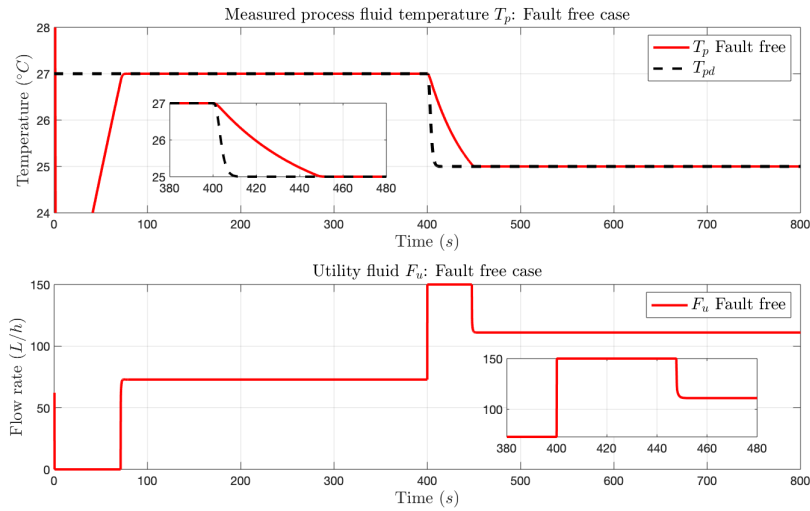


Figure 6.1: Measured process fluid temperature T_p and utility fluid flow rate F_u in fault free case

Simulation results: dynamic fault case

The considered fault is the same as that in Section 4.4, the heat transfer coefficient between the process fluid and plate wall h_p , and the inlet temperature of process fluid $T_{p,in}$. Their nominal values are $\beta = [7.5975 \times 10^3 \ 77]^T$.

The first fault f_{p1} is introduced in the decrease of heat transfer coefficient h_p at $200s$ i.e. $h_p^f = h_p + f_{p1}$, where $f_{p1} = -15\%h_p^0$.

Figure 6.2 and Figure 6.3 represent the faulty reactor without FTC and with FTC, respectively. When the fault occurs at $200s$, the measured temperature of the process fluid T_p is affected, as well as the control signal F_u . As shown in Figure 6.2, the control signal varies due to the influence of the fault, however, it still can not make the process fluid temperature T_p follow the expected value in presence of the fault.

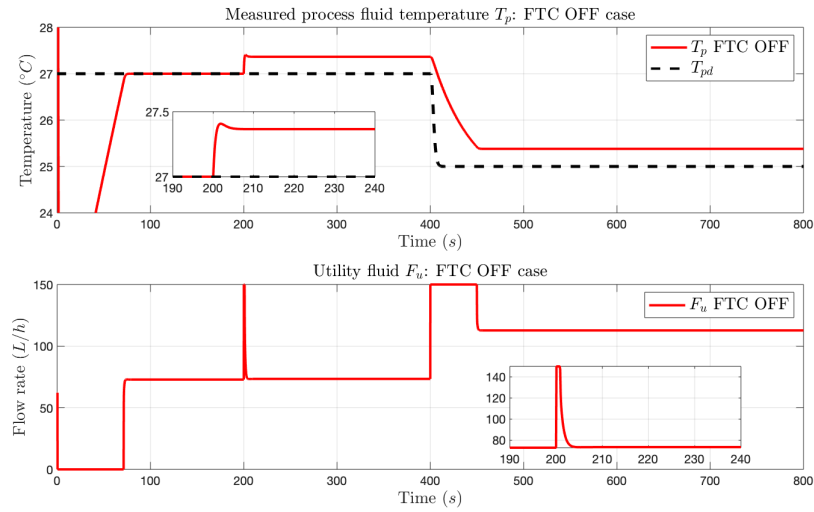


Figure 6.2: h_p is faulty at 200s, without FTC case

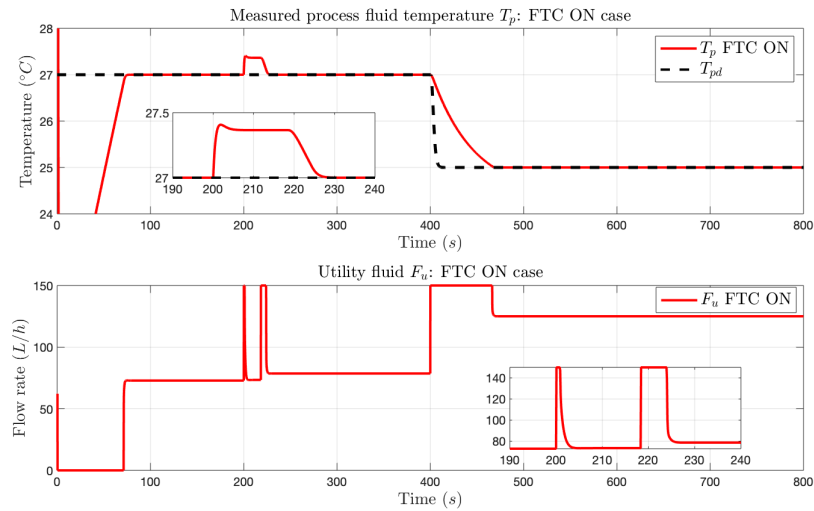


Figure 6.3: h_p is faulty at 200s, with FTC case

On the contrary, when the proposed FTC strategy is applied, the bad tracking performance disappears, as presented in Figure 6.3. Once the fault is isolated, the control signal is reconstructed by using the estimated fault value. Thus, the output temperature of process fluid T_p can track the expected value T_{pd} under the faulty situation. And it still well follows the desired temperature even if this reference value changes at $t = 400$ s.

The residuals used for fault detection and isolation are presented in Figure 6.4. Figure 6.5 and Figure 6.6 show the zoom in of the residuals. At about $t = 72$ s, the original residuals r_i change, when the auxiliary residuals go under the threshold

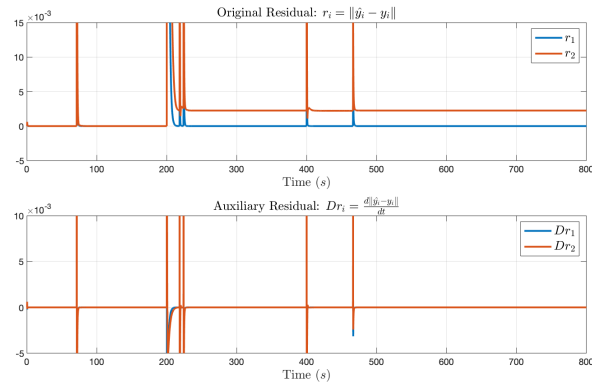


Figure 6.4: Original residual r_i and auxiliary residual Dr_i when h_p is faulty at 200s

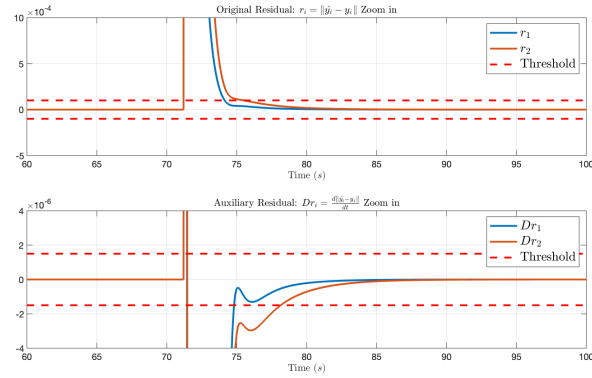


Figure 6.5: Zoom in 60s to 100s: original residual r_i and auxiliary residual Dr_i when h_p is faulty at 200s

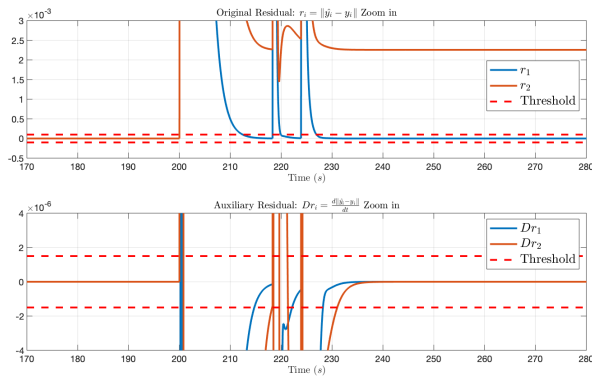


Figure 6.6: Zoom in 170s to 280s: original residual r_i and auxiliary residual Dr_i when h_p is faulty at 200s

$Th_{Dr} = \pm 2 \times 10^{-6}$, we check the values of the original residual r_i , and they all go under the threshold $Th_r = \pm 1 \times 10^{-4}$. Thus, this change is caused by a change of the control

signal and there is no fault at this time. At 200s, the residuals r_i change again. After 218.3s, the auxiliary residuals all go under the threshold, which means the value of the original residuals is stable. Then, we find that the first original residual r_1 , which corresponds to the first observer lies under the threshold, while the other residual r_2 stays at a nonzero constant. As discussed in the former part, this indicates that the fault occurs at the first parameter h_p . And the time used for fault isolation is 18.3s. And then, the residuals change at 400s and 470s, but the isolation result is always the same. The estimated faulty value \hat{f}_{p1} is also presented in Figure 6.7, and it matches with the given value f_{p1} .

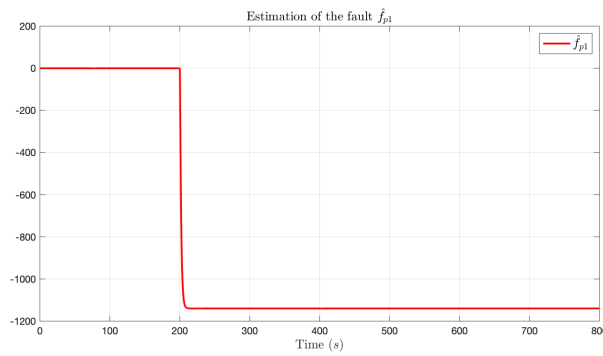


Figure 6.7: Estimated fault value \hat{f}_{p1} when h_p is faulty at 200s

In the second case, fault $f_{p2} = -5 \text{ }^\circ\text{C}$ is added to the inlet temperature of process fluid $T_{p,in}$ at $t_f = 200\text{s}$. Then, $T_{p,in}$ drops to the faulty case $T_{p,in}^f = T_{p,in} + f_{p2} = 73 \text{ }^\circ\text{C}$. Simulation results are shown in Figure 6.8 and Figure 6.9.

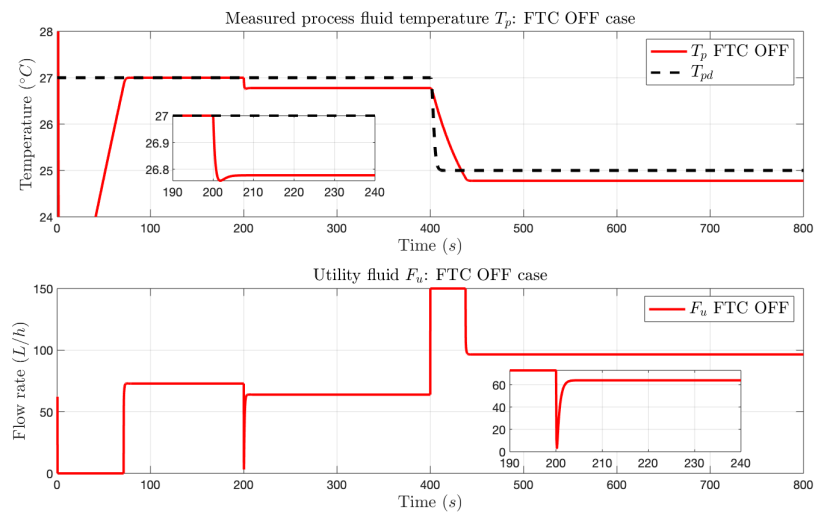


Figure 6.8: $T_{p,in}$ is faulty at 200s, without FTC case

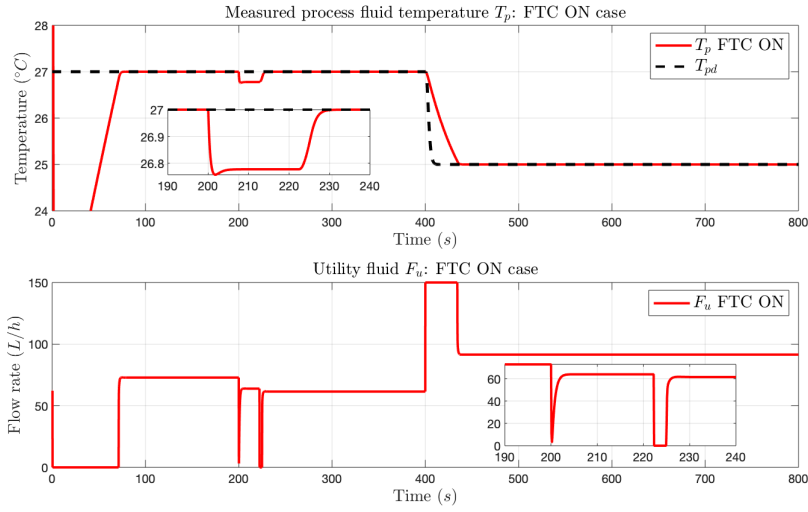


Figure 6.9: $T_{p,in}$ is faulty at 200s, with FTC case

Apparently, the measured process fluid temperature T_p can not track the expected T_{pd} in the presence of the fault, as presented in Figure 6.8. The decrease of $T_{p,in}$ causes a decrease in the temperature of process fluid directly, which makes it can not follow the desired temperature anymore. Actually, the control tries to compensate for this fault by adjusting the utility fluid flow rate, but it is not enough to eliminate the effect of the fault.

The performance of the proposed FTC strategy is presented in Figure 6.9. When the fault is isolated, the control signal is redesigned to adapt the existed faulty parameter and make the measured T_p always follow the expected value, even if the reference signal changes at 400s.

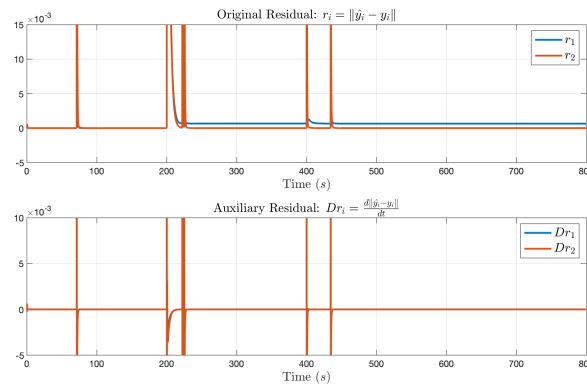


Figure 6.10: Original residual r_i and auxiliary residual Dr_i when $T_{p,in}$ is faulty at 200s

Figure 6.10 shows the residuals used for fault detection and isolation. The adjustment of F_u appears in the change of residuals, as well as the disturbing of the estimated

faulty value \hat{f}_{p2} at about $t = 72s$, as shown in Figure 6.11. The similar phenomenon happens at about $t = 219s$ and $t = 400s$. But, the fault is detected at about $200s$, because only at this time, the original residuals r_i vary to different values at the first time, r_2 equals zero while the residual r_1 stay at a nonzero constant. Thus, the fault is isolated at $T_{p,in}$, and the fault value is estimated by the corresponding second adaptive observer.

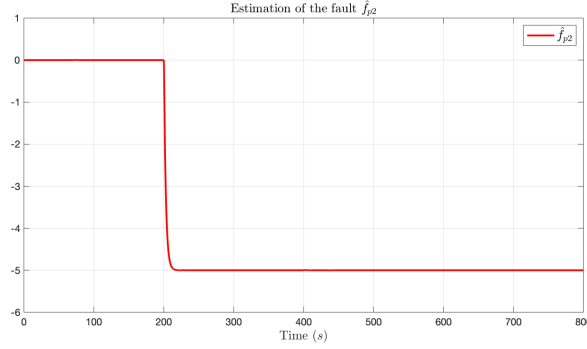


Figure 6.11: Estimated fault value \hat{f}_{p2} when $T_{p,in}$ is faulty at $200s$

With the proposed FTC scheme, simulation results show that the reference signal is well tracked even in the presence of a dynamic fault.

Simulation results: sensor fault case

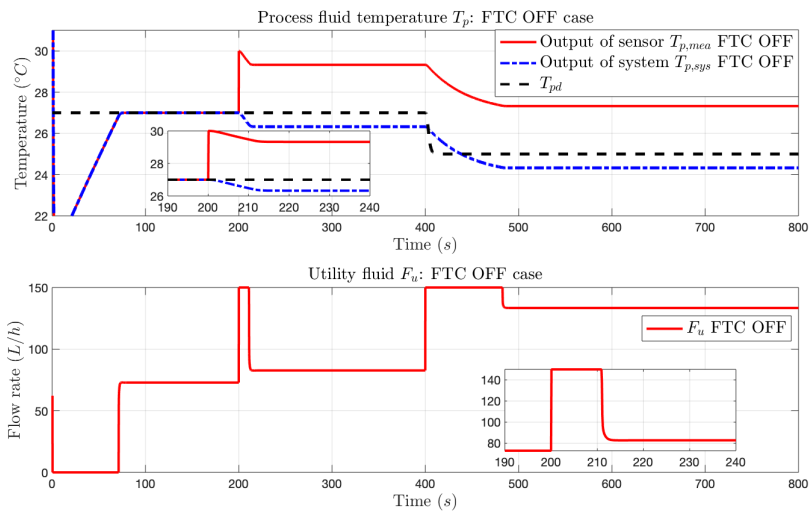


Figure 6.12: Sensor of T_p is faulty at $200s$, without FTC case

First, we consider a temperature sensor fault $f_{s1} = 3 \text{ }^\circ\text{C}$ occurring at the process fluid temperature sensor $s1$ at $t_f = 200s$. So the output of the faulty sensor is $y_1^f =$

$y_1 + f_{s1}$. Simulation results are presented in Figure 6.12 and Figure 6.13. The real output of the system $T_{p,sys}$ is presented in blue dot line, and the measured value (the output of the sensor) $T_{p,mea}$ is represented by the red line. The black dot line represents the desired process fluid temperature T_{pd} .

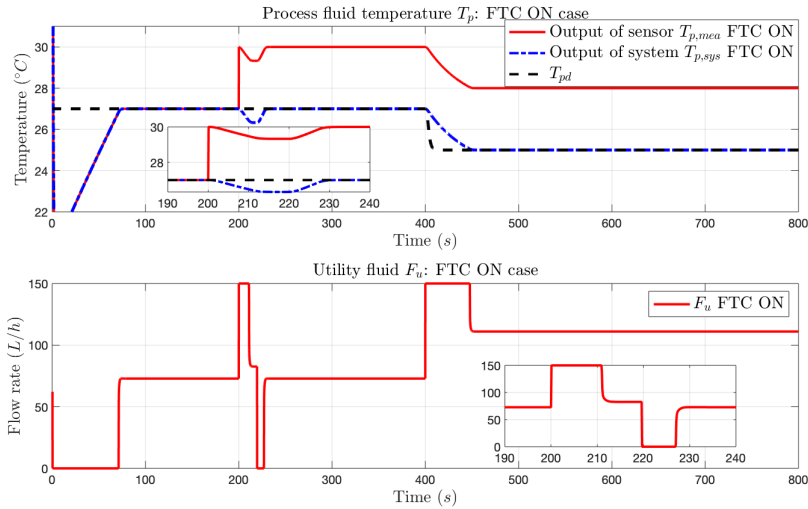


Figure 6.13: Sensor of T_p is faulty at 200s, with FTC case

We should pay attention that our objective is to make the real output process fluid temperature follow the desired value even in the case of a fault. As shown in Figure 6.12, not only the measured temperature (the output of sensor) is affected by the sensor fault, but also the real output value (the blue dot line) due to the closed-loop system. Under this situation, the tracking task can not be accomplished. However, in Figure 6.13, the real output T_p has a good tracking performance with the help of the proposed FTC strategy. At 400s, the reference signal is also changed like in the nominal case, but it still has a good tracking performance even though the sensor fault still exists. Since the sensor can not compensate the fault, the measured value (the output of sensor) $T_{p,mea}$ still has an offset with respect to the output of the system $T_{p,sys}$.

The dynamic of utility fluid temperature $T_{u,sys}$ and $T_{u,mea}$ under different situations, with and without FTC strategy, are presented in Figure 6.14. When the fault occurs in the first sensor, the temperature of utility fluid is also influenced. Since the fault is not located in the second sensor, the measured utility fluid temperature (the output of sensor) $T_{u,mea}$ is equal to the real output of system $T_{u,sys}$. However, without the application of FTC strategy, the utility fluid temperature cannot in line with that in fault free cases.

The residuals are shown in Figure 6.15. The fault is easily detected and isolated

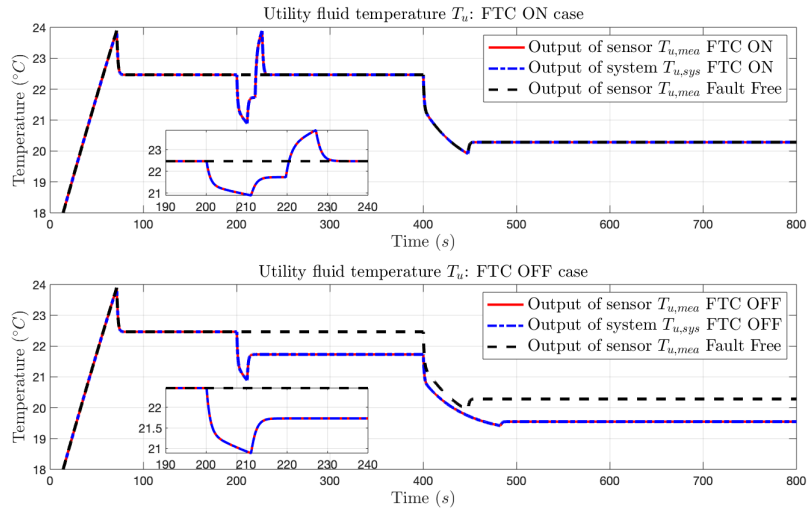


Figure 6.14: Utility fluid temperature when sensor of T_p is faulty at 200s

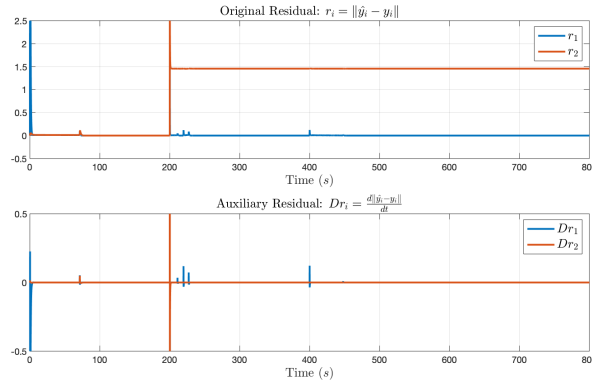


Figure 6.15: Original residual r_i and auxiliary residual Dr_i when sensor of T_p is faulty at 200s

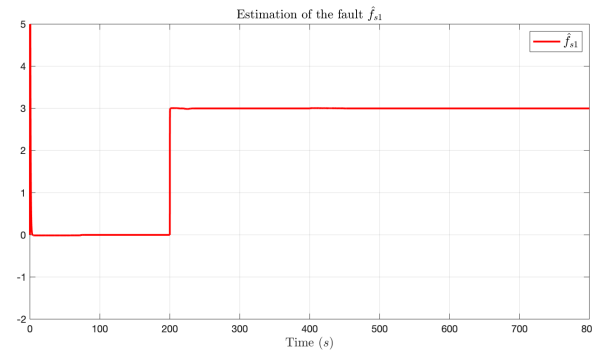


Figure 6.16: Estimated fault value \hat{f}_{s1} when sensor of T_p is faulty at 200s

by using the presented fault diagnosis scheme. r_1 equals to zeros while r_2 is a nonzero constant when all the auxiliary residuals go under the threshold at 219.2s. That is to

say, the fault occurs at the first sensor. The estimated faulty value \hat{f}_{s_1} is also shown in Figure 6.16, and the estimated fault equals the faulty value we applied. Then, this sensor fault is compensated during the redesign procedure of the control law F_u . At 400s, the residuals vary slightly because of the control single adjustment to follow the new reference signal.

Finally, a fault $f_{s_2} = 7\text{ }^\circ\text{C}$ is applied to the utility fluid temperature sensor s_2 at $t_f = 200\text{ s}$. Then, the faulty temperature measurement is $y_2^f = y_2 + f_{s_2}$.

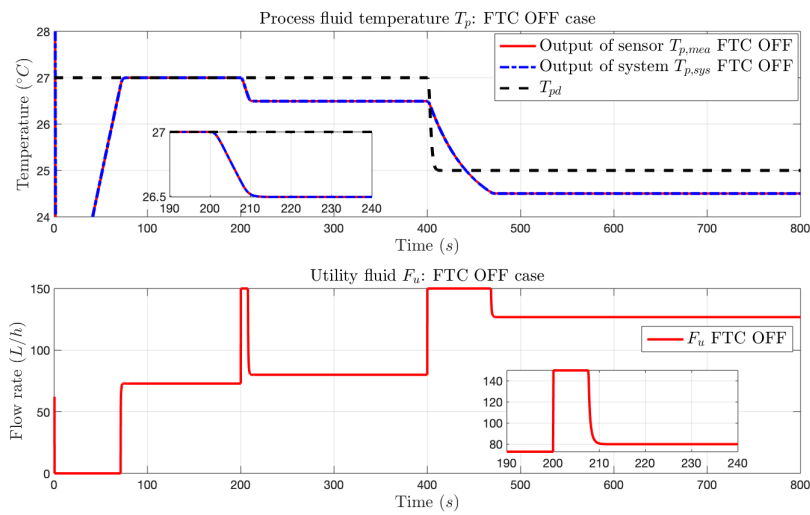


Figure 6.17: Sensor of T_u is faulty at 200s, without FTC case

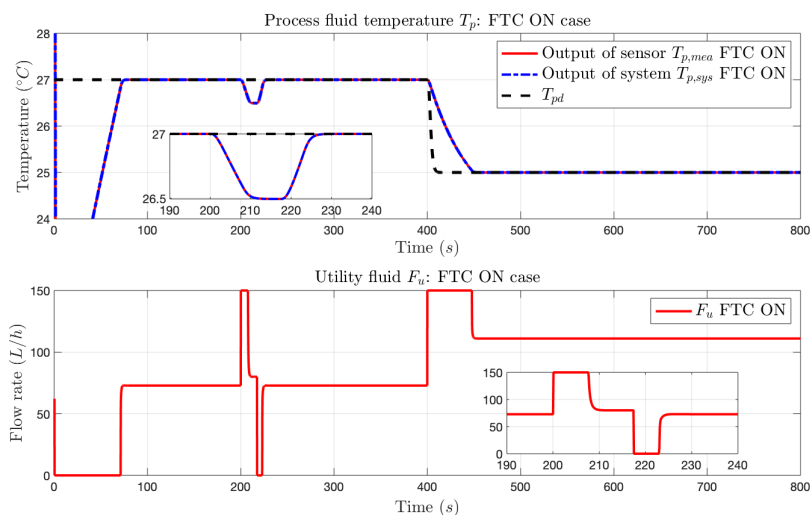


Figure 6.18: Sensor of T_u is faulty at 200s, with FTC case

Figure 6.17 shows the process fluid temperature T_p and the control signal F_u without the intervention of FTC, and Figure 6.18 shows the tracking performance with the

proposed FTC scheme. The output of the sensor is shown in the red line, and the output of the system is shown as a blue dot line. Even though the fault is applied on the sensor of utility fluid temperature T_u , the temperature of process fluid T_p is also affected. But their measured value $T_{p,mea}$ and the real system output $T_{p,sys}$ are the same. Then, adaptive observers are constructed to isolate the fault. Residuals are presented in Figure 6.19.

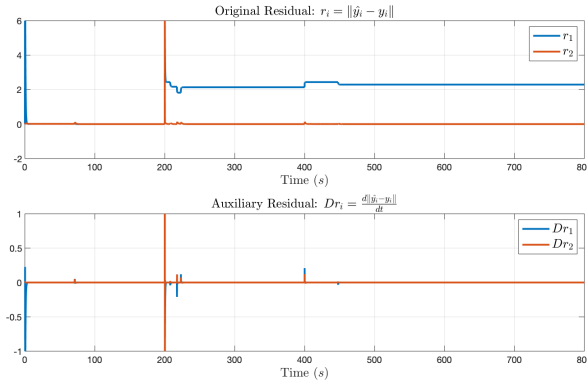


Figure 6.19: Original residual r_i and auxiliary residual Dr_i when sensor of T_u is faulty at 200s

Since the second residual r_2 returns to zero at about 207s, and the first residual remains nonzero, then the fault is isolated in the second sensor. Then, the control law is reconstructed to follow the reference signal. The estimated faulty value used for control compensation is presented in Figure 6.20, and it converges to the faulty value f_{s2} after a transition time. As shown in Figure 6.18 the process fluid can follow the reference signal once the controller is redesigned. And the tracking task is well finished when the desired temperature is changed at 400s in presence of the sensor fault.

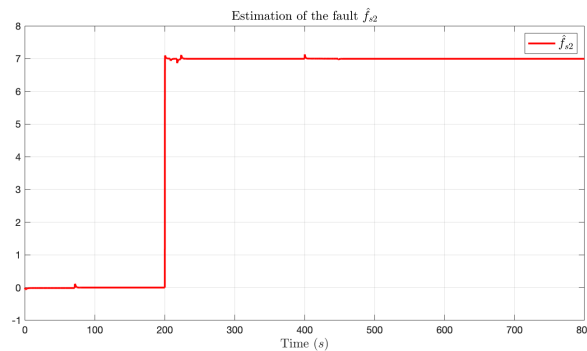


Figure 6.20: Estimated fault value \hat{f}_{s2} when sensor of T_u is faulty at 200s

To show the second sensor fault clearly, the utility fluid temperature is presented

in Figure 6.21 under different cases, with FTC, and without FTC. The nominal utility fluid temperature is presented in the black dot line. When there is a fault, the output of the system (blue dot line) and the output of the sensor (red line) are both changed. But the system output goes back to the nominal value because the FTC strategy works. However, without the intervention of FTC, the output of the system stays at a faulty value.

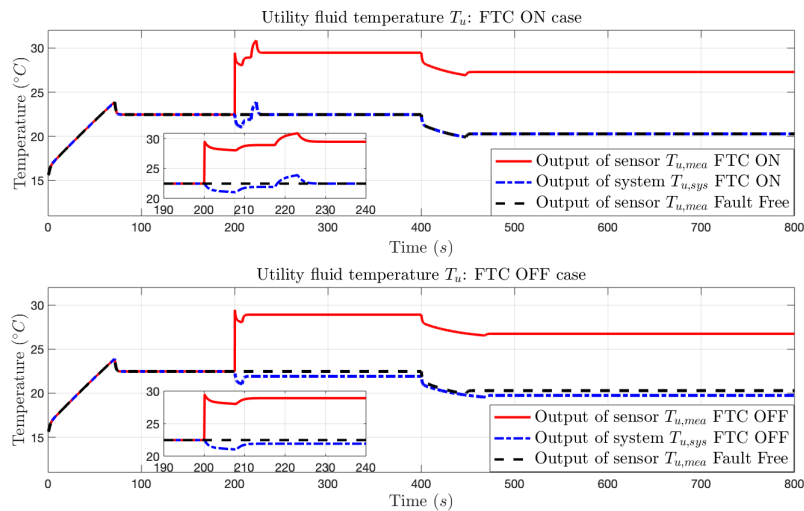


Figure 6.21: Utility fluid temperature when sensor of T_u is faulty at 200s

6.2.2 Backstepping fault tolerant control based on interval observers

Method presentation

In this part, the interval observer based FDD scheme presented in Section 4.5 is used to detect and isolate the fault. The practical domain of the value of each system parameter is divided into a certain number of intervals. After verifying all the intervals whether or not one of them contains the faulty parameter value of the system, the faulty parameter value is found, the fault is therefore isolated and identified.

To detect and isolate the fault, we will use the same manners to analyse the residual as presented in the adaptive observer based FTC case, that is to say, the combination of original residual (4.16) and auxiliary residual (6.5). But, we only need to pay attention to one special observer. In general, when we divide the practical domain of each parameter into intervals, the nominal value of the parameter is chosen to be one of the interval bounds. For simplicity, we defined the observer who uses the nominal

parameter value as the standard observer. By analysing the residual of the standard observer, we can detect the occurrence of the fault and prevent the fake alarm caused by input change. Firstly, the residual change indicates the state variation. And then, when the residual is stable i.e. the auxiliary residual goes under the threshold Th_{Dr} , if the original residual lies under the threshold Th_r , this change is caused by the input change, otherwise, this change is caused by a fault. Besides, to make sure the fault is isolated correctly, we will use the stable value of estimation error to calculate the isolation index, i.e. once the auxiliary residual goes under the threshold, if we make sure the occurrence of a fault, then the isolation index (4.33) (4.38) is calculated.

To clearly present the isolation results, we define a fault signature for each interval. That is to say, if the fault is located in this interval, then, the fault signature sends 1. Otherwise, the fault signature sends 0. Then, after the isolation and identification of fault, the control law is redesigned as (6.2) or (6.4).

The temperature of process fluid T_p and the dynamic flow rate of utility fluid F_u in fault free case have been presented in Figure 6.1.

Simulation results: dynamic fault case

The dynamic fault vector considered is $[h_p \ T_{p,in}]^T$, and their nominal values are $[h_p^0 \ T_{p,in}^0]^T = [7.5975 \times 10^3 \ 77]^T$. Both parameters are divided into five intervals, the bounds of each interval are given in Table 4.3 and Table 4.4. The interval diving of h_p is different percentages of its nominal value h_p^0 .

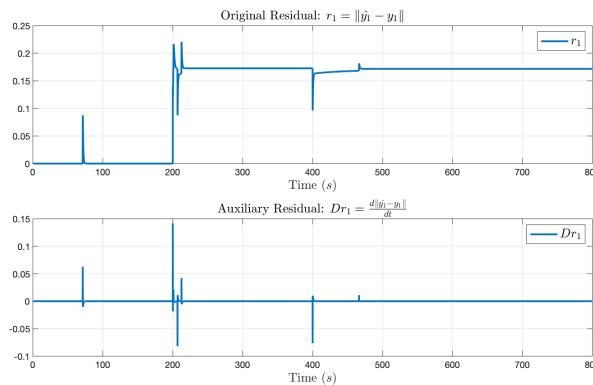


Figure 6.22: Original residual r_1 and auxiliary residual Dr_1 correspond to bound 1 of h_p when dynamic h_p is faulty at 200s

First of all, the fault is introduced in the first parameter h_p at 200s, it decreases to 85% of its nominal value. Figure 6.22 shows the performances of the original residual

and auxiliary residual corresponding to the standard observer, the first observer which uses the nominal value h_p^0 . Figure 6.23 and Figure 6.24 show the zoom in of the residual performances.

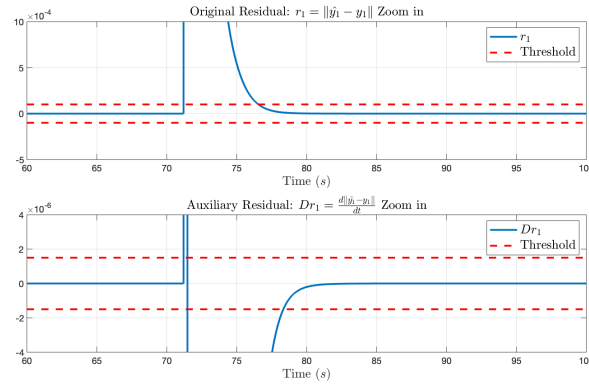


Figure 6.23: Zoom in 60s to 100s: original residual r_1 and auxiliary residual Dr_1 correspond to bound 1 of h_p when dynamic h_p is faulty at 200s

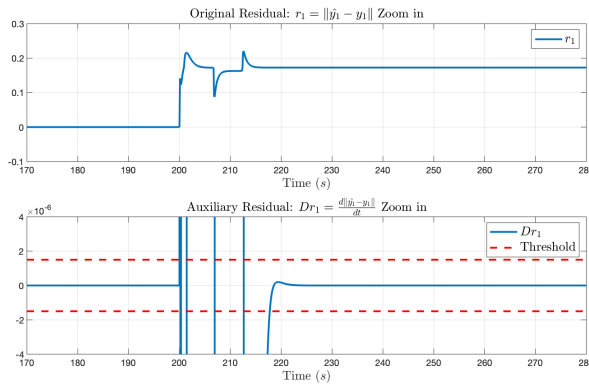


Figure 6.24: Zoom in 170s to 280s: original residual r_1 and auxiliary residual Dr_1 correspond to bound 1 of h_p when dynamic h_p is faulty at 200s

At about 72s, the residual r_1 is no longer zero, which indicates that there is a state change in the system. When the auxiliary residual Dr_1 goes under the threshold $Th_{Dr} = \pm 2 \times 10^{-6}$, we consider the residual r_1 is stable and check its value. We can find out that r_1 goes under the threshold $Th_r = \pm 1 \times 10^{-4}$. That is to say, That means this residual change is caused by the input change, not the fault. But, performances are different after 200s. The original residual r_1 stay at a nonzero value when the auxiliary residual Dr_1 goes under the threshold at $t = 207.5s$. This indicates that there is a fault in our system.

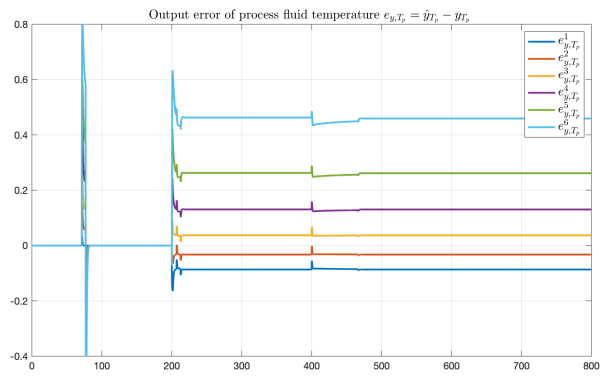


Figure 6.25: Output errors e_{y,T_p} correspond to intervals of h_p when dynamic h_p is faulty at 200s

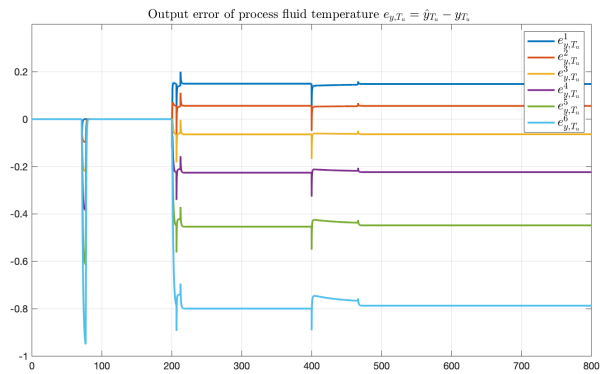


Figure 6.26: Output errors e_{y,T_u} correspond to intervals of h_p when dynamic h_p is faulty at 200s

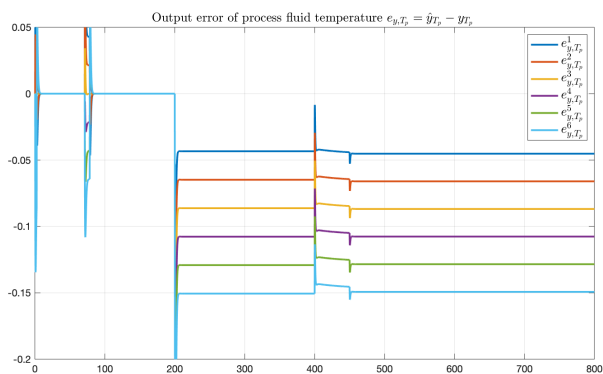


Figure 6.27: Output errors e_{y,T_p} correspond to intervals of $T_{p,in}$ when dynamic h_p is faulty at 200s

Figure 6.25 and Figure 6.26 present the output errors of process fluid temperature

and utility fluid temperatures between different interval observers and real system. After analyzing the performance of output errors of process fluid temperature and utility fluid temperatures, the fault is located in the second interval of h_p change immediately.

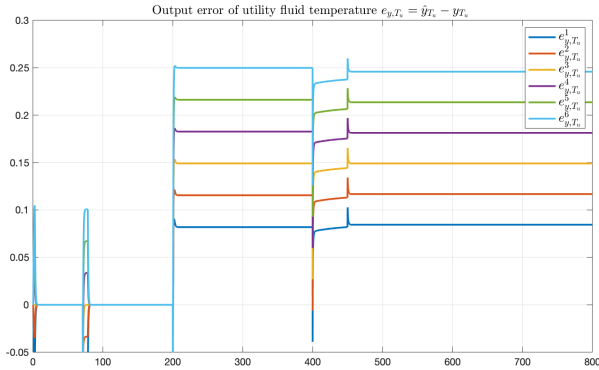


Figure 6.28: Output errors e_{y,T_u} correspond to intervals of $T_{p,in}$ when dynamic h_p is faulty at 200s

The output errors between the interval observers corresponding to $T_{p,in}$ change and real system are shown in Figure 6.27 and Figure 6.28. For both output error of process fluid temperature e_{y,T_p} and output error of utility fluid temperature e_{y,T_u} , they all stay on the same side of zero, either the negative side or the positive side. That is to say, the fault is not located in the intervals of $T_{p,in}$.

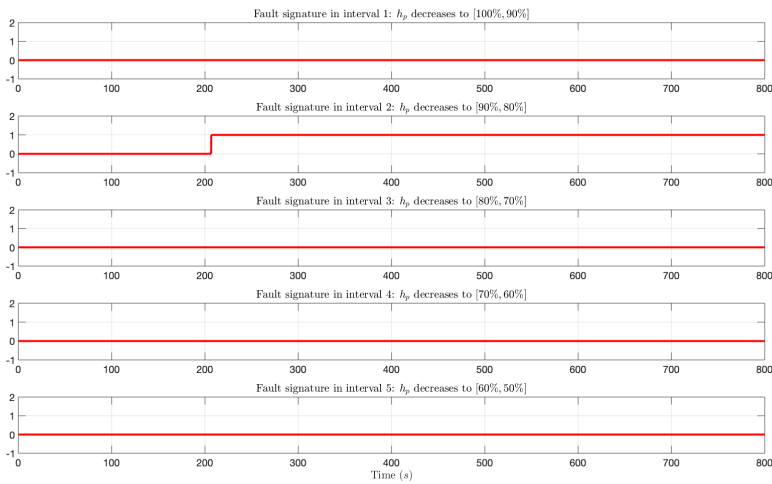


Figure 6.29: Fault signature correspond to intervals of h_p when dynamic h_p is faulty at 200s

Figure 6.29 presents the fault signature of different interval of h_p . It is obvious that, the fault signature of the second interval is equal to one after 200s, while others stay at zero. That is to say, the fault is located in the second interval of h_p .

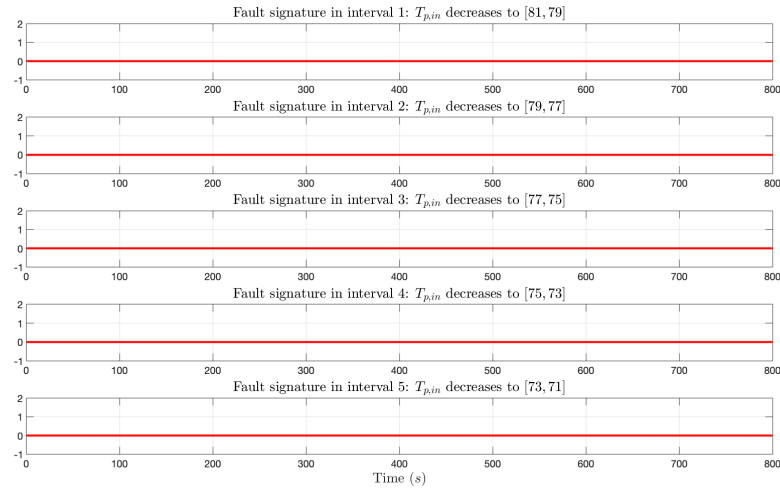


Figure 6.30: Fault signature correspond to intervals of $T_{p,in}$ when dynamic h_p is faulty at 200s

Fault signatures corresponding to parameter $T_{p,in}$ is shown in Figure 6.30. All the fault signatures stay at zero, and that indicates the fault is not contained in any interval of $T_{p,in}$.

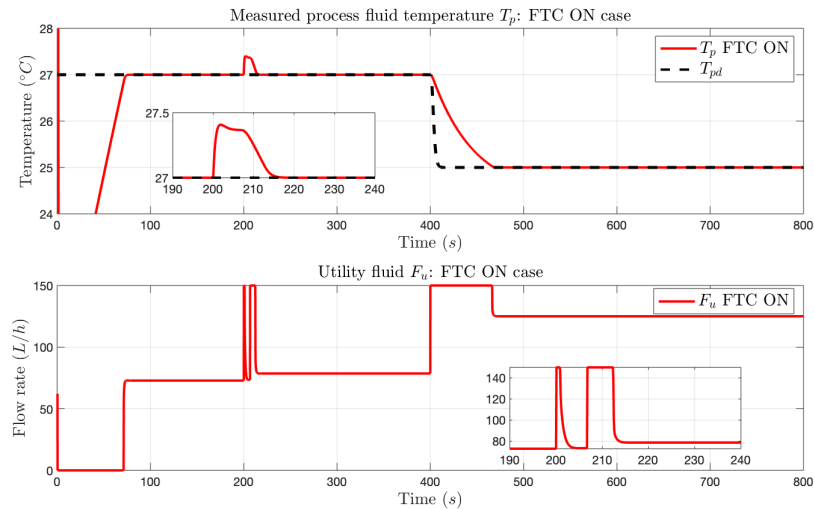


Figure 6.31: h_p is faulty at 200s, with FTC case

Therefore, the fault is isolated in the second interval of parameter h_p , and the identified fault information is used for controller reconstruction. The tracking performances

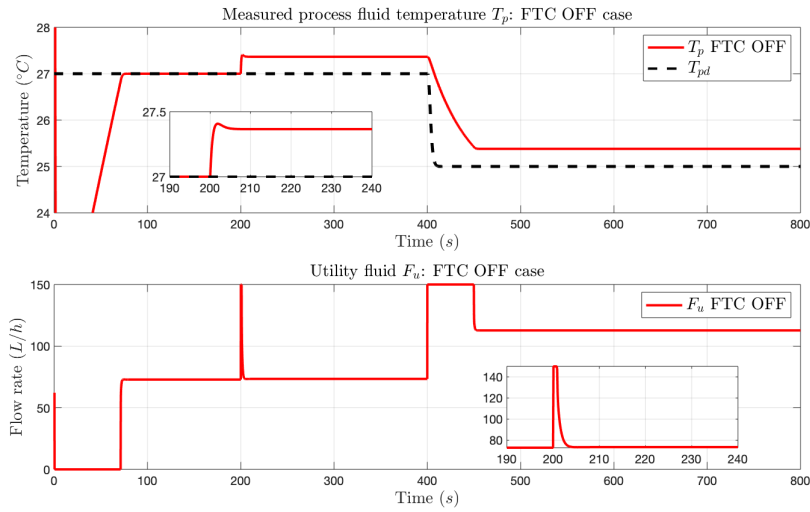


Figure 6.32: h_p is faulty at 200s, without FTC case

of process fluid temperature, as well as the dynamic of utility fluid flow rate under different situations, are presented in Figure 6.31 and Figure 6.32. At 200s, the process fluid temperature varies due to the effect of fault. The flow rate of utility is adjusted automatically, but it can not compensate for the influence of fault. Once the fault is isolated and the controller is re-designed, the temperature of process fluid can re-follow the desired temperature T_{pd} . Even though the reference signal changes at 400s, the HEX reactor still presents a good tracking performance. On contrast, the temperature of process fluid T_p cannot follow the expected value without the FTC strategy. The fault in h_p leads to a tracking offset, and this offset always exists since the fault is considered a permanent fault.

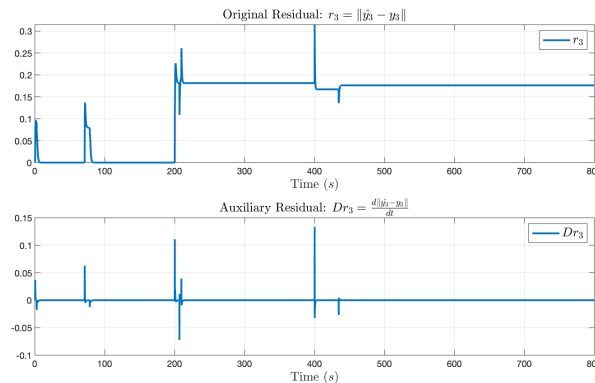


Figure 6.33: Original residual r_3 and auxiliary residual Dr_3 correspond to bound 3 of $T_{p,in}$ when dynamic $T_{p,in}$ is faulty at 200s

In the second case, the fault is introduced at the second parameter $T_{p,in}$, the inlet

temperature of process fluid decrease to $72\text{ }^\circ\text{C}$ from its nominal value $T_{p,in}^0 = 77\text{ }^\circ\text{C}$ at 200 s . In this case, our standard observer that uses the nominal value of $T_{p,in}^0$ is the third one, it is the bound of the second interval and the third interval. Figure 6.33 shows the performances of the original residual and auxiliary residual corresponding to the standard observer.

At about 72 s , the original residual r_3 has a variation, that indicates a state change in the system. After verifying its stable value, this state change is caused by the input signal change. However, after 200 s , it is no longer zero anymore, and its stable value indicates the occurrence of the fault.

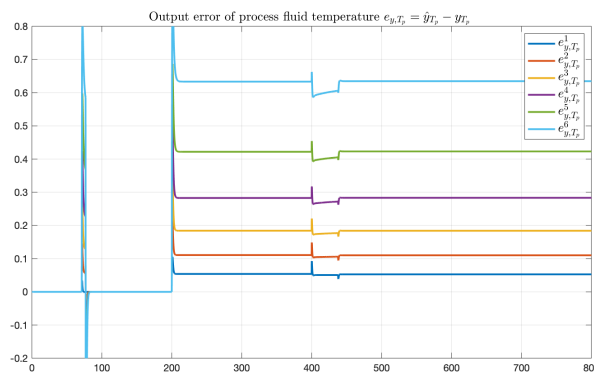


Figure 6.34: Output errors e_{y,T_p} correspond to intervals of h_p when dynamic $T_{p,in}$ is faulty at 200 s

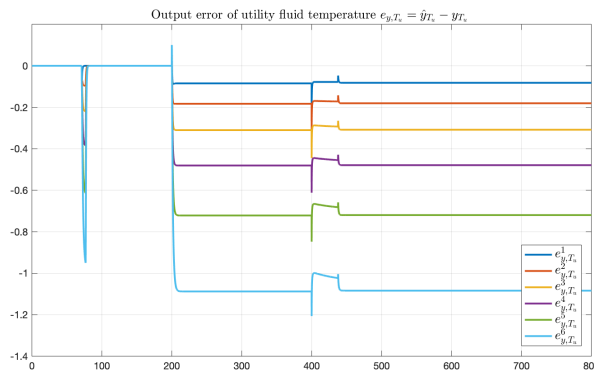


Figure 6.35: Output errors e_{y,T_u} correspond to intervals of h_p when dynamic $T_{p,in}$ is faulty at 200 s

Figure 6.34 and Figure 6.35 present the output error e_{y,T_p} and e_{y,T_u} corresponding to the intervals of h_p . According to the isolation principle, the fault is not located in the interval of h_p .

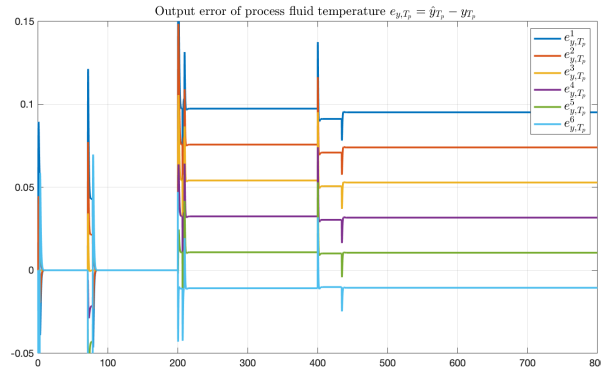


Figure 6.36: Output errors e_{y,T_p} correspond to intervals of $T_{p,in}$ when dynamic $T_{p,in}$ is faulty at 200s

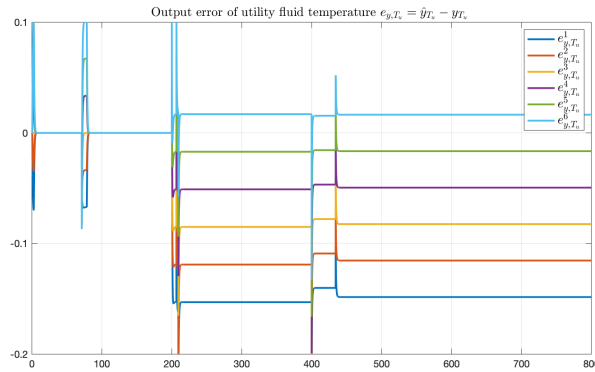


Figure 6.37: Output errors e_{y,T_u} correspond to intervals of $T_{p,in}$ when dynamic $T_{p,in}$ is faulty at 200s

Then, we check the performances of the observer whose parameter is changed at $T_{p,in}$. The output errors of process fluid temperature e_{y,T_p} between $T_{p,in}$ interval observers and real system are presented in Figure 6.36 and Figure 6.37. We can find that the output errors, which correspond to the fifth bound and the sixth bound of interval $T_{p,in}$, stay in different sides of zero. Therefore, we can conclude that the faulty parameter is contained in the fifth interval $[71, 73]$ of $T_{p,in}$ parameters.

Fault signatures of h_p intervals and $T_{p,in}$ intervals are presented in Figure 6.38 and Figure 6.39. Obviously, the fault is contained in the fifth interval of $T_{p,in}$ variation. The bounds of this interval are $[71, 73]$.

To tolerate the fault in $T_{p,in}$, the control signal is reconstructed. Different tracking performances of the process fluid temperature are presented in Figure 6.40 and Figure 6.41.

With the help of the FTC strategy, the dynamic of the process fluid temperature

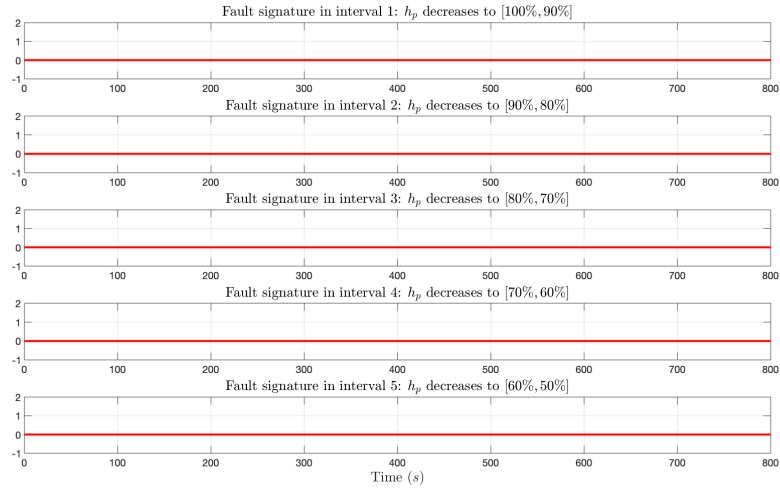


Figure 6.38: Fault signature correspond to intervals of h_p when dynamic $T_{p,in}$ is faulty at 200s

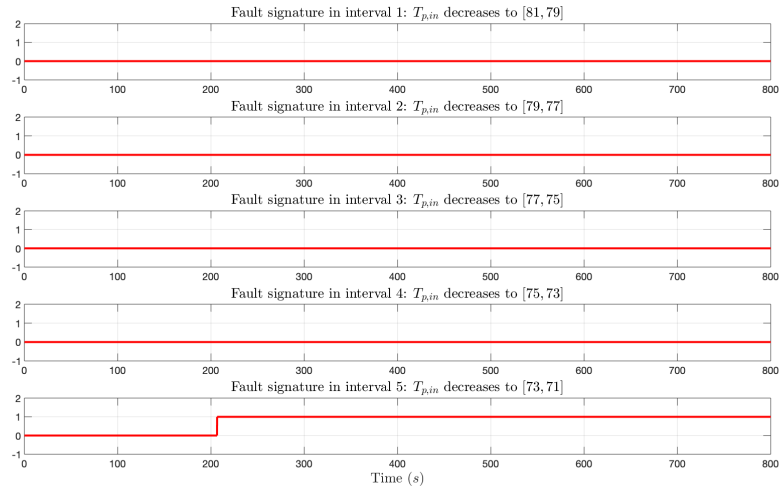


Figure 6.39: Fault signature correspond to intervals of $T_{p,in}$ when dynamic $T_{p,in}$ is faulty at 200s

T_p and the input signal change F_u are presented in Figure 6.40. After 200s, the output temperature T_p cannot follow the desired value anymore, because the inlet temperature of process fluid $T_{p,in}$ is affected by a fault. Even though the control signal tries to eliminate the difference between the reference signal and the real output, but it failed without the intervention of controller reconstruction, as shown in Figure 6.41. However, Figure 6.40 shows the importance of the proposed FTC strategy. The desired temperature is well followed by the output temperature T_p once the controller is

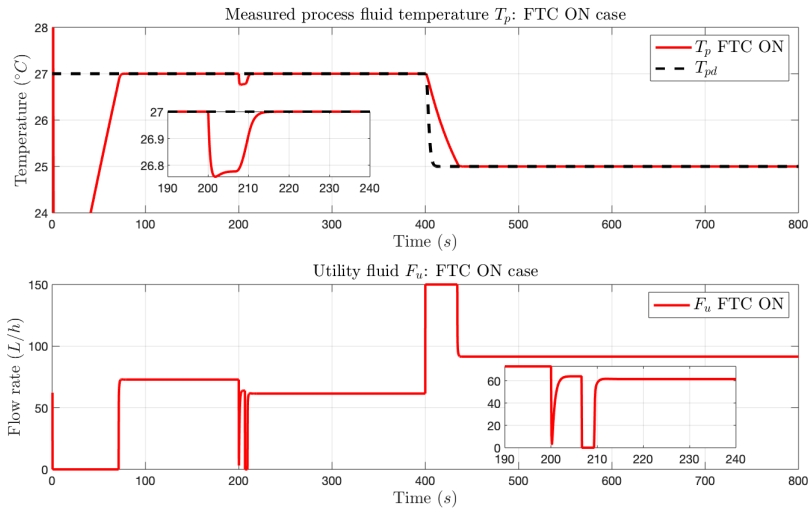


Figure 6.40: $T_{p,in}$ is faulty at 200s, with FTC case

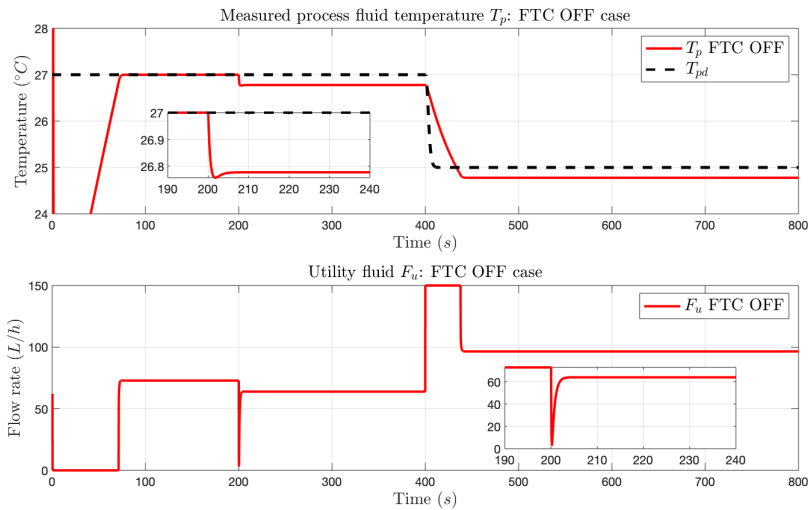


Figure 6.41: $T_{p,in}$ is faulty at 200s, without FTC case

reconstructed.

Therefore, we can conclude that the proposed FTC strategy based on interval observers can well detect, diagnose, and tolerant the dynamic fault, it can guarantee the tracking performance after the occurrence of the fault.

Simulation results: sensor fault case

In this part, two sensor faults are considered, the sensor of process fluid temperature T_p , and the sensor of utility fluid temperature T_u . The faulty values are $f_{s1} = 3^\circ C$, $f_{s2} = 7^\circ C$. The possible variation of each sensor is divided into four intervals with five

bounds. They are presented in Table 4.5 and Table 4.6.

At the beginning, we will consider the fault $f_{s1} = 3 \text{ }^\circ\text{C}$ in the first sensor, the process fluid temperature sensor $s1$. To identify the reason for state change, the standard observer is chosen as the first observer whose variation of Δ_{T_p} equals to zero. Figure 6.42 shows the residual of the standard observer.

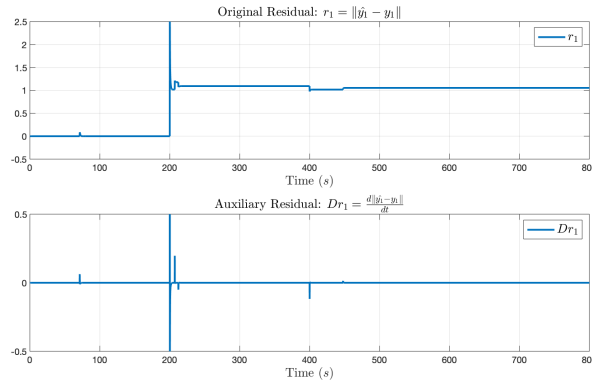


Figure 6.42: Original residual r_1 and auxiliary residual Dr_1 correspond to bound 1 of Δ_{T_p} when sensor T_p is faulty at 200s

At about 72s, there is a change in the original residual r_1 . When the auxiliary residual Dr_1 goes under the threshold $Th_{Dr} = \pm 2 \times 10^{-6}$, we consider the residual r_1 is stable and check its value. Result show that it goes under the threshold $Th_r = \pm 1 \times 10^{-4}$. That is to say, the change is caused by the input signal change. After 200s, the residual is no longer zero anymore. So, we can know that there is a fault. Then, the real outputs of each observer are added by the different variations in Table 4.5 and Table 4.6.

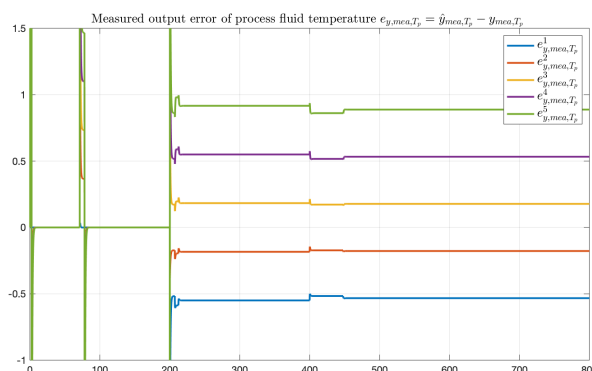


Figure 6.43: Output errors e_{y,mea,T_p} correspond to variation intervals of Δ_{T_p} when sensor T_p is faulty at 200s

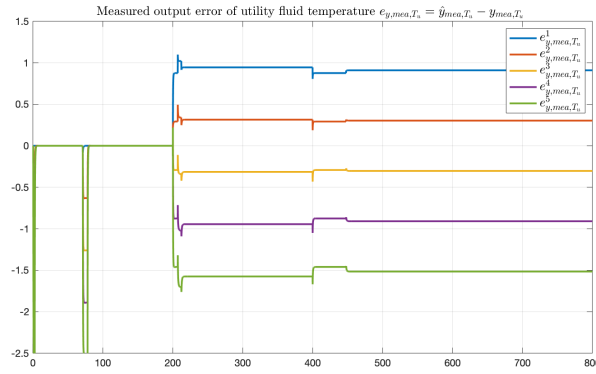


Figure 6.44: Output errors e_{y,mea,T_u} correspond to variation intervals of Δ_{T_p} when sensor T_p is faulty at 200s

Figure 6.43 and Figure 6.44 shows the performances of measured output error between the measurements of observers with Δ_{T_p} variations and the measurements of the system (the output of sensor). We can find that the zero is sandwiched by the second measured output error $e_{y,mea}^2$ and the third measured output error $e_{y,mea}^3$. That indicates the faulty value is located in the second interval $[2, 4]$ of variation Δ_{T_p} .

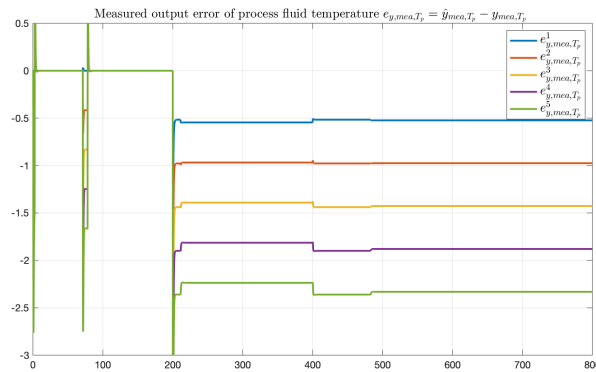


Figure 6.45: Output errors e_{y,mea,T_p} correspond to variation intervals of Δ_{T_u} when sensor T_p is faulty at 200s

In the other hand, for the observer has the parameter change in the second sensor Δ_{T_u} , their measurement errors are presented in Figure 6.45 and Figure 6.46. Unfortunately, the fault is not contained in these interval, because all the e_{y,mea,T_p} or all the e_{y,mea,T_u} locate in the same side of zero.

Fault signatures corresponding to different variation intervals Δ_{T_p} are also presented in Figure 6.47 and 6.48. After 200s, the second interval $[2, 4]$ of Δ_{T_p} gives one, while others stay at zero. That is to say, the faulty value is isolated in the second interval.

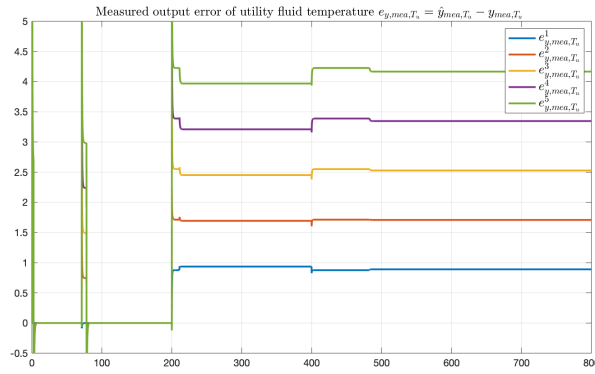


Figure 6.46: Output errors e_{y,mea,T_u} correspond to variation intervals of Δ_{T_u} when sensor T_p is faulty at 200s

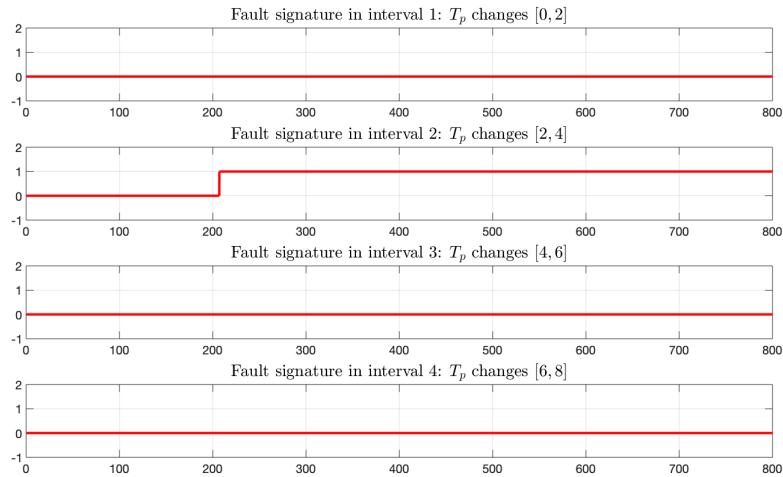


Figure 6.47: Fault signature correspond to variation intervals of Δ_{T_p} when sensor T_p is faulty at 200s

Figure 6.49 and Figure 6.50 shows the tracking performances of process fluid temperature T_p and the dynamic of utility fluid flow rate F_u under two different situation, with FTC strategy, and without FTC strategy. As shown in both figures, the process fluid temperature varies due to the influence of sensor fault at 200s. Not only the output of the sensor (the measurement of the system) but also the output of the system is affected by the sensor fault. And then, the control signal F_u is adjusted automatically to eliminate the tracking error. However, in Figure 6.50, the effect of fault cannot be compensated easily. The offset between the output of system $T_{p,sys}$ and the desired value $T_{p,d}$ always exist without the help of FTC. The good news is that the output of system $T_{p,sys}$ can re-track the desired temperature after a few seconds with the help of

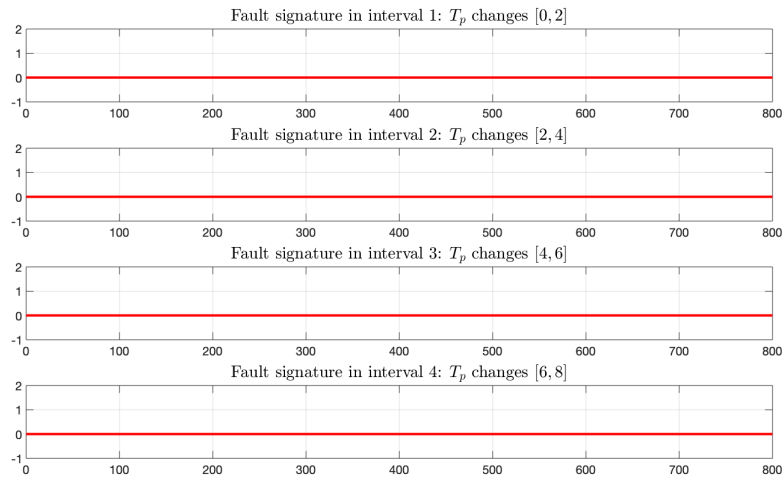


Figure 6.48: Fault signature correspond to variation intervals of ΔT_u when sensor T_p is faulty at 200s

the FTC strategy, as shown in Figure 6.49.

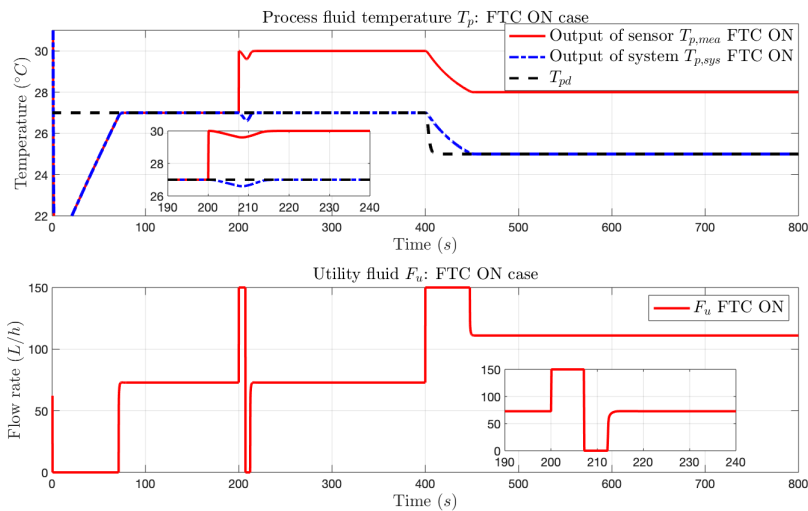


Figure 6.49: Sensor of T_p is faulty at 200s, with FTC case

We should pay attention to that, our control objective is to make the output of the system follows the desired temperature. If the fault occurs in one of the sensors, there is always an offset between the output of the sensor and the output of the system, unless the faulty sensor is replaced. And the value of offset is the value of fault.

Figure 6.51 gives the performances of utility fluid temperature under the two situations. The black dot line represents the output of sensor T_u under fault free case. In this case, since the fault does not occur in the utility fluid temperature sensor, the

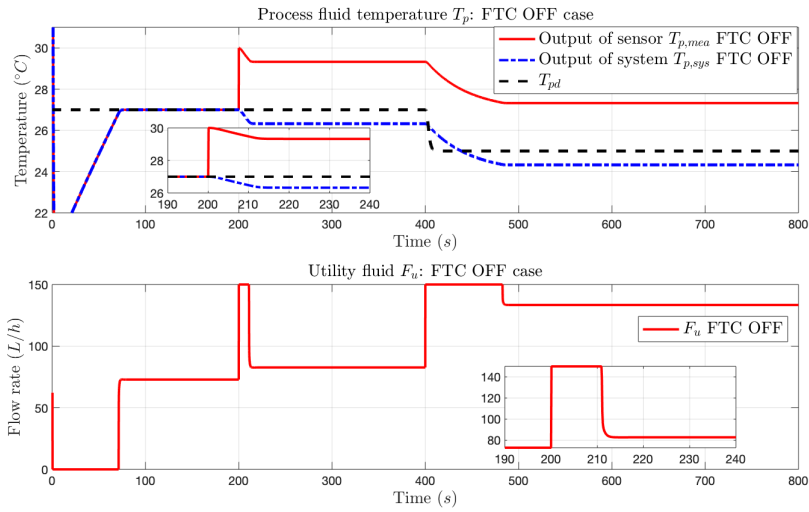


Figure 6.50: Sensor of T_p is faulty at 200s, without FTC case

output of the sensor is equal to the output of the system in both cases. When the fault is introduced in the first sensor at 200s, the utility fluid temperature is also affected, both output of sensor $T_{u,mea}$ and output of system $T_{u,sys}$ are not equal to the value under fault free case. Fortunately, this difference is eliminated with the help of the proposed FTC method. In the contrast, this difference always exists without the use of FTC.

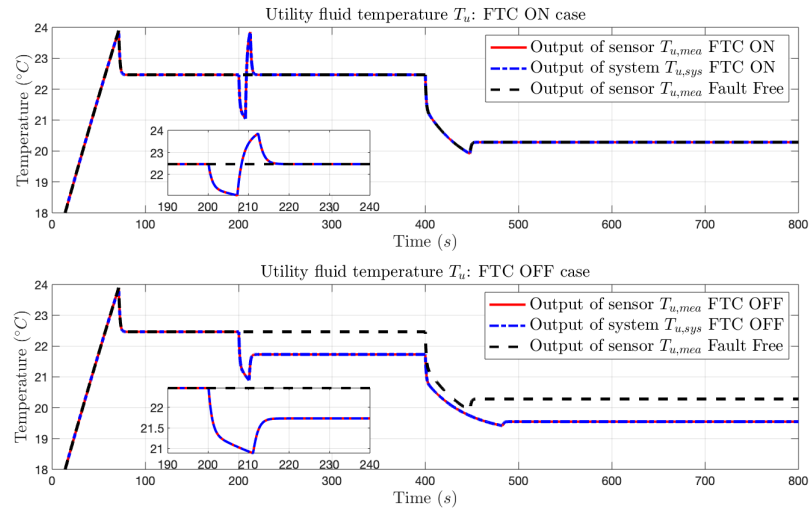


Figure 6.51: Utility fluid temperature when sensor of T_p is faulty at 200s

In the second case, the sensor fault $f_{s2} = 7 \text{ } ^\circ\text{C}$ is introduced in the utility fluid temperature sensor $s2$ at 200s. Then, the faulty output of sensor (the measurement of the system) is $y_2^f = y_2 + f_{s2}$.

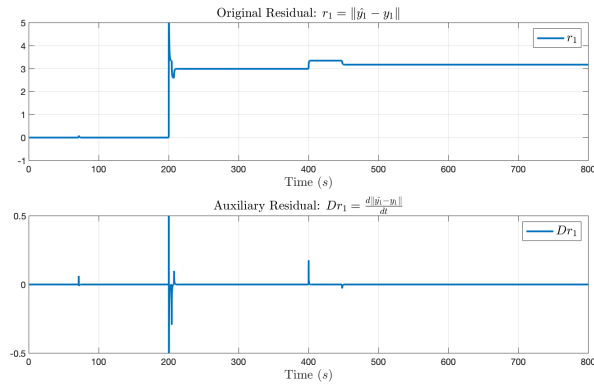


Figure 6.52: Original residual r_1 and auxiliary residual Dr_1 correspond to bound 1 of Δ_{T_u} when sensor T_u is faulty at 200s

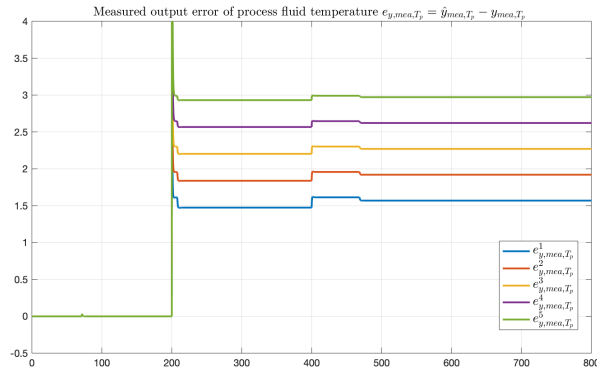


Figure 6.53: Output errors e_{y,mea,T_p} correspond to variation intervals of Δ_{T_p} when sensor T_u is faulty at 200s

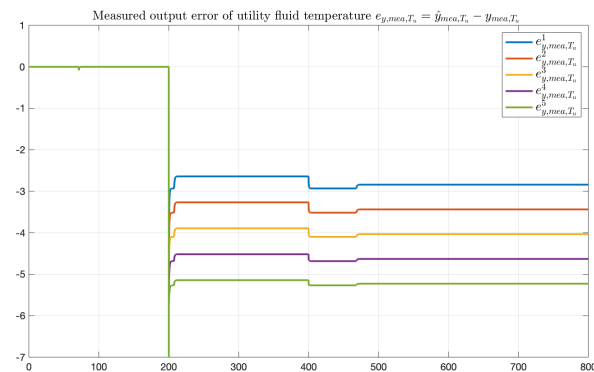


Figure 6.54: Output errors e_{y,mea,T_u} correspond to variation intervals of Δ_{T_p} when sensor T_u is faulty at 200s

To detect the fault correctly, the first observer is named as the standard observer

since its variation is zero, which means it uses the same parameter value as the real system before the fault is introduced. The performance of the residuals is presented in Figure 6.52. The standard observer can help us find out the reason for state change, it is caused by input change or caused by a fault. At 200s, the state change is caused by a fault.

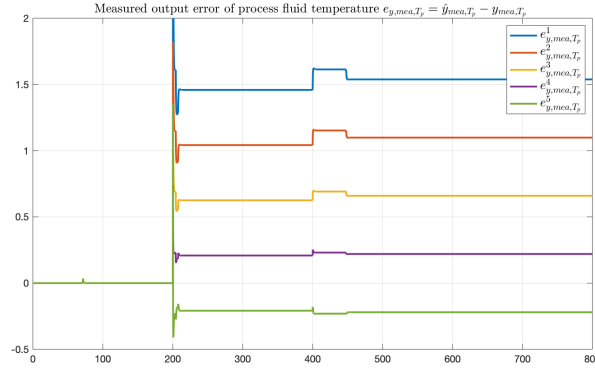


Figure 6.55: Output errors e_{y,mea,T_p} correspond to variation intervals of Δ_{T_u} when sensor T_u is faulty at 200s

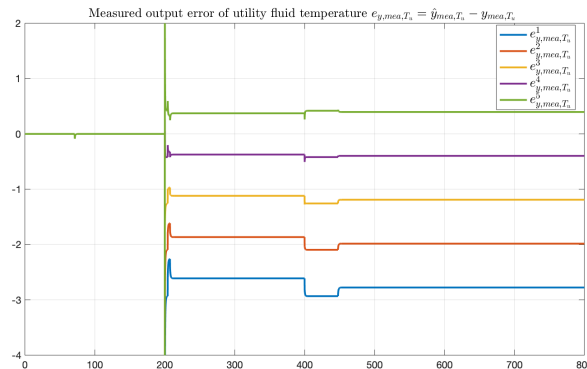


Figure 6.56: Output errors e_{y,mea,T_u} correspond to variation intervals of Δ_{T_u} when sensor T_u is faulty at 200s

The measured output errors $e_{y,mea}$ between the variation Δ_{T_p} interval observers and the measurement of the system are presented in Figure 6.53 and Figure 6.54. We also check the performance of the observers whose measured output change at Δ_{T_u} . Their measured output errors $e_{y,mea}$ are presented in Figure 6.55 and Figure 6.56. we can easily find that the fault is contained in the fourth interval of Δ_{T_u} variation.

Fault signature of each interval is shown in Figure 6.57 and 6.58. The fourth fault signature of Δ_{T_u} sends one after 200s to indicate the faulty value is contained. Other

fault signatures keep zero because the faulty value is not contained in these intervals.

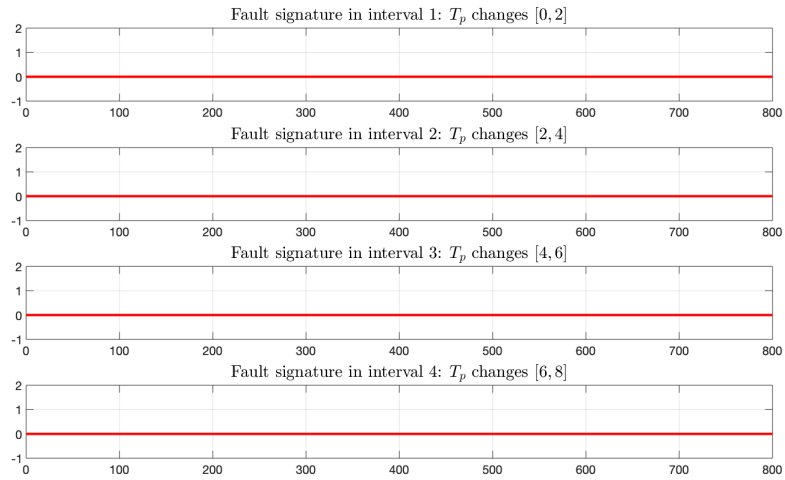


Figure 6.57: Fault signature correspond to variation intervals of Δ_{T_p} when sensor T_u is faulty at 200s

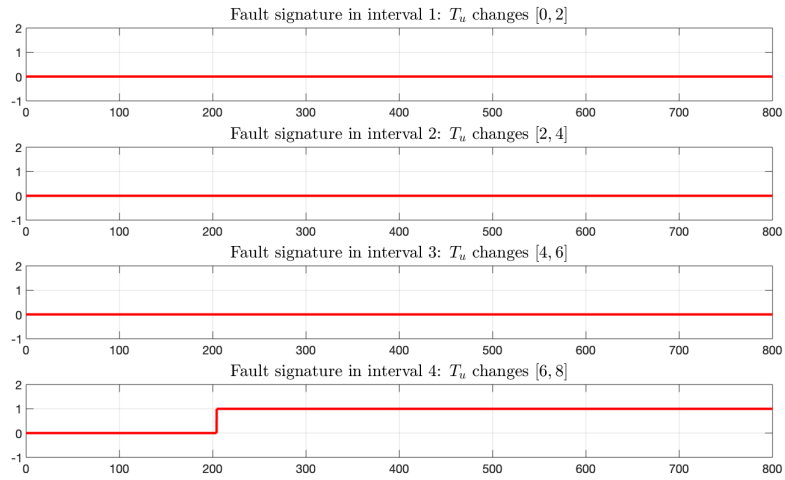


Figure 6.58: Fault signature correspond to variation intervals of Δ_{T_u} when sensor T_u is faulty at 200s

Figure 6.59 and Figure 6.60 present the tracking performance of process fluid temperature T_p and the variation of input signal F_u are presented under different situations, with and without FTC strategy. Before 200s, the process fluid temperature can well follow the desired value T_{pd} . Because the fault occurs in the second sensor, the output of the first sensor $T_{p,mea}$ always equals the real output of the system $T_{p,sys}$. However, the output of process fluid temperature is still influenced by the faulty sensor s_2 . And

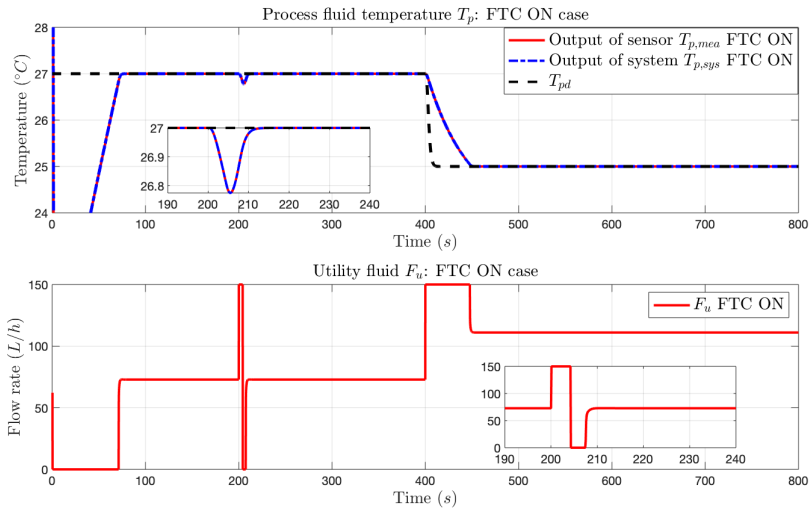


Figure 6.59: Sensor of T_u is faulty at 200s, with FTC case

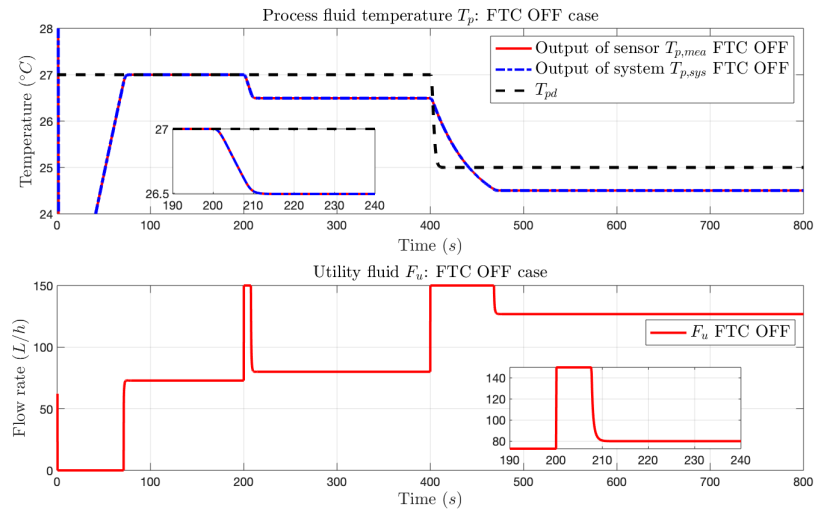


Figure 6.60: Sensor of T_u is faulty at 200s, without FTC case

the tracking difference always exists after 200s without the application of TFC strategy, see in Figure 6.60. Fortunately, this tracking error is eliminated by the reconstruction of the control signal, as shown in Figure 6.59.

The measured utility fluid temperature $T_{u,mea}$ and the real utility fluid temperature output of system $T_{u,sys}$ under different cases are presented in Figure 6.61. As we described before, the fault is introduced in the second sensor, i.e. the sensor of utility fluid temperature, so there is an offset between the measured value and the real output of the system. The value of the offset is the faulty value we applied 5°C . Obviously, the influence of sensor s_2 fault is eliminated with the application of the proposed FTC

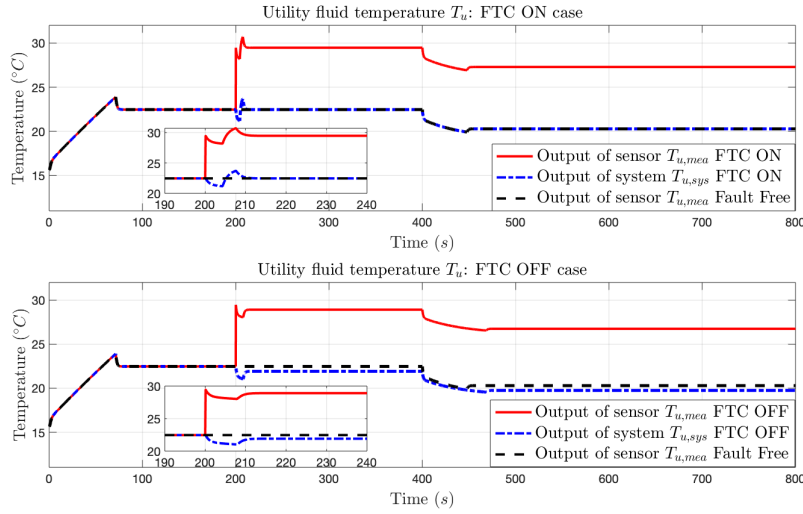


Figure 6.61: Utility fluid temperature when sensor of T_u is faulty at 200s

method.

Therefore, we can conclude that the proposed interval observer based FTC strategy works. The reference signal can be well tracked even with the existence of dynamic fault or sensor fault.

6.3 Comparison between these two methods

In this part, we will compare the adaptive observer based FTC strategy and the interval observer based FTC strategy proposed in Section 6.2 and Section 6.3. According to the presented simulation results, both FTC strategies can achieve our objective, that is to make the temperature of process fluid T_p stays at the desired temperature $T_{p,d}$ by adjusting the flow rate of utility fluid F_u under the interruption of dynamic fault or sensor fault.

The main idea of both observer based FTC strategies proposed are control reconfiguration. The nominal controller is based on the backstepping technique. Once the fault is detected and diagnosed, the control law is reconstructed according to the fault information. So, the fault diagnosis procedure is quite important for our FTC scheme. If the fault can be quickly isolated and identified, the better tracking performance we can get.

The only difference between the presented FTC strategies is their fault diagnosis scheme. One uses a bank of adaptive observers to isolate the fault, each adaptive observer corresponds to one possible faulty parameter. The other is based on parameter

interval dividing, the working domain of each parameter is divided into several intervals, and observers are constructed whose parameter is changed to the preselected interval bounds. To prevent the fake alarm caused by input signal change, we will evaluate the original residual until its value is stable. And the auxiliary residual is the tools to check the stability of the original residual. Therefore, the fault can be immediately isolated as long as we can make sure the state change in the system is caused by a fault, not by the input signal change. To compare the performance of the proposed FTC method, the same values including initial values, fault values and threshold, are used for both observer based FTC scheme.

Table 6.1: Comparison between adaptive observer based FTC strategy and interval observer based FTC strategy

Fault	Magnitude f	Adaptive observer based FTC		Interval observer based FTC	
		Isolation Instant (s)	Estimation \hat{f}	Isolation Instant (s)	Estimation \hat{f}
h_p	$-15\% h_p^0$	218.3	$-15\% h_p^0$	207.5	$-15\% h_p^0$
$T_{p,in}$	-5	222.2	-5	206.6	-5
T_p	3	219.6	3	207.1	3
T_u	7	217.4	7	212.1	7

Table 6.1 shows the comparison between these two strategies. The first column represents the type of fault. And the first and second rows represent the dynamic fault in h_p , the heat transfer coefficient between process channel and plate wall, and $T_{p,in}$, the inlet temperature of the process fluid. The third and fourth row represent the sensor fault in T_p and T_u . The time of fault occurrence is 200s, and both of these methods can detect the fault immediately, at 200.1s. Besides, the fault can be identified accurately. In Table 6.1, we can see that the biggest difference between these two methods is their isolation time. The interval observer based FTC strategy uses less time than the adaptive observer based FTC method to isolate the fault. Thus, the controller can be redesigned earlier than the adaptive observer based FTC method, and the influence of fault can be quickly eliminated. This can be seen from the simulation results presented in the former section.

As we described before, each adaptive observer gives an estimation of the fault, and it is a time wasting procedure. Unfortunately, the fault can not be isolated until the fault value is well estimated for the adaptive observer based method. For the interval

observer based method, by calculating the average value of the interval bounds that contain the faulty value, the faulty value can be easily and quickly obtained.

However, the faulty value estimation of the interval observer based method highly relies on the parameter dividing. For example, the faulty value equals 0.8, but the interval contains the faulty parameter is $[0, 1]$. Then, according to (4.34), we take the faulty value estimation as 0.5, which is different from the real faulty value 0.8. Fortunately, this difference can be decreased or eliminated by dividing more intervals, for instance, we minimize the interval to $[0.6, 1]$, then the faulty value is well estimated. But, more intervals will increase the complexity of calculation at the same time. Besides, the interval observer based FTC method needs a great number of observers compared to the adaptive observer based method. For example, there are n possible faulty parameters in the system, and their practical domains are divided into m intervals, which means there are $m + 1$ bounds. Thus, $n \times (m + 1)$ observers need to be constructed for the interval observer based FTC strategy, while only n adaptive observers are needed for the adaptive observer based FTC strategy. Nevertheless, with the development of computer technology, the calculation complexity will not be a problem.

6.4 Summary

In this section, two active FTC strategies have been proposed based on the backstepping control law obtained in Chapter 5 and the FDD schemes presented in Chapter 4. The fault was firstly detected, isolated, and identified. Then, the controller is reconfigured by using the estimated fault information. Since accurate fault information is important for our FTC scheme, different observers were used to providing the details of the fault, adaptive observer, and interval observer. Then, the adaptive observer based FTC strategy and the interval observer based FTC strategy have been applied to the HEX reactor. Both dynamic fault and sensor fault were considered in this chapter. The effectiveness of both FTC strategies has been proved according to the simulation results. They both provided a satisfactory tracking performance even the system has been affected by the unexpected fault. Besides, the performances of the proposed FTC strategies have been compared. Their advantages and disadvantages have been analyzed. The adaptive observer based FTC strategy has less calculation complexity. While the interval observer based FTC strategy presents a faster fault isolation speed.

Chapter 7

Conclusion and suggestion of future works

In this chapter, the main results obtained in this thesis are summarized, and conclusions of this thesis are presented. Based on these conclusions and other observations made during the research, new research directions for further developments are suggested.

7.1 Conclusion

This thesis focuses on observer based fault diagnosis scheme and active fault tolerant control strategy based on backstepping technique. The proposed FTC schemes can not only be applied to an intensified HEX reactor system but also can be used for other industrial systems. The fault is firstly detected, isolated, and identified by nonlinear observers, and then, the estimated fault information is used for controller reconstruction to make the whole system still achieve the desired performance with the interruption of unexpected fault. The main results of this thesis are summarized as follows:

- Modeling of an intensified heat-exchanger/reeactor (HEX reactor).

The HEX reactor considered in this thesis is an intensified device that combines heat exchanger and chemical reactor in the same module. The pilot consists of three process plates sandwiched between four utility plates, both process plate and utility plate are engraved by laser machining to obtain cross-section channels, which are named as process channel and utility channel, respectively. Reactants are injected into the process channel and the chemical reaction is taken place here, while the utility fluid, (usually water) is fed into the utility channel to bring in or take reaction heat away as soon as possible. This intensified channel-based structure makes it provide excellent thermal and hydrodynamic performances.

To provide an accurate model for further control use, a cell-based modeling scheme has been proposed in this thesis. The HEX reactor has been divided into 17 units firstly according to its physical structure. Each unit consists of 15 cells with different functions. According to the mass balance and energy balance, every cell is represented by one particular mathematical equation. After connecting all these cells in order, an integrated HEX reactor model is obtained. The effectiveness of the proposed model has been proved by comparing the simulation results with experimental data under two different situations, with and without consideration of chemical reaction. Results prove that the performance of the proposed model can well reflect the dynamic of the HEX reactor in reality.

- Application of nonlinear observer based FDD methods.

In order to supervise and investigate the dynamic of the considered HEX reactor system, two kinds of nonlinear observers, adaptive observer and interval observer, have been studied in Section 4. Firstly, an overview of the recent observers applied to chemical process systems has been presented. Since the adaptive observer

and interval observer can not only focus on the estimation of the internal states but also the estimation of the parameters, they are typically investigated in this section. Two kinds of FDD schemes based on adaptive observer and interval observer have been presented and applied to the considered HEX reactor.

The adaptive observer based FDD scheme uses a bank of adaptive observers to detect and isolate the fault, each adaptive observer corresponds to one possible faulty parameter. Once the fault is isolated, the corresponding adaptive observer can give the estimation of the faulty parameter. The interval observer based FDD method relies on the construction of interval observers. The working domain of each parameter is divided into several intervals, and then, observers are constructed by changing the possible faulty parameter into the preselected interval bound value. The fault is isolated by verifying if the faulty value is contained in the interval.

In this chapter, both dynamic fault and sensor have been taken into consideration. With the occurrence of fault, there was a degradation in the performance of the HEX reactor. By applying the presented FDD methods based on different observers, the fault can be well detected, isolated and identified.

- Nonlinear control signal design for the considered HEX reactor based on backstepping technique.

For the considered HEX reactor, temperature control is a principal problem. Therefore, a nominal control law has been designed based on the backstepping technique. To guarantee the safety and productivity of chemical reactions, our control objective is to make the temperature of the process fluid maintain at the desired value. Considering a simplified working situation of the HEX reactor, without chemical reaction, the backstepping control law has been proposed and applied to the reactor. According to the presented simulation results, the proposed nominal control law can make the process fluid temperature well follow the desired temperature.

- Observer based fault tolerant control schemes design and their applications for the HEX reactor under dynamic fault or sensor fault case.

Based on the FDD schemes presented in Section 5 and the backstepping control law obtained in Section 5, two active fault tolerant control strategies have been proposed in Section 6 to deal with the HEX reactor with the interruption of dynamic fault and sensor fault. Both FTC strategies are based on the idea

of controller reconfiguration. The fault is firstly detected and diagnosed by an observer based FDI scheme, and then, the controller is re-designed by using the estimated fault information to guarantee the performance of the faulty system.

After applying the FTC strategies based on different observers, adaptive observer and interval observer, to the HEX reactor, both of them can provide a satisfactory tracking performance for the process fluid temperature even though the system is affected by a dynamic fault or sensor fault. Besides, the performances of these two strategies have been compared. Simulation results show that both of them can well isolate and estimate the faulty parameter, but the interval observer based FTC strategy has a faster isolation speed.

To summarize, the observer based backstepping fault tolerant control strategies proposed in this thesis can make the system still achieve the desired performance even though it is influenced by a dynamic fault or sensor fault. Besides, the designed fault tolerant schemes are applicable for various types of engineering systems. The application to the considered HEX reactor has shown the effectiveness of the proposed FTC strategies.

7.2 Future works

Based on the work mentioned above, it is motivated to keep on researching about the following problems.

- Application of proposed FTC strategies to the HEX reactor with consideration of chemical reaction.

In the case study, the proposed FTC strategies are both applied to the HEX reactor where only the heat exchange part is considered. When the chemical reaction is introduced, the HEX reactor may be bothered with various faults with the increase of the system complexity. Therefore, how to guarantee the system performance after the implementation of the chemical reaction is another interest for investigation.

- Application of proposed FTC strategies under the interruption of measurement noise.

In reality, the existence of measurement noise will make it difficult to detect and diagnose the fault. So, how to avoid the fake fault detection alarm and guarantee the fault tolerant performance are the questions worthy of future research.

- Fault tolerant control strategy design for actuator fault case.

The proposed FTC strategies are both based on the controller reconfiguration. For the considered dynamic fault and sensor fault, the control law can be easily re-designed. However, what if the fault occurs in the actuator. The fault tolerant scheme can not be done by simply changing its parameters to the faulty situation. Therefore, it is another direction of future study.

- Combination of the proposed adaptive observer based FTC strategy and interval observer based FTC strategy.

As mentioned in the last section, both of the proposed FTC strategies have their advantages and disadvantages. The adaptive observer based FTC scheme can provide an accurate faulty value estimation while it takes a longer time for fault isolation. In the contrast, the interval observer based FTC scheme has a faster isolation speed, but the fault estimation highly relies on parameter interval dividing. Thus, is there a possibility to take advantage of these two observers at the same time? For example, replacing the observer corresponding to each interval bounds with adaptive observers, which can give an accurate estimation of the faulty parameter. Then, once the faulty value is isolated in one of the intervals, its estimation can be given by the adaptive observer other than calculating the average value of the bounds in (4.34) or (4.39). This is also a research interest in future work.

Bibliography

- [1] M. Abid. “Fault detection in nonlinear systems: An observer-based approach”. In: *Universitat Duisburg-Essen* (2010).
- [2] A. Akhenak, E. Duviella, L. Bako, and S. Lecoeuche. “Online fault diagnosis using recursive subspace identification: Application to a dam-gallery open channel system”. In: *Control Engineering Practice* 21.6 (2013), pp. 797–806.
- [3] J. M. Ali, N. H. Hoang, M. A. Hussain, and D. Dochain. “Review and classification of recent observers applied in chemical process systems”. In: *Computers & Chemical Engineering* 76 (2015), pp. 27–41.
- [4] J. M. Ali, N. H. Hoang, M. A. Hussain, and D. Dochain. “Hybrid observer for parameters estimation in ethylene polymerization reactor: A simulation study”. In: *Applied Soft Computing* 49 (2016), pp. 687–698.
- [5] H. Alwi, C. Edwards, O. Stroosma, and J. Mulder. “Fault tolerant sliding mode control design with piloted simulator evaluation”. In: *Journal of Guidance, Control, and Dynamics* 31.5 (2008), pp. 1186–1201.
- [6] Z. Anxionnaz, M. Cabassud, C. Gourdon, and P. Tochon. “Heat exchanger/reactors (HEX reactors): concepts, technologies: state-of-the-art”. In: *Chemical Engineering and Processing: Process Intensification* 47.12 (2008), pp. 2029–2050.
- [7] Z. Anxionnaz, F. Theron, P. Tochon, R. Couturier, C. Gourdon, M. Cabassud, et al. “RAPIC project: toward competitive heat-exchanger/reactors”. In: *EPIC, 3rd European Process Intensification Conference*. 2011.
- [8] Z. Anxionnaz-Minvielle, M. Cabassud, C. Gourdon, and P. Tochon. “Influence of the meandering channel geometry on the thermo-hydraulic performances of an intensified heat exchanger/reactor”. In: *Chemical Engineering and Processing: Process Intensification* 73 (2013), pp. 67–80.

- [9] G. Arji, H. Ahmadi, M. Nilashi, T. A. Rashid, O. H. Ahmed, N. Aljojo, et al. “Fuzzy logic approach for infectious disease diagnosis: A methodical evaluation, literature and classification”. In: *Biocybernetics and Biomedical Engineering* 39.4 (2019), pp. 937–955.
- [10] W. Benaissa, S. Elgue, N. Gabas, M. Cabassud, D. Carson, and M. Demissy. “Dynamic behaviour of a continuous heat exchanger/reactor after flow failure”. In: *International Journal of Chemical Reactor Engineering* 6.1 (2008).
- [11] M. E. H. Benbouzid. “A review of induction motors signature analysis as a medium for faults detection”. In: *IEEE transactions on industrial electronics* 47.5 (2000), pp. 984–993.
- [12] M. Benosman and K.-Y. Lum. “Passive actuators’ fault-tolerant control for affine nonlinear systems”. In: *IEEE Transactions on Control Systems Technology* 18.1 (2009), pp. 152–163.
- [13] G. Besançon. “Remarks on nonlinear adaptive observer design”. In: *Systems & control letters* 41.4 (2000), pp. 271–280.
- [14] G. Besançon. *Nonlinear observers and applications*. Vol. 363. Springer, 2007.
- [15] M. Blanke, R. Izadi-Zamanabadi, S. A. Bøgh, and C. P. Lunau. “Fault-tolerant control systems—a holistic view”. In: *Control Engineering Practice* 5.5 (1997), pp. 693–702.
- [16] M. Blanke, M. Kinnaert, J. Lunze, M. Staroswiecki, and J. Schröder. *Diagnosis and fault-tolerant control*. Vol. 2. Springer, 2006.
- [17] M. Blanke, M. Staroswiecki, and N. E. Wu. “Concepts and methods in fault-tolerant control”. In: *Proceedings of the 2001 American Control Conference. (Cat. No. 01CH37148)*. Vol. 4. IEEE, 2001, pp. 2606–2620.
- [18] M. Bo, J. Zhi-nong, and W. Zhong-qing. “Development of the task-based expert system for machine fault diagnosis”. In: *Journal of Physics: Conference Series*. Vol. 364. 1. IOP Publishing, 2012, p. 012043.
- [19] M. Bodson and J. E. Groszkiewicz. “Multivariable adaptive algorithms for reconfigurable flight control”. In: *IEEE transactions on control systems technology* 5.2 (1997), pp. 217–229.
- [20] G. Bornard, F. Celle-Couenne, and G. Gilles. “Observability and observers”. In: *Nonlinear Systems*. Springer, 1995, pp. 173–216.

- [21] H. Chen and S. Lu. “Fault diagnosis digital method for power transistors in power converters of switched reluctance motors”. In: *IEEE Transactions on Industrial Electronics* 60.2 (2012), pp. 749–763.
- [22] J. Chen and R. J. Patton. *Robust model-based fault diagnosis for dynamic systems*. Vol. 3. Springer Science & Business Media, 2012.
- [23] W. Chen and M. Saif. “An actuator fault isolation strategy for linear and non-linear systems”. In: *Proceedings of the 2005, American Control Conference, 2005*. IEEE. 2005, pp. 3321–3326.
- [24] W. Chen and M. Saif. “Adaptive sensor fault detection and isolation in uncertain systems”. In: *2007 American Control Conference*. IEEE. 2007, pp. 3240–3245.
- [25] U.-P. Chong et al. “Signal model-based fault detection and diagnosis for induction motors using features of vibration signal in two-dimension domain”. In: *Strojniški vestnik* 57.9 (2011), pp. 655–666.
- [26] X. Dai and Z. Gao. “From model, signal to knowledge: A data-driven perspective of fault detection and diagnosis”. In: *IEEE Transactions on Industrial Informatics* 9.4 (2013), pp. 2226–2238.
- [27] S. X. Ding. *Model-based fault diagnosis techniques: design schemes, algorithms, and tools*. Springer Science & Business Media, 2008.
- [28] D. Dochain. “State observers for tubular reactors with unknown kinetics”. In: *Journal of process control* 10.2-3 (2000), pp. 259–268.
- [29] D. Dochain. “State and parameter estimation in chemical and biochemical processes: a tutorial”. In: *Journal of process control* 13.8 (2003), pp. 801–818.
- [30] M. Döhler and L. Mevel. “Subspace-based fault detection robust to changes in the noise covariances”. In: *Automatica* 49.9 (2013), pp. 2734–2743.
- [31] G. Dong, W. Chongguang, B. Zhang, and M. Xin. “Signed directed graph and qualitative trend analysis based fault diagnosis in chemical industry”. In: *Chinese Journal of Chemical Engineering* 18.2 (2010), pp. 265–276.
- [32] Z. Dong, J. Zhao, J. Duan, M. Wang, and H. Wang. “Research on agricultural machinery fault diagnosis system based on expert system”. In: *2018 2nd IEEE Advanced Information Management, Communicates, Electronic and Automation Control Conference (IMCEC)*. IEEE. 2018, pp. 2057–2060.

- [33] G. J. Ducard. *Fault-tolerant flight control and guidance systems: Practical methods for small unmanned aerial vehicles*. Springer Science & Business Media, 2009.
- [34] S. Elgue, A. Conte, C. Gourdon, and Y. Bastard. “Direct fluorination of 1, 3-dicarbonyl compound in a continuous flow reactor at industrial scale”. In: *Chemica Oggi/Chemistry Today* 30.4 (2012).
- [35] J. Etchells. “Process intensification: safety pros and cons”. In: *Process Safety and Environmental Protection* 83.2 (2005), pp. 85–89.
- [36] H. Fang, N. Tian, Y. Wang, M. Zhou, and M. A. Haile. “Nonlinear Bayesian estimation: From Kalman filtering to a broader horizon”. In: *IEEE/CAA Journal of Automatica Sinica* 5.2 (2018), pp. 401–417.
- [37] M. Farza, H. Hammouri, S. Othman, and K. Busawon. “Nonlinear observers for parameter estimation in bioprocesses”. In: *Chemical Engineering Science* 52.23 (1997), pp. 4251–4267.
- [38] A. Fekih. “Fault diagnosis and fault tolerant control design for aerospace systems: A bibliographical review”. In: *2014 American Control Conference*. IEEE, 2014, pp. 1286–1291.
- [39] D. Fragkoulis. “Détection et localisation des défauts provenant des actionneurs et des capteurs: application sur un système non linéaire”. PhD thesis. Université de Toulouse, Université Toulouse III-Paul Sabatier, 2008.
- [40] D. Fragkoulis, G. Roux, and B. Dahhou. “Detection, isolation and identification of multiple actuator and sensor faults in nonlinear dynamic systems: Application to a waste water treatment process”. In: *Applied Mathematical Modelling* 35.1 (2011), pp. 522–543.
- [41] P. M. Frank. “Fault diagnosis in dynamic systems using analytical and knowledge-based redundancy: A survey and some new results”. In: *automatica* 26.3 (1990), pp. 459–474.
- [42] P. M. Frank. “On-line fault detection in uncertain nonlinear systems using diagnostic observers: a survey”. In: *International journal of systems science* 25.12 (1994), pp. 2129–2154.
- [43] P. M. Frank. “Analytical and qualitative model-based fault diagnosis—a survey and some new results”. In: *European Journal of control* 2.1 (1996), pp. 6–28.

- [44] Z. Gao and P. J. Antsaklis. “Stability of the pseudo-inverse method for reconfigurable control systems”. In: *international Journal of Control* 53.3 (1991), pp. 717–729.
- [45] Z. Gao and P. J. Antsaklis. “Reconfigurable control system design via perfect model following”. In: *International Journal of Control* 56.4 (1992), pp. 783–798.
- [46] Z. Gao, C. Cecati, and S. X. Ding. “A survey of fault diagnosis and fault-tolerant techniques—Part I: Fault diagnosis with model-based and signal-based approaches”. In: *IEEE Transactions on Industrial Electronics* 62.6 (2015), pp. 3757–3767.
- [47] Z. Gao, C. Cecati, and S. X. Ding. “A survey of fault diagnosis and fault-tolerant techniques—Part I: Fault diagnosis with model-based and signal-based approaches”. In: *IEEE Transactions on Industrial Electronics* 62.6 (2015), pp. 3768–3774.
- [48] E. A. Garcia and P. Frank. “On the relationship between observer and parameter identification based approaches to fault detection”. In: *IFAC Proceedings Volumes* 29.1 (1996), pp. 6349–6353.
- [49] E. A. Garcia and P. M. Frank. “Deterministic nonlinear observer-based approaches to fault diagnosis: a survey”. In: *Control Engineering Practice* 5.5 (1997), pp. 663–670.
- [50] J. Gauthier and G. Bornard. “Observability for any $u(t)$ of a class of nonlinear systems”. In: *IEEE Transactions on Automatic Control* 26.4 (1981), pp. 922–926.
- [51] X. Gong and W. Qiao. “Bearing fault diagnosis for direct-drive wind turbines via current-demodulated signals”. In: *IEEE Transactions on Industrial Electronics* 60.8 (2013), pp. 3419–3428.
- [52] A. Green, B. Johnson, and A. John. “Process intensification magnifies profits”. In: *Chemical engineering (New York, NY)* 106.13 (1999), pp. 66–73.
- [53] Y. Gritli, L. Zarri, C. Rossi, F. Filippetti, G.-A. Capolino, and D. Casadei. “Advanced diagnosis of electrical faults in wound-rotor induction machines”. In: *IEEE Transactions on Industrial Electronics* 60.9 (2012), pp. 4012–4024.
- [54] D. He, R. Li, and J. Zhu. “Plastic bearing fault diagnosis based on a two-step data mining approach”. In: *IEEE Transactions on Industrial Electronics* 60.8 (2012), pp. 3429–3440.

- [55] M. He, Z. Li, X. Han, M. Cabassud, and B. Dahhou. “Development of a Numerical Model for a Compact Intensified Heat-Exchanger/Reactor”. In: *Processes* 7.7 (2019), p. 454.
- [56] R. Hermann and A. Krener. “Nonlinear controllability and observability”. In: *IEEE Transactions on automatic control* 22.5 (1977), pp. 728–740.
- [57] L. Hong and J. S. Dhupia. “A time domain approach to diagnose gearbox fault based on measured vibration signals”. In: *Journal of Sound and Vibration* 333.7 (2014), pp. 2164–2180.
- [58] C.-S. Hsieh. “Performance gain margins of the two-stage LQ reliable control”. In: *Automatica* 38.11 (2002), pp. 1985–1990.
- [59] M.-D. Hua, G. Ducard, T. Hamel, R. Mahony, and K. Rudin. “Implementation of a nonlinear attitude estimator for aerial robotic vehicles”. In: *IEEE Transactions on Control Systems Technology* 22.1 (2013), pp. 201–213.
- [60] X. Hulhoven, A. V. Wouwer, and P. Bogaerts. “Hybrid extended Luenberger-asymptotic observer for bioprocess state estimation”. In: *Chemical engineering science* 61.21 (2006), pp. 7151–7160.
- [61] W. Hwang and K. Huh. “Fault detection and estimation for electromechanical brake systems using parity space approach”. In: *Journal of Dynamic Systems, Measurement, and Control* 137.1 (2015).
- [62] R. Isermann. “Process fault detection based on modeling and estimation methods—A survey”. In: *automatica* 20.4 (1984), pp. 387–404.
- [63] R. Isermann. *Fault-diagnosis systems: an introduction from fault detection to fault tolerance*. Springer Science & Business Media, 2005.
- [64] R. Isermann. *Fault-diagnosis applications: model-based condition monitoring: actuators, drives, machinery, plants, sensors, and fault-tolerant systems*. Springer Science & Business Media, 2011.
- [65] R. Isermann and P. Balle. “Trends in the application of model-based fault detection and diagnosis of technical processes”. In: *Control engineering practice* 5.5 (1997), pp. 709–719.
- [66] H. A. Izadi, Y. Zhang, and B. W. Gordon. “Fault tolerant model predictive control of quad-rotor helicopters with actuator fault estimation”. In: *Proceedings of the 18th IFAC World Congress*. Vol. 18. 1. 2011, pp. 6343–6348.

- [67] I. Izadi, S. L. Shah, D. S. Shook, and T. Chen. “An introduction to alarm analysis and design”. In: *IFAC Proceedings Volumes* 42.8 (2009), pp. 645–650.
- [68] A. Jarrou. “Diagnostic de défauts et commande tolérante aux défauts des systèmes à énergie renouvelable”. PhD thesis. Université de Lorraine, 2020.
- [69] J. Jiang. “Fault-tolerant control systems-an introductory overview”. In: *Acta Automatica Sinica* 31.1 (2005), pp. 161–174.
- [70] J. Jiang and X. Yu. “Fault-tolerant control systems: A comparative study between active and passive approaches”. In: *Annual Reviews in control* 36.1 (2012), pp. 60–72.
- [71] G. M. Joksimović, J. Riger, T. M. Wolbank, N. Perić, and M. Vašak. “Stator-current spectrum signature of healthy cage rotor induction machines”. In: *IEEE Transactions on Industrial Electronics* 60.9 (2012), pp. 4025–4033.
- [72] R. E. Kalman and R. S. Bucy. “New results in linear filtering and prediction theory”. In: (1961).
- [73] M. Kinnaert. “Fault diagnosis based on analytical models for linear and nonlinear systems-a tutorial”. In: *IFAC Proceedings Volumes* 36.5 (2003), pp. 37–50.
- [74] P. V. Kokotovic. “The joy of feedback: nonlinear and adaptive”. In: *IEEE Control Systems Magazine* 12.3 (1992), pp. 7–17.
- [75] I. Konstantopoulos and P. Antsaklis. “An eigenstructure assignment approach to control reconfiguration”. In: *Proceedings of the 4th IEEE Mediterranean Symposium on Control et Automation, Chania, Crete, Greece*. 1996, pp. 328–333.
- [76] B. Koppen-Seliger, P. Frank, and A. Wolff. “Residual evaluation for fault detection and isolation with RCE neural networks”. In: *Proceedings of 1995 American Control Conference-ACC'95*. Vol. 5. IEEE. 1995, pp. 3264–3268.
- [77] M. Kordestani, K. Salahshoor, A. A. Safavi, and M. Saif. “An adaptive passive fault tolerant control system for a steam turbine using a PCA based inverse neural network control strategy”. In: *2018 World Automation Congress (WAC)*. IEEE. 2018, pp. 1–6.
- [78] C. Kravaris, J. Hahn, and Y. Chu. “Advances and selected recent developments in state and parameter estimation”. In: *Computers & chemical engineering* 51 (2013), pp. 111–123.

- [79] M. Krstic, P. V. Kokotovic, and I. Kanellakopoulos. *Nonlinear and adaptive control design*. John Wiley & Sons, Inc., 1995.
- [80] Z. Li and B. Dahhou. “Parameter intervals used for fault isolation in non-linear dynamic systems”. In: *International Journal of Modelling, Identification and Control* 1.3 (2006), pp. 215–229.
- [81] Z. Li and B. Dahhou. “A new fault isolation and identification method for non-linear dynamic systems: Application to a fermentation process”. In: *Applied Mathematical Modelling* 32.12 (2008), pp. 2806–2830.
- [82] D. Looze, J. Weiss, J. Eterno, and N. Barrett. “An automatic redesign approach for restructurable control systems”. In: *IEEE Control systems magazine* 5.2 (1985), pp. 16–22.
- [83] D. Luenberger. “Observers for multivariable systems”. In: *IEEE Transactions on Automatic Control* 11.2 (1966), pp. 190–197.
- [84] J. Lunze and J. H. Richter. “Reconfigurable fault-tolerant control: a tutorial introduction”. In: *European journal of control* 14.5 (2008), pp. 359–386.
- [85] J. M. Maciejowski and C. N. Jones. “MPC fault-tolerant flight control case study: Flight 1862”. In: *IFAC Proceedings Volumes* 36.5 (2003), pp. 119–124.
- [86] M. Mansouri, M. N. Nounou, and H. N. Nounou. “Multiscale kernel pls-based exponentially weighted-glrt and its application to fault detection”. In: *IEEE Transactions on Emerging Topics in Computational Intelligence* 3.1 (2017), pp. 49–58.
- [87] R. Marino and P. Tomei. “Adaptive observers with arbitrary exponential rate of convergence for nonlinear systems”. In: *IEEE Transactions on Automatic Control* 40.7 (1995), pp. 1300–1304.
- [88] J. Marzat, H. Piet-Lahanier, F. Damongeot, and E. Walter. “Model-based fault diagnosis for aerospace systems: a survey”. In: *Proceedings of the Institution of Mechanical Engineers, Part G: Journal of aerospace engineering* 226.10 (2012), pp. 1329–1360.
- [89] M. R. Maurya, R. Rengaswamy, and V. Venkatasubramanian. “A signed directed graph and qualitative trend analysis-based framework for incipient fault diagnosis”. In: *Chemical Engineering Research and Design* 85.10 (2007), pp. 1407–1422.

- [90] T. Moor. “A discussion of fault-tolerant supervisory control in terms of formal languages”. In: *Annual Reviews in Control* 41 (2016), pp. 159–169.
- [91] S. Nandi, T. C. Ilamparithi, S. B. Lee, and D. Hyun. “Detection of eccentricity faults in induction machines based on nameplate parameters”. In: *IEEE Transactions on Industrial Electronics* 58.5 (2010), pp. 1673–1683.
- [92] S. Nandi, H. A. Toliyat, and X. Li. “Condition monitoring and fault diagnosis of electrical motors—A review”. In: *IEEE transactions on energy conversion* 20.4 (2005), pp. 719–729.
- [93] E. B. Nauman. *Chemical reactor design, optimization, and scaleup*. John Wiley & Sons, 2008.
- [94] H. M. Odendaal and T. Jones. “Actuator fault detection and isolation: An optimised parity space approach”. In: *Control Engineering Practice* 26 (2014), pp. 222–232.
- [95] L. E. Olivier, I. K. Craig, and Y. Chen. “Fractional order and BICO disturbance observers for a run-of-mine ore milling circuit”. In: *Journal of Process Control* 22.1 (2012), pp. 3–10.
- [96] A. Al-Othman. “A fuzzy state estimator based on uncertain measurements”. In: *Measurement* 42.4 (2009), pp. 628–637.
- [97] R. J. Patton. “Fault-tolerant control: the 1997 situation”. In: *IFAC Proceedings Volumes* 30.18 (1997), pp. 1029–1051.
- [98] R. J. Patton and J. Chen. “Review of parity space approaches to fault diagnosis for aerospace systems”. In: *Journal of Guidance, Control, and Dynamics* 17.2 (1994), pp. 278–285.
- [99] M. Rodrigues. “Diagnostic et commande active tolerante aux defauts appliques aux systemes decrits par des multi-modeles lineaires”. PhD thesis. 2005.
- [100] F. Sallem. “Détection et isolation de défauts actionneurs basées sur un modèle de l’organe de commande”. PhD thesis. Université de Toulouse, Université Toulouse III-Paul Sabatier, 2013.
- [101] P. A. Samara, G. N. Fouskitakis, J. S. Sakellariou, and S. D. Fassois. “A statistical method for the detection of sensor abrupt faults in aircraft control systems”. In: *IEEE Transactions on Control Systems Technology* 16.4 (2008), pp. 789–798.

- [102] M. R. Shahriar, T. Ahsan, and U. Chong. “Fault diagnosis of induction motors utilizing local binary pattern-based texture analysis”. In: *EURASIP Journal on Image and Video Processing* 2013.1 (2013), p. 29.
- [103] N. Sheibat-Othman, N. Laouti, J.-P. Valour, and S. Othman. “Support vector machines combined to observers for fault diagnosis in chemical reactors”. In: *The Canadian Journal of Chemical Engineering* 92.4 (2014), pp. 685–695.
- [104] H. Shen, L. Su, and J. H. Park. “Reliable mixed H_∞ /passive control for T–S fuzzy delayed systems based on a semi-Markov jump model approach”. In: *Fuzzy Sets and Systems* 314 (2017), pp. 79–98.
- [105] C. Shi, D. M. Blei, and V. Veitch. “Adapting neural networks for the estimation of treatment effects”. In: *arXiv preprint arXiv:1906.02120* (2019).
- [106] E. Sobhani-Tehrani and K. Khorasani. *Fault diagnosis of nonlinear systems using a hybrid approach*. Vol. 383. Springer Science & Business Media, 2009.
- [107] A. I. Stankiewicz, J. A. Moulijn, et al. “Process intensification: transforming chemical engineering”. In: *Chemical engineering progress* 96.1 (2000), pp. 22–34.
- [108] M. Staroswiecki. “Fault tolerant control using an admissible model matching approach”. In: *Proceedings of the 44th IEEE Conference on Decision and Control*. IEEE. 2005, pp. 2421–2426.
- [109] M. Staroswiecki, H. Yang, and B. Jiang. “Progressive accommodation of aircraft actuator faults”. In: *IFAC Proceedings Volumes* 39.13 (2006), pp. 825–830.
- [110] B. Tang, W. Liu, and T. Song. “Wind turbine fault diagnosis based on Morlet wavelet transformation and Wigner-Ville distribution”. In: *Renewable Energy* 35.12 (2010), pp. 2862–2866.
- [111] D. Theilliol, D. Sauter, and J. Ponsart. “A multiple model based approach for fault tolerant control in non-linear systems”. In: *IFAC Proceedings Volumes* 36.5 (2003), pp. 149–154.
- [112] F. Theron, Z. Anxionnaz-Minvielle, M. Cabassud, C. Gourdon, and P. Tochon. “Characterization of the performances of an innovative heat-exchanger/reactor”. In: *Chemical Engineering and Processing: Process Intensification* 82 (2014), pp. 30–41.
- [113] S. Thomas. *Reconfiguration and bifurcation in flight controls*. Drexel University, 2004.

- [114] B. Thonon and P. Tochon. “Compact multifunctional heat exchangers: a pathway to process intensification”. In: *Re-Engineering the Chemical Processing Plant: Process Intensification* (2003), p. 121.
- [115] P. Tochon, R. Couturier, Z. Anxionnaz, S. Lomel, H. Runser, F. Picard, et al. “Toward a competitive process intensification: a new generation of heat exchanger-reactors”. In: *Oil & Gas Science and Technology—Revue d’IFP Energies nouvelles* 65.5 (2010), pp. 785–792.
- [116] P. Tochon, R. Couturier, and F. Vidotto. *Method for producing a heat exchanger system, preferably of the exchanger/reactor type*. US Patent 8,468,697. June 2013.
- [117] C. Tutivén Gálvez. “Fault detection and fault tolerant control in wind turbines”. In: (2018).
- [118] E. R. Van Oort. “Adaptive backstepping control and safety analysis for modern fighter aircraft”. In: (2011).
- [119] V. Venkatasubramanian, R. Rengaswamy, and S. N. Kavuri. “A review of process fault detection and diagnosis: Part II: Qualitative models and search strategies”. In: *Computers & chemical engineering* 27.3 (2003), pp. 313–326.
- [120] V. Venkatasubramanian, R. Rengaswamy, S. N. Kavuri, and K. Yin. “A review of process fault detection and diagnosis: Part III: Process history based methods”. In: *Computers & chemical engineering* 27.3 (2003), pp. 327–346.
- [121] V. Venkatasubramanian, R. Rengaswamy, K. Yin, and S. N. Kavuri. “A review of process fault detection and diagnosis: Part I: Quantitative model-based methods”. In: *Computers & chemical engineering* 27.3 (2003), pp. 293–311.
- [122] L. Wen, X. Li, L. Gao, and Y. Zhang. “A new convolutional neural network-based data-driven fault diagnosis method”. In: *IEEE Transactions on Industrial Electronics* 65.7 (2017), pp. 5990–5998.
- [123] A. Widodo and B.-S. Yang. “Support vector machine in machine condition monitoring and fault diagnosis”. In: *Mechanical systems and signal processing* 21.6 (2007), pp. 2560–2574.
- [124] Z. Xiaoqiang, X. Yongfei, and W. Tao. “Fault detection of batch process based on multi-way Kernel T-PLS”. In: *Journal of Chemical and Pharmaceutical Research* 6.7 (2014), pp. 338–346.

- [125] X. Xu, D. Cao, Y. Zhou, and J. Gao. “Application of neural network algorithm in fault diagnosis of mechanical intelligence”. In: *Mechanical Systems and Signal Processing* (2020), p. 106625.
- [126] R. Yan and R. X. Gao. “Hilbert–Huang transform-based vibration signal analysis for machine health monitoring”. In: *IEEE Transactions on Instrumentation and measurement* 55.6 (2006), pp. 2320–2329.
- [127] S. Yin, S. X. Ding, A. Haghani, H. Hao, and P. Zhang. “A comparison study of basic data-driven fault diagnosis and process monitoring methods on the benchmark Tennessee Eastman process”. In: *Journal of process control* 22.9 (2012), pp. 1567–1581.
- [128] D. Zappalá, P. J. Tavner, C. J. Crabtree, and S. Sheng. “Side-band algorithm for automatic wind turbine gearbox fault detection and diagnosis”. In: *IET Renewable Power Generation* 8.4 (2014), pp. 380–389.
- [129] S. Zeghlache, K. Kara, and D. Saigaa. “Fault tolerant control based on interval type-2 fuzzy sliding mode controller for coaxial trirotor aircraft”. In: *ISA transactions* 59 (2015), pp. 215–231.
- [130] M. Zhang. “Fault diagnosis & root cause analysis of invertible dynamic system”. PhD thesis. Université Paul Sabatier-Toulouse III, 2017.
- [131] M. Zhang, Z. Li, M. Cabassud, and B. Dahhou. “An integrated FDD approach for an intensified HEX/Reactor”. In: *Journal of Control Science and Engineering* 2018 (2018).
- [132] Q. Zhang. *Fault detection and isolation based on adaptive observers for nonlinear dynamic systems*. Citeseer, 1999.
- [133] Q. Zhang. “A new residual generation and evaluation method for detection and isolation of faults in non-linear systems”. In: *International Journal of Adaptive Control and Signal Processing* 14.7 (2000), pp. 759–773.
- [134] Y. Zhang, N. Yang, and S. Li. “Fault isolation of nonlinear processes based on fault directions and features”. In: *IEEE Transactions on Control Systems Technology* 22.4 (2013), pp. 1567–1572.
- [135] Y. Zhang and J. Jiang. “Bibliographical review on reconfigurable fault-tolerant control systems”. In: *Annual reviews in control* 32.2 (2008), pp. 229–252.

- [136] F. Zidani, D. Diallo, M. E. H. Benbouzid, and R. Nait-Said. “A fuzzy-based approach for the diagnosis of fault modes in a voltage-fed PWM inverter induction motor drive”. In: *IEEE Transactions on industrial electronics* 55.2 (2008), pp. 586–593.